CENTRO DE INVESTIGACIÓN Y DE ESTUDIOS AVANZADOS DEL INSTITUTO POLITÉCNICO NACIONAL

UNIDAD ZACATENCO
DEPARTAMENTO DE FARMACOLOGÍA

El precondicionamiento farmacológico aumenta STIM1 y Orai1 a través de ROS y la vía MAPK en cardiomiocitos de rata adulta

M en C. JOICE THOMAS GAVALI

Para obtener el grado de:
DOCTORA EN CIENCIAS
EN LA ESPECIALIDAD DE
FARMACOLOGÍA

DIRECTOR DE TESIS:

DR. JORGE ALBERTO SÁNCHEZ RODRÍGUEZ

CIUDAD DE MÉXICO Septiembre, 2020

RESEARCH AND STUDIES CENTER
ADVANCED POLYTECHNIC INSTITUTE
NATIONAL

ZACATENCO UNIT
DEPARTMENT OF PHARMACOLOGY

Pharmacological preconditioning upregulates STIM1 and Orai1 via ROS and the MAPK pathway in adult rat cardiomyocytes

M en C. JOICE THOMAS GAVALI

IN PARTIAL FULFILMENT OF THE REQUIREMENTS FOR THE AWARD OF THE DEGREE OF
DOCTOR IN SCIENCE
SPECIALIZATION IN PHARMACOLOGY

DIRECTOR OF TESIS:

DR. JORGE ALBERTO SÁNCHEZ RODRÍGUEZ

MÉXICO CITY September, 2020

Acknowledgement

I owe my gratitude to all those people who have made this thesis possible and because of whom my graduate experience would be one to cherish forever. Firstly, I would like to thank my advisor Dr. Jorge Alberto Sánchez Rodríguez, for the continuous support of my Ph.D. study and related research, for his patience, motivation, and immense knowledge. I could not have imagined having a better learning and experience under his mentorship.

My sincere gratitiude to all my committee members: Dra. Maria del Carmen García García, Dr. Juan Carlos Gómora Martínez, Dr. José Antonio Terrón Sierra, Dr. Pablo Muriel de la Torre and Dr. Benjamín Florán Garduño for their thought-provoking questions, insightful comments and constructive criticism. I am greatly benefitted by their comments to focus and improve on my objectives.

I would like to thank my lab auxiliaries Dra. Elba Dolores Carrillo Valero and Ascensión Hernández Pérez (Tere) for their technical assistance, continuous support and suggestions that helped me overcome technical problems and achieve my objectives. I would also like to acknowledge our lab technicians Oscar Ramírez Herrera and Sergio Gomez Ortiz for their assistance during experiments.

My special thanks to all my friends for their moral support and encouragement during hard times of my PhD. Thank you very much Neeshu, Shiv, Tauqeer, Gayathri, Eshwar, Gaurav, Samanatha, Khemlal, Kari, Sanyog, Mohan, Prashant, Shakti and my two little champs Meshika and Ishaan.

I also would like to thank my labmates for their encouragement and for providing a stimulating and fun-filled environment in the lab, Raùl, Maikel ,Willibaldo, Ruben, Erick and Andres.

My heartfelt thanks to my parents, Mr. Thomas Gavali and Mrs Ruth Gavali, Johnlove my brother and my sisters Jolly and Jenisa for their love, patience and support without which any of this would have been possible. I would like to thank Vasanth Kumar Prabhakar my fiancé for his support and encouragement in my hour of need. Thank you, all my family members, for your inspirational appreciation and love.

Finally, I appreciate the financial aid from CONACYT who funded parts of the research discussed in this dissertation and supported with a scholarship for four years during my doctoral study.

Joice Thomas Gavali

INDICE

Abbreviations 5
RESUMEN 7
ABSTRACT 7
1.INTRODUCTION 8
1.1 Ischemia 8
1.2 Ischemic Preconditioning 10
1.3 Pharmacological Preconditioning 11
1.4 Store-operated calcium channels (SOCs) 14
1.5 Store-operated calcium channels (SOCs) in heart 19
1.6 Store-operated calcium channels (SOCs) and ROS 20
2 Materials and Methods: 22
2.1The composition of solutions used is given in the tables described below: 22
2.2. Pharmacological agents 25
2.3. Animals 25
2.4. Isolation of Hearts 26
2.5. Isolation of ventricular myocytes 26
2.6. Cardiomyocyte treatments 27
2.7. Membrane Fractionation and western blotting 27
2.8. Measurement of ROS production 28
2.9. Immunochemistry 29
2.10. qRT-PCR 30
2.11. Data analysis 31
3. RESULTS 32
3.1. Upregulation of STIM1 and Orai1 proteins by PPC 32
3. 2 The distribution pattern of STIM1 is disrupted by PPC 33
3.3 PPC increases the expression of Orai 1 34
3.4 Pharmacological preconditioning and ROS production. 35
3.5.The role of mitoKATP channels and ROS on upregulation of STIM1 and Orai1 proteins by PPC36
3.6. The role of mitoKATP channels and ROS on STIM 1 distribution changes by PPC 38
3.7. The role of mitoKATP channels and ROS on localization of Orai 1 by PPC 39
3.8. PPC and SGK 1 40
3.9. Increased STIM1 protein levels produced by de novo protein synthesis 41
3.10. Increased STIM1 protein levels produced by de novo protein synthesis 43
3.11. PPC increases the mRNA expression of STIM1 and Orai1 45

3.12. Regulation of Orai1 and STIM1 expression by PPC are mediated by the MAPK/ERK pathway 45
3.13. Regulation of Orai1 and STIM1 expression by PPC are mediated by the MAPK/ERK pathway is through ROS 46
3.14. Regulation of STIM1 by PPC is mediated by the MAPK/ERK pathway 47
3.15. Regulation of Orai 1 by PPC is mediated by the MAPK/ERK pathway 48
3.16. Regulation of STIM1 and Orai 1 distribution pattern by PPC are mediated by the MAPK/ERK pathway through ROS 49
3.17. PPC induces translocation of transcription factors NFkB and c-Fos into the nucleus 51
3.18. Translocation of NFκB and c-Fos into the nucleus by PPC is mediated by ROS 52
3.19. Translocation of NFκB and c-Fos into the nucleus by PPC is via MAPK/ERK pathway 53
4. DISCUSSION 54
4.1. Up-regulation of Stim 1 and Orai1 by PPC 54
4.2. The effect ROS on up-regulation of Stim 1 and Orai1 54
4.3. Upregulation of STIM1 and Orai1 by PPC involves ROS activation of the MAPK signaling pathway 55
4.4. Upregulation of Stim 1 and Orai1 expression by PPC and SOCE 57
4.5. Role of NFκB in upregulation and ROS of Stim 1 and Orai1 expression 62
4.6. The involvement of pERK and c-Fos in upregulation of Stim 1 and Orai1 by PPC and role of ROS 64
4.7. Cav1.2 channels and SOCs 66
CONCLUSION 67
6. APPENDIX 68
A. Preliminary data shows that PPC increases NFκB 68
B. Glycosylation pattern in Orai 1 68
C. Stim1 and Orai1 colocalization 71
D. Calmodulin is involved in disruption of Stim 1 in PPC 73
E. Intracellular Ca^{2+} plays a role in change in localization of Stim 1 and Orai 1. 74
7. REFERENCE 77

Abbreviations

MPT - Mitochondrial permeability transition.

$\Delta\psi_m$ - Mitochondrial membrane potential.

ROS – Reactive oxygen species.

mitoKATP- Mitochondrial ATP-sensitive K^+ channel.

IP- Ischemic Preconditioning.

MPTP- Mitochondrial permeability transition pore.

PKC- Protein kinase C.

MAPK- Mitogen activated protein kinase.

PPC- Pharmacological preconditioning.

Dzx- Diazoxide.

SR- Sarcoplasmic reticulum.

ER- Endoplasmic reticulum.

PLB- Phospholamban.

NCX- Na+/Ca2+ exchanger.

MCU- Mitochondrial Ca^{2+}uniporter.

SOCs- Store-operated calcium channels.

VGCC- Voltage gated calcium channel.

PLC- *Phospholipase* C.

TPEN- N,N,N',N'-tetrakis(2-pyridylmethyl)ethane-1,2-diamine.

CRAC- Ca^{2+} release activated channels.

PM- Plasma membrane.

SOCE- Store-operated Ca^{2+} entry.

BSO- Buthionine sulfoximine.

H_2O_2- Hydrogen peroxide.

ERK-Extracellular signal regulated kinases.

5-HD- 5-hydroxydecanoate.

NAC- N-acetyl cysteine.

AP1- Activator protein 1.

SGK 1- Serine/threonine-protein kinase.

NF-κB- *Nuclear factor kappa* B.

RESUMEN

Antecedentes: El precondicionamiento farmacológico (PPC) con diazóxido, un abridor de canales de K^+ sensible al ATP mitocondrial, conduce a la cardioprotección frente a la isquemia. El PPC reduce la amplitud de los transitorios de Ca^{2+} durante los potenciales de acción como resultado de la regulación a la baja de los canales de Ca^{2+} tipo L (González et al., 2010). Sin embargo, se ignora si la expresión de otros canales iónicos relacionados con la homeostasis del Ca^{2+} se altera por el PPC. En esta tesis, encontramos que el PPC regula la expresión de STIM y Orai (componentes principales de la entrada de Ca^{2+} controlada por los depósitos intracelulares (s*tore operated* Ca^{2+} *entry*).

ABSTRACT

Background: Pharmacological preconditioning (PPC) using diazoxide, a mitochondrial ATP-sensitive K^+ channel opener, leads to cardioprotection against ischemia. PPC reduces Ca^{2+} transients during action potentials as a result of down-regulation of L-type Ca^2 channels (González et al., 2010). However, changes in the expression of other channels involved in Ca^{2+} homeostasis have remained unexplored. In this study, we found that PPC regulates the expression of STIM and Orai (major components of Store Operated Ca^{2+} Entry).

Methods: We used diazoxide to produce PPC in hearts and isolated cardiomyocytes from adult male Wistar rats. The expression and localization of Stim 1 and Orai1 were assessed by Western blot and by immunofluorescence, respectively. The expression levels of Stim 1 and Orai1 mRNA were quantified using qRT-PCR.

Results: PPC increased the expression of STIM1 and Orai1, both at the mRNA and protein levels. In addition, confocal microscopy revealed a change in the distribution pattern of Stim 1

and Orai1 by PPC. The effect of diazoxide was prevented by the ROS scavenger NAC and by the mitoKATP channel blocker 5-HD. The increase in the expression of STIM1 and Orai1 involved *de novo* protein synthesis, as evidenced by the selective protein synthesis inhibitor, cycloheximide. We also found that up-regulation of Stim 1 and Orai1 expression by PPC is mediated by the ERK pathway, as revealed by the specific inhibitor U0126.

Conclusion: Our results demonstrate that PPC up-regulates the expression of STIM1 and Orai1. This effect is mediated by ROS via the MAPK/ERK pathway.

1.INTRODUCTION

1.1 Ischemia

Myocardial infarction, ischemia and heart failure are leading causes of morbidity and mortality in human. Cardiac ischemia is a pathophysiological process in which the heart lacks enough supply of oxygen and blood flow to contract normally. It is mainly caused by narrowing and blockage of one or more coronary arteries. The ischemia is a condition which denote deficient blood supply to tissues due to obstruction of the arterial inflow. The term ischemia was first used in the early nineteenth century (Kalogeris *et el*., 2012).

During ischemia, cells depend on anaerobic glycolysis for their ATP supply, leading to accumulation of lactate, protons, and NAD+, and a subsequent drop in cytosolic pH. To reestablish normal pH, the cell extrudes H^+ ions in exchange for Na^+ via the plasmalemmal Na^+/H^+ exchanger (NHE) (Baines, 2009a, b, 2010, 2011; Murphy and Steenbergen, 2008). Na^+ ions are, in turn, exchanged for Ca^{2+} by the plasmalemmal Na^+/Ca^{2+} exchanger. The increase in cytosolic Ca^{2+} may lead to cell death following ischemia/reperfusion. One of the ways cells deal with this lethal increase in Ca^{2+} is to take it up into the mitochondria via the mitochondrial Ca^{2+} uniporter, a protein that uses the negative membrane potential ($\Delta\psi m$) to drive uptake of the positively charged Ca^{2+} ions into the matrix (Contreras *et al*., 2010; Szydlowska and

Tymianski, 2010**;** Talukder *et al*., 2009). However, if the elevations in mitochondrial Ca^{2+} become excessive, they can trigger the mitochondrial permeability transition pore response dissipating the membrane potential, impairing ATP production and inducing apoptosis (Kalogeris *et al*., 2012).

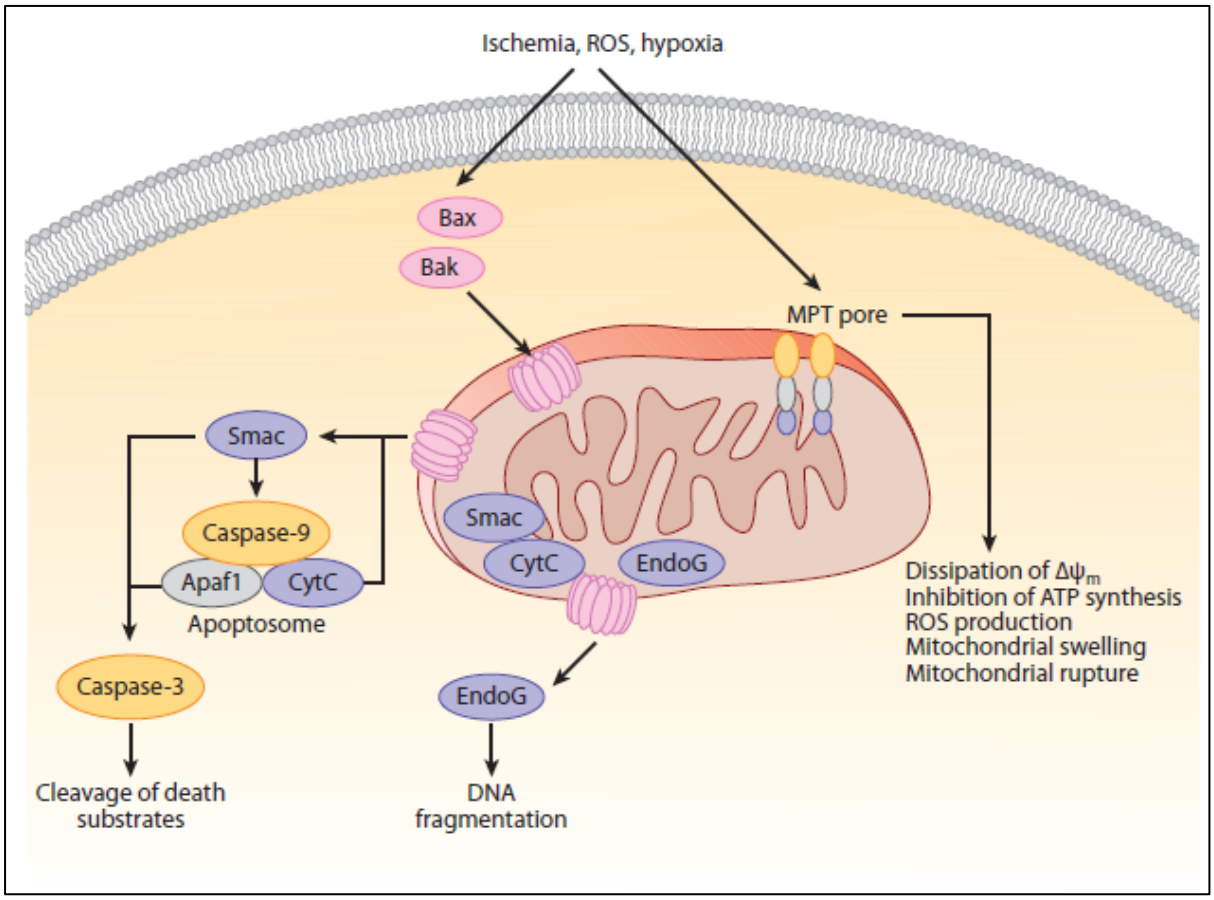

Figure 1.1 Mechanisms of mitochondria dependent cardiac cell death.

Ischemia and ROS induced cardiomyocyte death is through two mitochondria-dependent processes. The first involves the induction of the intrinsic apoptotic pathway. Activation and integration of proapoptotic Bcl2 proteins such as Bax and Bak into the mitochondrial membrane enable the efflux of proteins such as cytochrome *c* (CytC), Smac/DIABLO, and endonuclease-G (endoG). These in turn induce caspase activation and the degradation of DNA. The second pathway involves the activation of the mitochondrial permeability transition (MPT) pore. Opening of the MPT pore dissipates $\Delta\psi_m$ and inhibits ATP synthesis. This event leads

to increased production of ROS, swelling and rupture of the mitochondrion (Christopher P. Baines, 2010).

1.2 Ischemic Preconditioning

In contrast to the effects of stress or ischemia, opening of mitochondrial ATP-sensitive K^+ (mitoKATP) causes an influx of K^+ ions, with diffusion of water and uptake of anions, resulting in matrix swelling. This effect preserves the low permeability of the outer membrane for nucleotides and then the creates favorable gradient for ATP synthesis and transfer to cytoplasm. Activation of mitoKATP controls the matrix volume, preserving a narrow intermembrane space, necessary for an effective oxidative phosphorylation. Opening of mitoKATP produces a mild depolarization of membrane potential with reduced uptake of Ca^{2+} into the mitochondrial matrix, preventing Ca^{2+} overload and the opening of MPTP (Testai *et al*., 2015).

Several studies have been done on the functional recovery and to reduce the extent of infarction after ischemic episodes. Heart muscles can be protected from ischemia by Ischemic Preconditioning (IP). IP was first defined by Murry et al. in 1986 as repetitive cycles of brief periods of ischemia and reperfusion that protected the heart against prolonged ischemia. IP has been shown to enhance the recovery of cardiac function, decrease the incidence of arrhythmias, and reduce infarct size in hearts subjected to ischemia-reperfusion (I/R) injury. Preconditioning of heart by brief periods of ischemia or by administration of K^+ channel opener was found to protect the heart from ischemia-reperfusion injury. Two distinct mechanisms have been reported to involve in cardioprotection. (1) Mitochondrial ROS production triggered by mitoKATP channel opening which will lead to the activation of several protein kinases such as PKC and MAPK which are involved in gene transcription and cell growth. (2) Matrix contraction because of prevention of high electron transport rates by mitoKATP channel opening. Mitochondrial K_{ATP} channel regulates mitochondrial volume by preventing the disruption of intermembrane space. (Garlid et al. 2003).

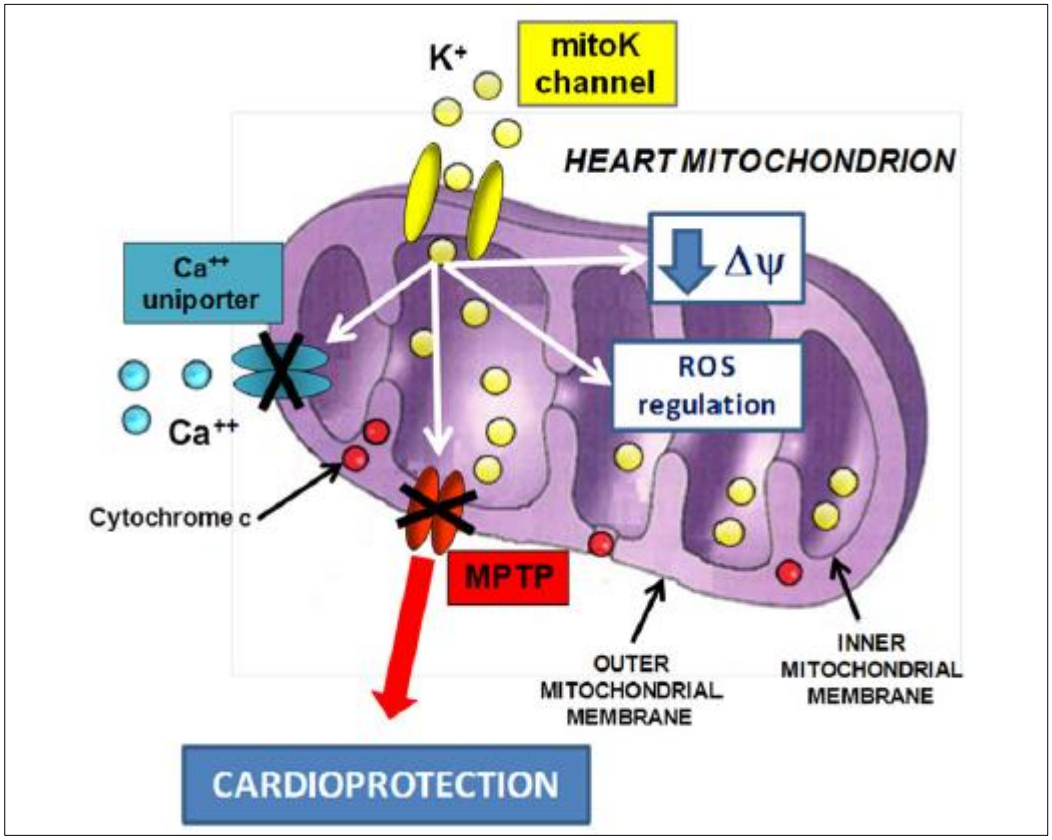

Figure 1.2. Schematic description of the different mechanisms that links the activation of mitoKATP channels and control of mitochondrial Ca^{2+} movements and modulation of the MPTP. Activation of mitoKATP channels induces inward flow of potassium ions, weak membrane depolarization, and reduced driving force for Ca^{2+} accumulation in the matrix by limiting the opening of MPTP. This mechanism reduces the release of mitochondrial proapoptotic factors during reperfusion and thus preserves mitochondrial membrane integrity (Testai et al. 2015).

1.3 Pharmacological Preconditioning

Ischaemic preconditioning (IPC) can be mimicked by pharmacological agents like diazoxide, which, among other actions, opens mitoKATP channels. Furthermore, both IPC and pharmacological preconditioning (PPC) can be antagonized by mitoKATP channel blockers. Based on this pharmacological evidence, mitoKATP channels are proposed to be central in

protection of the heart muscle by IPC and PPC (Gonzalez *et al*., 2015; Garlid *et al*., 1997; Pain *et al*., 2000).

Diazoxide significantly reduces the deleterious effects of ischemia by stabilizing mitochondrial membrane potential through the opening of mitoKATP channels. As membrane potential is being stabilized, mitochondrial Ca^{2+} overload is reduced thus preventing leakage of cytochrome c into cytosol and destruction of cristae. All these events lead to protection of cardiomyocytes from apoptosis (Dhalla *et al*.,2002).

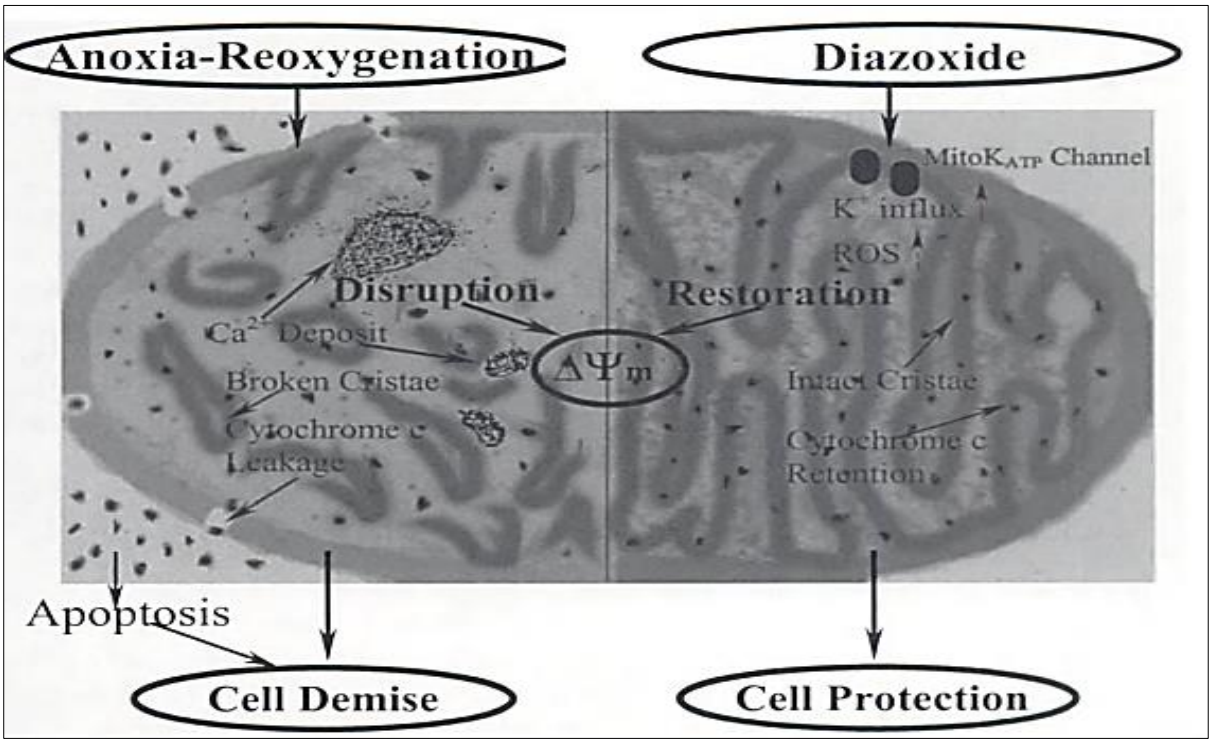

Figure 1.3. The mechanism of effect of diazoxide on cardiomyocytes during anoxia-reoxygenation. Diazoxide opens mitochondrial KATP channel and restores mitochondrial membrane potential reducing mitochondrial Ca^{2+} overload and preventing the release of cytochrome c from mitochondria to cytosol. All these events lead to inhibition of apoptosis and protect myocytes against the damage caused by anoxia-reoxygenation. Changes as a result of $\Delta\psi_m$ during anoxia and reoxygenation are shown on the left half of the diagram (Dhalla *et al*., 2002).

Pharmacological activation of mitoKATPs depends on reactive oxygen species (ROS) generated in mitochondria during preconditioning, which prevents mitochondrial Ca^{2+} overloading and MPTP opening (Lesnefsky *et al*., 2017). In addition to mitochondrial channels, L-type calcium channels also play a role in PPC in adult rat cardiomyocytes. PPC reduces both Cav1.2 channel current amplitudes and action potential-produced surges in myoplasmic Ca^{2+} concentrations, mitigating I/R-induced damage (González *et al*., 2010). However, PPC-induced changes in the functions of other types of channels involved in Ca^{2+} homeostasis is understudied.

Ca^{2+} acts as an intracellular second messenger serves a remarkable diversity of roles that span a range of biological processes from birth through development, and regulated cell function as well as apoptosis. Ca^{2+} ions are critical mediators of cardiac excitation–contraction coupling, the process through which the heart chamber contracts and relaxes. The development of contraction depends on an increase in cytoplasmic Ca^{2+} concentration. During the cardiac action potential, Ca^{2+} enters the cell through depolarization induced Ca^{2+} channels as an inward Ca^{2+} current (I_{Ca}), which contributes to the action potential plateau (Figure 1.4). Ca^{2+} entry triggers Ca^{2+} release from the sarcoplasmic reticulum (SR). The combination of Ca^{2+} influx and release raises the free intracellular Ca^{2+} concentration ($[Ca^{2+}]i$), allowing Ca^{2+} to bind to the myofilament protein troponin C, which then switches on the contractile machinery. For relaxation to occur, intracellular must decline which then allows Ca^{2+} to dissociate from troponin. For relaxation to occur, Ca^{2+} is then removed from the cytosol through four transporters, namely the SR Ca^{2+}pump, the sarcolemmal Ca^{2+} ATPase, NCX, and MCU (Bers, 2002).

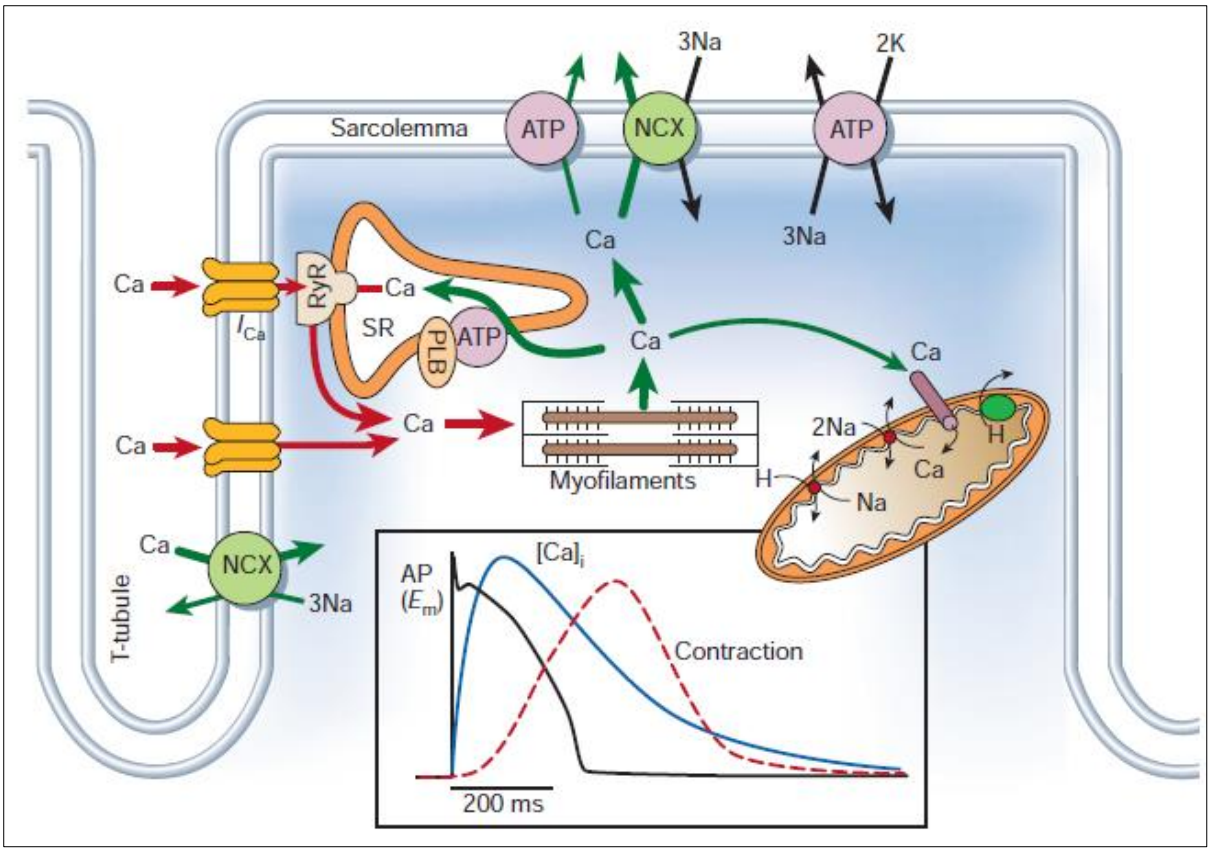

Figure 1.4. Ca2+ transport in ventricular myocytes. Inset shows the time course of an action potential, Ca^{2+} transient and contraction measured in a rabbit ventricular myocyte. NCX, ATP, PLB and SR (Bers, 2002).

1.4 Store-operated calcium channels (SOCs)

Voltage and store-operated Ca^{2+} channels are the major routes of Ca^{2+} influx in mammalian cells. In metazoans, one of the primary sources of Ca^{2+} signals in both excitable and particularly in non-excitable cells is the family of store-operated calcium channels (SOCs). These channels are typically activated by the engagement of cell surface receptors that through G proteins or a tyrosine kinase cascade activate phospholipase C to cleave phosphatidylinositol 4,5-bisphosphate (PIP2) and produce inositol 1,4,5-trisphosphate (IP3). SOCs are so named because they respond to the reduction of ER intraluminal Ca^{2+}, a consequence of IP3-induced Ca^{2+} release through IP3 receptors in the ER membrane (Figure 1.5). Store-operated channels are unique among ion channels, from their molecular basis to their biophysical properties and

mode of regulation. Because of their intimate physical and functional connections to the ER, they play a homeostatic role in providing Ca^{2+} to refill the ER after Ca^{2+} has been released and pumped out across the plasma membrane (Prakriya and Lewis, 2015).

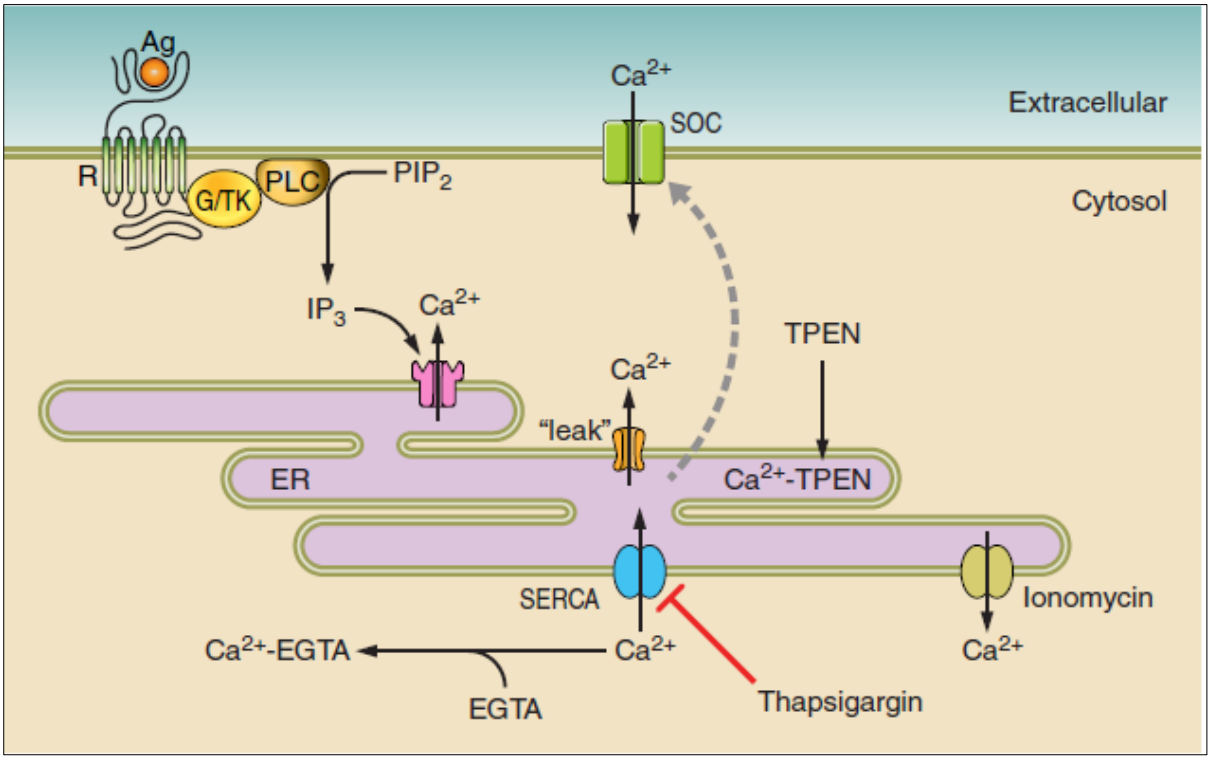

Figure 1.5. Store-operated calcium entry. Under physiological conditions, extracellular agonists bind to receptors and activate PLC through a G protein or tyrosine kinase-coupled pathway. PLC cleaves PIP2 to produce IP3, which releases Ca^{2+} from the ER. SOCs are activated by the depletion of sarcoplasmic Ca^{2+}. SOCs can also be activated experimentally by chelating intracellular Ca^{2+} with EGTA, inhibiting SERCA pumps with thapsigargin, releasing Ca^{2+} from the ER with ionomycin, or chelating intraluminal Ca^{2+} with TPEN (Prakriya and Lewis, 2015).

The endoplasmic reticulum (ER) Ca^{2+} sensor protein, STIM1, undergoes a complex activation process in response to sarcoplasmic Ca^{2+} store depletion, and translocates into ER plasma

membrane (PM) junctions where it tethers and activates PM Orai1 Ca^{2+} channels. Ca^{2+} entering through Orai1 channels maintains Ca^{2+} homeostasis, sustaining Ca^{2+} oscillations and mediates Ca^{2+} signals to control gene expressions (Amcheslavsky et al.,2015).

Putney first described the concept of capacitative Ca^{2+} entry (Putney, 1986). According to this, the concerted control of both Ca^{2+} influx and Ca^{2+} release from intracellular stores maintains Ca^{2+} homeostasis. Several studies showed that ER/SR depletion can trigger subsequent influx of extracellular Ca^{2+} into the cytoplasm to replenish Ca^{2+} in intracellular stores (Takemura and Putney, 1989; Muallem *et al*., 1990). Entry of extracellular Ca^{2+} upon store depletion was later suggested to be mediated by Ca^{2+} release activated channels (CRAC) by a process referred to as SOCE (Hoth and Penner, 1992; Patterson *et al.,* 1999).

CRAC activity was first described in 1992 (Hoth and Penner, 1992), but its mechanism of activation was not known until 2005 STIM1 was identified as the intracellular CRAC component that acts as the Ca^{2+} sensor. Upon store depletion, STIM1 aggregates and activates the PM Ca^{2+} channel that is necessary for SOCE (Roos *et al*., 2005; Zhang *et al*., 2005). The first physiological description of STIM1 as a key component of CRAC was done in *Drosophila* S2 cells where SOCE is the predominant Ca^{2+} entry mechanism. Using RNA interference screens of candidate genes, they reported that *Stim* loss altered SOCE (Roos *et al*., 2005; Zhang *et al*., 2005). This discovery took place one year after intracellular STIM1 was identified as the PM component of CRAC. The *Orai* gene, so named after the mythological keepers of heaven's gate, was described as a result of genetic mapping of mutations linked to impaired lymphocyte function (Zhang *et al.,* 2006). The mechanism of SOCE mechanism was then revised to involve two key players:(1) STIM, a transmembrane Ca^{2+} sensor protein that is located into the SR/ER membrane; and (2) Orai, an integral PM protein , subunit of the CRAC channel (Soboloff *et al*., 2012). Once the key genes governing SOCE were identified, the interplay between STIM1

and Orai1 was examined. Investigators reported that Orai protein monomers multimerize to form a Ca^{2+} channel whose activity is triggered by interaction with STIM1 (Penna *et al*., 2008).

STIM-Orai Activating Region(SOAR) and CRAC Activation Domain (CAD) were identified as active STIM1 sites necessary to trigger the CRAC current (Park *et al*., 2009; Yuan *et al*., 2009). In addition, high-resolution crystal structures of the CAD and the N-terminal region of STIM1 as well as the full-length Orai channel have been characterized (Stathopulos *et al*., 2008;Hou *et al*., 2012; Yang *et al*., 2012). These latter discoveries represent major landmarks towards the explanation of the conformational changes of STIM1-Orai complexes as well as the possible interactions with key proteins involved in Ca^{2+} handling mechanisms.

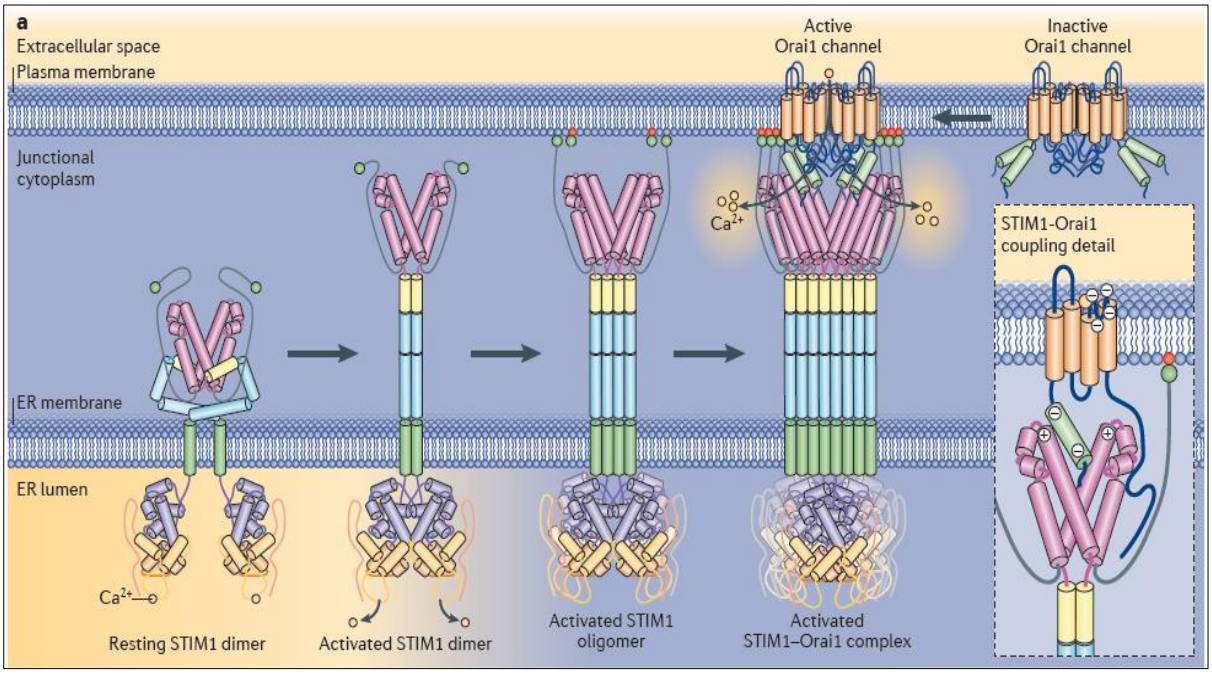

Figure 1.6. STIM activation and organization of the Ca^{2+} signaling junction. Hypothetical model of stromal interaction molecule 1 (STIM1) activation and interaction with Orai1. Activation of the STIM1 dimer starts by dissociation of $Ca^{2+}$from the EF hand of STIM1. This causes EF-hand–SAM domains within the STIM1 dimer to interact, which induces an extended configuration of the cytoplasmic coiled-coil domains, dissociation of the Cα3 inhibitory helix from SOAR, and the carboxy-terminal flexible domains recede and expose SOAR. STIM1

continues to oligomerize and migrates into ER–plasma membrane junctions and active SOAR is fully exposed. Large aggregates STIM1 are anchored within ER–PM junctions to activate Orai1 proteins (Soboloff *et al*., 2012).

Excitable and non-excitable cells are differentiated by their characteristics to increase depolarization induced concentration of intracellular Ca^{2+}. Excitable cells such as neurons and cardiomyocytes have VGCCs that are activated by depolarization induced mechanism and are needful for contraction, relaxation and electrical excitability. In contrast to non-excitable cells such as lymphocytes and mast cells don't have voltage gated Ca^{2+} influx but have CRAC channels (Wang *et al*., 2010). STIM and Orai proteins are the key mediators of SOCE, a nearly ubiquitous process in non-excitable cells. CRAC channels are activated after depletion the intracellular Ca^{2+} stores and are important for regulation of gene expression, cell proliferation and cell differentiation. Excitable cells also exhibit store-operated Ca^{2+} channel proteins, but these contribute little to Ca^{2+} influx, whereas non-excitable cells exhibit VGCC proteins, but they don't have voltage-gated Ca^{2+} currents. Previous studies have reported that SOCE coexists with VGCC in excitable cells, including neurons, skeletal muscle cells, and cardiomyocytes (Harraz and Altier, 2014, Park *et al*., 2010, Wang *et al*., 2010).

Activation of Stim 1 by store depletion or mutational modification inhibits VGCC (Cav1.2) channels while activating store-operated Orai channels. These both actions are mediated by the short STIM-Orai activating region (SOAR) of STIM1. STIM1 interacts with Cav 1.2 where it reciprocally controls CRAC and VGCC hitherto to operate independently. Such coordinated control of CaV1.2 and Orai channels has major implications for Ca^{2+} signal generation in excitable and non-excitable cells (Wang *et al*.,2010).

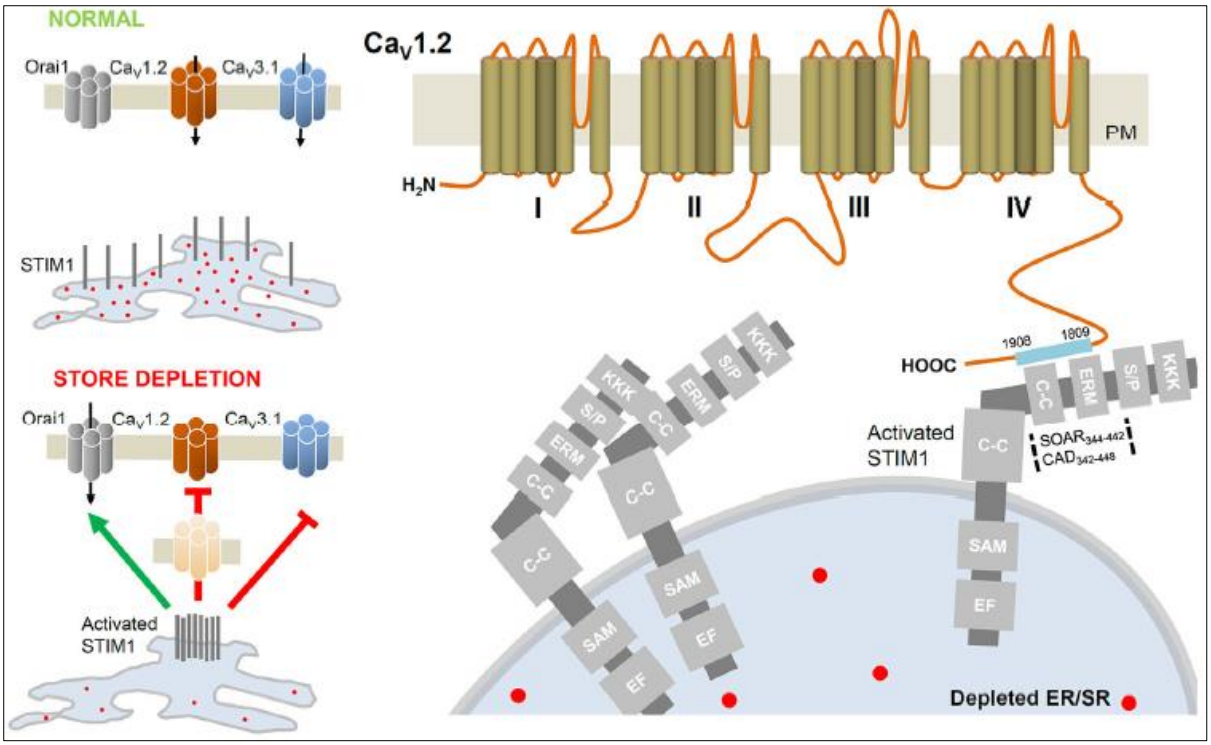

Figure 1.7. STIM1-mediated regulation of VGCC.(A) In resting conditions, the EF-hand of STIM1 is always associated Ca^{2+}. Upon sarcoplasmic depletion, STIM1 molecules aggregate closer to ER-PM junction to activate Orai channels but inhibit CaV1.2(L-type) and CaV3.1 (T-type) channels.STIM1 then internalizes CaV1.2 by removing functional channels from the cell surface. **(B)** Detailed interaction sites of STIM1 with C-terminus Cav1.2. The CAD or SOAR region of Stim 1 interacts with the C-terminus of CaV1.2. (Harraz and Altier,2014).

1.5 Store-operated calcium channels (SOCs) in heart

The expression of Stim 1 was first detected in the heart in 2001 (Williams *et al*., 2001), but its physiological function in cardiomyocytes has not studied yet. Although the role of SOCs in the adult heart is yet to know, inhibition of SOCs have been shown to enhance functional recovery of heart muscle tissues in I/R (Liu et al., 2006; Collins et al., 2013) which suggest that SOCE might play a role in Ca^{2+} overload.

In 2002, Hunton *et al* reported for the first time the existence of SOCE in neonatal rat ventricular myocytes (NRVMs) and adult cardiomyocytes. They also demonstrated that SOCE was needed for activation of hypertrophic signaling pathways including nuclear translocation of NFAT by IP3-generating agonists such as phenylephrine and angiotensin II. While the physiological role of SOCE in the adult heart continues to be debated, SOCE is thought to be involved in development because high expression levels of STIM1 are seen in neonatal cardiomyocytes (Hulot *et al.*, 2011 and Luo *et al.*,2012). Additionally, SOCE has been implicated in pathological conditions of the heart, such as cardiac hypertrophy, a disorder that leads to upregulation of STIM1 (Correll *at al*., 2015; Hulot *et al.*,2001 and Luo *et al.*, 2012). Apart from its potential role in cardiomyocyte hypertrophy little is known about the physiological role of STIM1-mediated SOCE in adult cardiomyocytes and whether and how expression of STIM1 and Orai1 may be altered in other pathophysiological states remain largely unexplored.

1.6 Store-operated calcium channels (SOCs) and ROS

Store independent activation of SOCs have reported in several studies. In oxidative stress conditions, reactive thiol groups of proteins undergoes S-glutathionylation, a reversible reaction between cysteine residues of a protein and glutathione (GSH) that regulates redox signaling and oxidative stress responses. Exposure of COS7 cells to H_2O_2 or BSO activates Stim 1. Stim 1 then oligomerizes and redistributes from ER to ER-PM junction to activate SOCE. A similar store-independent Ca^{2+}entry was studied in mouse embryonic fibroblasts (MEFs) but was ineffective in MEFs lacking STIM1, indicating STIM1 as an important oxidative stress sensor. STIM1 knockout DT40 chicken B-lymphocytes inhibited SOCE after exposure of BSO or H_2O_2 whereas they showed activation of SOCE after re-expression of STIM1 (Hawkins et al.,2010). Several studies showed that induction of hypoxia or oxidative stress with either the O_2 scavenger sodium dithionite or tert-butyl hydroperoxide (tBHP)

promotes redistribution of STIM1 at ER-PM junctions in various cell lines. stimulated ROS produced by hypoxia and oxidant signaling causes store-depletion and triggers SOCs activation in human A549 adenocarcinomic alveolar basal epithelial cells and143B osteosarcoma cells, respectively (Gusarova *et al*.,2011, Mungai *et al*.,2011 and Mancarella *et al*.,2011).

In this study, we examined the effects of PPC with diazoxide on the transcription and protein expression of STIM1 and Orail, and on the intracellular localization of the transcription factors c-FOS and NFκB, We used western blot and quantitative reverse transcriptase polymerase chain reaction (qRT-PCR) experiments to quantitate protein and mRNA transcript levels in presence of various drugs aimed at probing the mechanisms mediating PPC. We examined whether ROS and the MAPK/ERK pathway may be involved in the upregulation of Orai1 and STIM1 proteins by PPC and tested the possibility that changes in the expression of SOCE components by PPC depend on c-FOS and NF-κB transcription factors.

2 Materials and Methods:

2.1The composition of solutions used is given in the tables described below:

Tyrode solution

Reagents	**Concentrations**
NaCl	137 mM
KCl	5.4 mM
$MgCl_2$	1 mM
HEPES	10 mM
Glucose	10 mM

pH set to 7.47 with 1N NaOH at 25°C; Osmolality: 305 mOsm

Krebs-Henseleit buffer

Reagents	**Concentrations**
NaCl	117.8 mM
NaH_2PO_4	1.2 mM
KCl	6 mM
NaHCO3	24.3 mM
MgSO4	1.2 mM
EDTA	0.027 mM
Glucose	5.1 mM
CaCl2	1.6 mM

pH set to 7.4 with 1N NaOH; gassed with 95% O_2, 5% CO_2

10X PBS

Reagents	Concentrations/Litre
KCl	2 g
NaCl	80 g
KH_2PO_4	2 g
Na_2HPO_4	11.5 g

pH set to 7.4 with 1N NaOH

10X protein running buffer

Reagents	Concentrations/Litre
Tris Base	30.2 g
Glycine	144 g
SDS	10 g

pH set to 8.3 with concentrated HCl

4X sample loading buffer

Reagents	Concentrations
Tris HCL (pH 6.8)	0.2 M
SDS	0.8 g/10ml
Glycerol	40%
β-Mercaptoethanol 14.7 M	0.4 ml/10 ml
EDTA 0.5 M	0.05 M
Bromophenol blue	8 mg/10 ml

Protein transfer buffer

Reagents	Concentrations/100 ml
Tris Base	0.532 g
Glycine	0.293 g
SDS 10%	0.375 ml
Methanol	20%

Blocking solution

4.5 % non-fat milk powder in 1X PBS solution

Coomassie blue staining solution

Reagents	Concentrations/200 ml
Glacial acetic acid	10%
Methanol:H_2O	1:1
Coomassie brilliant blue R-250	0.5 g

Ponceau red staining solution

Reagents	Concentrations
Acetic acid	1%
Ponceau red	0.5 g/100 ml

Destaining solution

Reagents	Concentrations
Methanol	30%
Acetic acid	10%

2.2. Pharmacological agents

Reagents	Concentrations
Diazoxide (Dzx)	100 μM; 20 mg/kg
5-HD	100 μM
NAC	2-4 mM
Cycloheximide	10 μM
U0126 (MAPK/ERK inhibitor)	5 mM

2.3. Animals

Adult male (250–300 g) Wistar rats were used in this study. Our experimental protocols were approved by the Division of Laboratory Animal Units, Cinvestav-IPN, in compliance with federal law and Consejo Nacional de Ciencia y Tecnología (CONACYT) regulations.

Previous to extraction of the heart rats were anesthetized with 50 mg/kg of sodium pentobarbital, injected intraperitoneally. A 500-U/kg heparin sodium solution was also administered intraperitoneally.

2.4. Isolation of Hearts

Hearts were rapidly excised, arrested in modified Krebs-Henseleit buffer and perfused in a Langendorff apparatus with an aortic cannula. Unless otherwise stated, all chemicals and materials were purchased from Sigma–Aldrich (St. Louis, MO, USA). Isolated hearts were subjected to the following treatments: The control group was perfused for 90 min with Krebs-Henseleit buffer. The diazoxide (Dzx)-treated (Tocris, Bristol, UK) group was perfused for 90 min in Krebs-Henseleit buffer also containing 100 μM Dzx. In the NAC-Dzx group, the ROS scavenger NAC (4 mM) was added to Krebs-Henseleit buffer for15 min. Thereafter, hearts were perfused for 90 min in this buffer to which Dzx was added (100 μM). The NAC-treated group was perfused for 90 min with Krebs-Henseleit buffer to which NAC (4 mM) was added. Experiments using the mKATP channel antagonist 5-HD (100 μM) were done with a protocol similar to that used with NAC.

2.5. Isolation of ventricular myocytes

Rats were anesthetized with 50 mg/kg of sodium pentobarbital, injected intraperitoneally. A 500-U/kg heparin sodium solution was also administered intraperitoneally. Hearts were perfused for 5 minutes at 37^{o}C with Ca^{2+}-free Tyrode's solution. Hearts were recirculated for 60 minutes with Tyrode's solution supplemented with 70-U/mL type II collagenase (Worthington, Lakewood, NJ), and 0.5-mg/100 mL type XIV protease (Sigma). Ventricles were minced and shaken 2–3 times at 45 rpm for 7 minutes in the same solution. The dislodged cells were filtered through a cell strainer (100 mm nylon BD Falcon) and centrifuged at 28g for 2 minutes. The pellet was resuspended in Tyrode's solution with 1% bovine serum albumin.

2.6. Cardiomyocyte treatments

The pellet was resuspended for 90 min in Tyrode solution plus 1% BSA in control experiments, or in an identical solution containing diazoxide (100 μM), 5-hydroxydecanoate (5-HD; 100 μM), N-acetyl-L-cysteine (NAC; 2 or 4 mM) for the indicated time periods. Cardiomyocytes of cycloheximide (CHX) group, were exposed to 10 μM cycloheximide (CHX), a selective inhibitor of protein synthesis for 30 min and then incubated for 90 min in the same solution with 100 μM Dzx added. The U0126 plus diazoxide group used the selective noncompetitive inhibitor of the MAPKs, MEK1 and MEK2, U0126 (1,4-diamino-2,3-dicyano-1,4-bis(methylthio) butadiene, 5 mM; Sigma), added to cardiomyocytes for 1 hour and then cardiomyocytes were incubated for further 90 min in the same solution with diazoxide. All drugs were removed by washing 3 times with Tyrode solution containing bovine serum albumin (1 mg/mL) and 1-mM Ca^{2+}. Thereafter, cells were centrifuged at 28g for 2 minutes, and total protein were extracted for western blot analysis.

2.7. Membrane Fractionation and western blotting

For preparation of the membrane compartment, heart tissue was homogenized in ice-cold lysis buffer containing, in mM: 20 Tris (pH 7.4), 5.0 EDTA, 250 sucrose, 1.0 phenylmethanesulfonylfluoride, and 2.5% protease inhibitor mix. Tissue homogenates (20% w/v) were centrifuged at 1,000*g* for 10 min to remove nuclei and debris, and the supernatant was ultracentrifuged at 110,000*g* for 75 min at 4 °C to pellet the crude membrane fraction (both the sarcolemmal and microsomal subfractions). The resulting pellet was resuspended in solubilization buffer (50 mM Tris (pH 7.4), 100mM NaCl, 50mM LiCl, 5mM EDTA, 0.5% (v/v) triton X-100, 0.5% (w/v) sodium deoxycholate, 0.05% (w/v) SDS, and 0.02% (w/v) sodium azide). After incubation for 30 min on ice, the remaining insoluble material was

collected by centrifugation (14,000*g*, 10 min, 4 °C). Protein content of the supernatant (particulate membrane fraction) was measured with Bradford assay.

In some experiments, dissociated myocytes were used for Western blotting by resuspension in lysis buffer containing: 20 mM Tris (pH 7.5), 100 mM NaCl, 1% triton X-100 and protease inhibitors. Lysis was achieved by continuous agitation for 60 min at 4°C followed by five cycles of sonication. Samples were centrifuged at 13,000*g* for 10 min at 4°C and the soluble fraction used for Western blots. Protein content was measured with Bradford assay.

We subjected membrane fraction or total fraction samples (50-60 mg) to 10% sodium dodecyl sulfate–polyacrylamide gel electrophoresis (180 V, 120 minutes), transferred the resultant proteins bands onto nitrocellulose membranes, blocked the membranes with 4.5% nonfat dried milk in PBS, and probed the membranes with anti-STIM1 monoclonal antibody (1:1000; Abcam), anti-Orai1 polyclonal antibody (1:3000; Abcam), anti–phospho-44/42 MAPK (Erk1/2) polyclonal antibody (1:1000; Cell Signaling Technology), anti-actin monoclonal antibody (1:2000; anti- Sigma Aldrich), anti SGK 1 (1:500; Abcam) and GAPDH monoclonal antibody (1:10,000; Sigma Aldrich) in PBS for 12–14 hours at 4ºC. After rinsing, the blots with PBS-tween 20 (0.1%), they were incubated for 1 hour with anti-rabbit (1:50,000) or anti-mouse (1:75,000) horseradish peroxidase conjugated secondary antibody (Invitrogen, Carlsbad, CA) in PBS and rinsed with PBS-tween 20 (0.1%). Antibody labeling was detected with Immobilon Western reagent (Millipore Co, Billerica, MA) according to the manufacturer's instructions.

2.8. Measurement of ROS production

ROS was measured using the cell-permeant fluorescent probe, 5-(and-6)-chloromethyl-2′,7′-dichlorodihydrofluorescein diacetate, acetyl ester (CM-H2DCFDA, Molecular Probes/Invitrogen). Cardiomyocytes were loaded with 10 μM CM-H2DCFDA and incubation

in the dark for 30 min at room temperature. Loaded myocytes were incubated in dye-free solution for over 30 min to allow conversion of the dye into its ROS-sensitive form. Immediately after dye loading, ROS production was measured every 5 min for 90 min, in myocytes in Tyrode solution, with or without diazoxide (100 µM). The effect of DZX on ROS production was estimated by measuring fluorescence signals first for 15 minutes under control conditions and then for 90 minutes with Dzx.

2.9. Immunochemistry

Freshly isolated adult rat cardiomyocytes were suspended in tyrode solution containing 1 mM Ca^{2+} plus 5 % Fetal Bovine Serum (Thermofisher scientific) and were plated onto laminin treated slides and allowed to settle for 2 hours at 37^{o}C before being treated with drugs. Once cardiomyocytes are attached they were treated for 90 min in control experiments, or in an identical solution containing diazoxide (100 µM), 5-hydroxydecanoate (5-HD; 100 µM), N-acetyl-L-cysteine (NAC; 2 or 4 mM) for the indicated time periods. In the U0126 plus diazoxide group, the selective noncompetitive inhibitor of the MAPKs, MEK1 and MEK2, U0126 (1,4-diamino-2,3-dicyano-1,4-bis(methylthio) butadiene, 5 mM; Sigma) was added to cardiomyocytes for 1 hour and then cardiomyocytes were incubated for additional 90 min in the same solution with diazoxide. In the cycloheximide group, the selective inhibitor of protein synthesis cycloheximide (10µM; Sigma) was added to cardiomyocytes for 30 mins and then cardiomyocytes were further incubated 90 min in the same solution with diazoxide. Removal of all drugs was done by washing 3 times with tyrode solution containing 1mM Ca^{2+}. Immediately after treatments, cells were fixed using 4% paraformaldehyde in PBS for 15 min at 4^{o}C. After three washes with PBS, cells were permeabilized and blocked in PBS containing 0.3 % triton X-100 and 5% donkey serum for 1 hour at room temperature. Cells were then incubated overnight at 4 °C with the primary antibody in PBS containing 0.3% Triton X-100 and 0.5% BSA . Primary antibodies used were: monoclonal anti-STIM1 (1:50; Abcam,

Cambridge, UK), polyclonal anti -Orai1 (1:50; Thermofisher Scientific, Waltham, MA, USA), monoclonal anti c-FOS (1:50, Santa Cruz), monoclonal anti NFκBp65 (1:50; Santa Cruz, CA, USA). After washing three times in PBS, cells were incubated for 1 h at room temperature with secondary antibodies: Alexa Fluor 555-conjugated donkey anti-rabbit (1:200; Thermofisher Scientific, Waltham, MA, USA) for Stim1 and Alexa Fluor 488-conjugated donkey anti-mouse (1:200; Thermofisher Scientific, Waltham, MA, USA) for Orai1, NFκB and c-FOS. Thereafter, preparations were washed three times in PBS and were incubated for 10 min at room temperature with Hoechst nuclear stain (1:1000; Invitrogen, Carlsbad, CA, USA). Negative controls were identically processed but without primary antibodies.

Labeling was visualized under a laser scanning confocal microscope (Leica, Wetzlar, Germany, model TCSSP8) with argon (488 nm) and helium/neon (543 nm) lasers used with an optimized pinhole diameter. Confocal images were obtained as Z-stacks of single optical sections, which were superimposed as a single image in Leica LAS AF 2.6.0 build 7268 software. Immunofluorescence was quantified in ImageJ 1.44 p (NIH, Bethesda, MD, USA) after the images were threshold adjusted (pixel value used to find edges of immunolabeling closed regions) at an intensity of twice the mean intensity and three (for STIM1) or five (for Orai1) times the standard deviation. The threshold area was outlined under particle analysis (size 0-infinity; circularity 0-1).

2.10. qRT-PCR

RNA was isolated from cardiomyocytes with RLT buffer and a RNeasy Mini Kit (Qiagen, Hilden, Germany), and cDNAs were synthesized with a Taqman reverse transcription kit (Thermofischer, Waltham, MA, USA). Transcript levels were determined in TaqMan assays (Rn02397170_m1, Rn01506496_m1; Applied Biosystems, Foster City, CA, USA) and an iCycler iQ machine (Bio-Rad, Hercules, CA) with TaqMan Gene Expression Master Mix (Thermofischer, Waltham, MA, USA). mRNA expression was assessed relative to the

ribosomal RNA 18S (Hs999999_s1, Applied Biosystems, Foster City, CA, USA), as recommended by the manufacturer. Relative changes in expression were calculated by the $2^{-\Delta\Delta CT}$ method (Livak and Schmittgen.,2001).

2.11. Data analysis

The data, which are expressed as means ± standard errors of the mean (SEMs), were tested for normal distribution, analyzed with independent t-tests (when two groups were compared) or with analyses of variance (ANOVAs) followed by multiple comparison Dunnett's tests (each treatment group vs. control group) as appropriate. A significance criterion of $p < 0.05$ was used.

3. RESULTS

3.1. Upregulation of STIM1 and Orai1 proteins by PPC

We found that the abundance of STIM1 and Orai1 proteins significantly increased by PPC. Among the several isoforms, STIM1 and Orai1 are predominant in heart and were recognized by specific antibodies. Figure 1*A* shows representative western blots of STIM1 and actin from whole membrane fractions of ventricles of control (lane a) and Dzx-treated hearts (lane b). PPC led to an increase in the density of the STIM1 band with no changes in the density of the actin band which was used as a standard for normalization. The graph in Fig. 1*B* summarizes results from several experiments performed as in in Fig. 1*A* . On the other hand, Orai1 protein was also upregulated by PPC. Fig. 1*C* shows representative western blots of Orai1 and actin bands under control conditions (lane a) and in Dzx-treated cardiomyocytes (lane b). The density of the actin band remained unchanged and was used to normalize the values of Orai1 abundance. Fig. 1*D* shows mean density values (± SEM) of Orai1 bands under experimental conditions as in Fig. 1*C*. Orai1 abundance increased by ~50%, similar to the increase observed in the density of STIM1 band under the same experimental conditions (Fig. 1*B*).

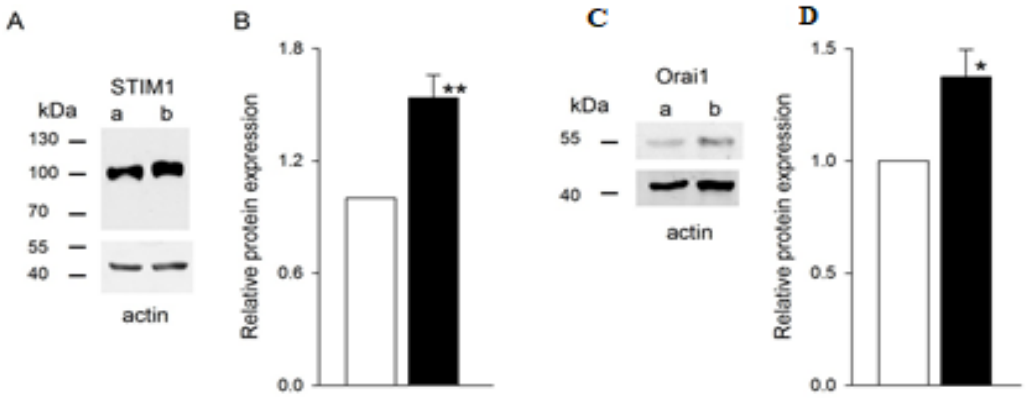

Figure 3.1. PPC increases STIM1 and Orai1 expression. A: Representative western blots of STIM1 and actin of whole membrane fractions from control (lane a) and Dzx-treated hearts

(lane b). B: Mean values (±SEM, *n*=7) of normalized densities of STIM1 bands. C: Representative western blots of Orai1 and actin of whole membrane fractions from control (lane a) and Dzx-treated hearts (lane b). D: Mean values of normalized densities of Orai1 bands (± SEM, *n*=4). *p<0.05, **p<0.01.

3. 2 The distribution pattern of STIM1 is disrupted by PPC

The effects of PPC were not limited to upregulation of STIM1, there were also changes in its distribution pattern as revealed by immunofluorescence imaging. This is shown in Fig. 2 *A-E.* Illustrated are representative zoomed images of cardiomyocytes under control conditions and after PPC (Fig. 2*A*). In control cardiomyocytes STIM1 had a characteristic cross-striated distribution. STIM1 is organized into both puncta and linear structures along the Z-disk. In contrast, a clear alteration of this pattern was seen in PPC cardiomyocytes. Fig. 1*B* shows mean values of fluorescence along the longitudinal axis of control and Dzx-treated myocytes illustrated in Fig. 2*C*. Peaks of fluorescence were regularly spaced in control cardiomyocytes and this pattern was lost by PPC. In addition, and consistent with the western blot results (Fig. 1 *A-B*), the number of particles and its mean size were incremented (Fig.2*C-D*), leading to an increase in the ratio of total particle area and cell area (Fig.2*E*). On the other hand, Orai1 protein was also upregulated by PPC.

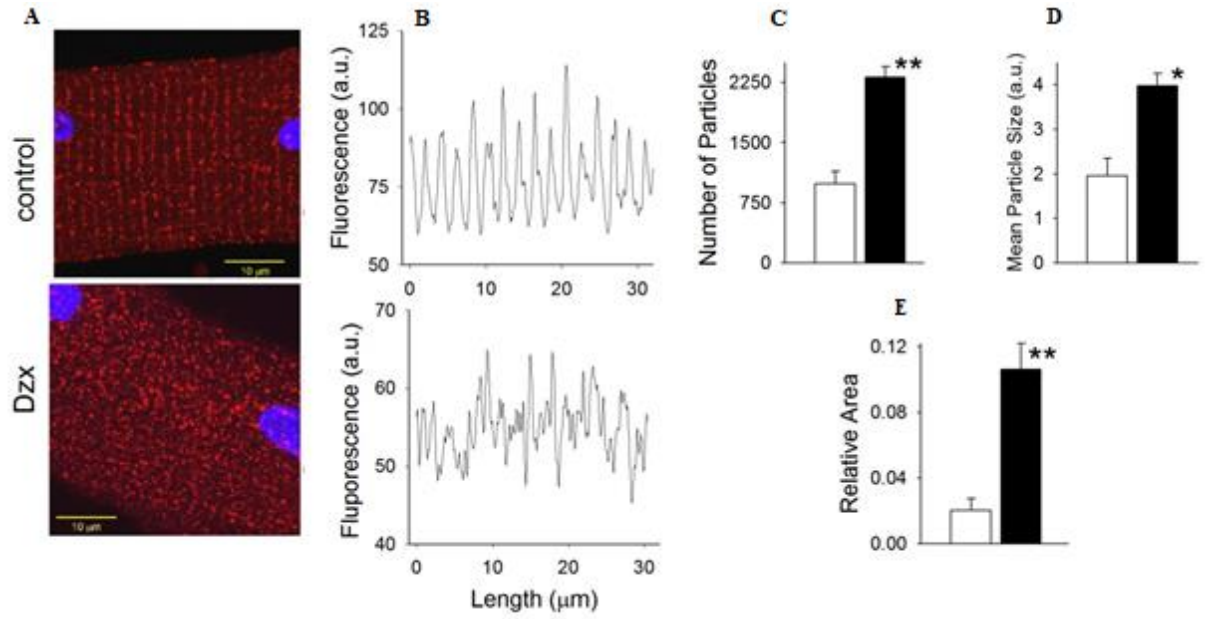

Figure 3.2. Confocal microscopy images of myocytes under control conditions and after PPC. Images show localization of STIM1 (red) with DAPI-labeled nuclei (blue). Calibration bars: 10 μm. B: Mean values of fluorescence intensity along the longitudinal axis from myocytes shown in A. C-E: Particle analysis of myocytes under the same conditions as in A . Illustrated are mean values of number of particles (C); particle size (D) and ratio of total particle area and cell area (E) (± SEM, n=5-10). Empty bars, control; filled bars, Dzx.

3.3 PPC increases the expression of Orai 1

The localization of Orai1 in control and PPC cardiomyocytes was assessed by immunofluorescence (Fig. 3*A*). We found that Orai1 is located along the surface membrane in control and PPC cardiomyocytes and consistent with western blot results, a large increase in the abundance of Orai1 was observed (Fig. 3*A*). Particle analysis of confocal images from several experimental replicates revealed an increase in the number of particles in PPC cardiomyocytes (Fig. 3*B*).

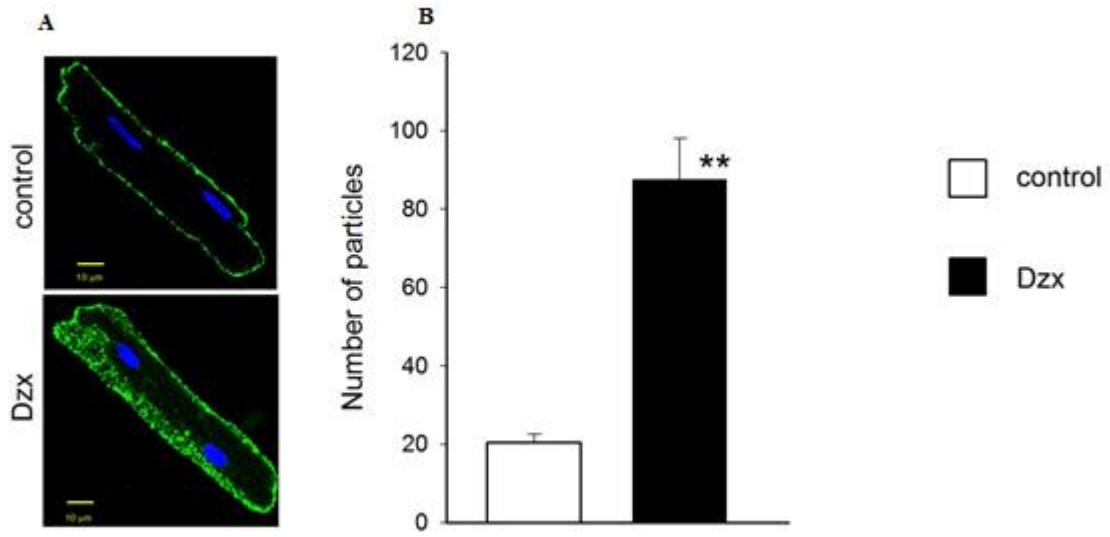

Figure 3.3.A: Representative immunofluorescence images of myocytes showing the distribution of Orai1 under the indicated experimental conditions. B: the graph shows the mean values (±SEM, n=6-10) of number of particles of Orai1 from confocal images of myocytes under experimental conditions as in A. **p<0.01.

3.4 Pharmacological preconditioning and ROS production.

Dzx opens mitoKATP channels and increases the rate of ROS production by mitochondria (Pain et al., 2000; Lesnefsky et al., 2017). Therefore, to assess whether dzx increase ROS production, ROS levels were measured with the cell-permeant fluorescent probe CM-H2DCFDA and found that dzx increased ROS production within minutes. Figure 4 summarizes the results from several experiments, showing mean relative fluorescence values as a function of time. A significant increase in ROS production was observed in myocytes incubated in dzx containing solution compared with controls.

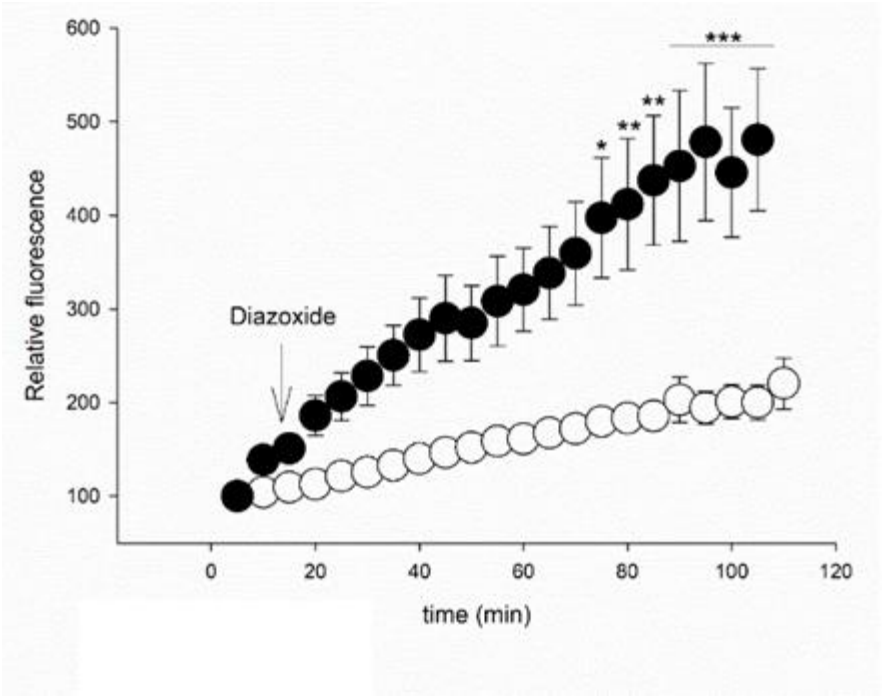

Figure 3.4. Pharmacological preconditioning and ROS production**.** The graph shows mean values (±SEM) of ROS production in control (open circles, $n = 7$) and PPC cardiomyocytes (filled circles, $n = 7$) as a function of time. $^{*}p < 0.05$, $^{**}p < 0.01$, $^{***}p < 0.001$.

3.5.The role of mitoKATP channels and ROS on upregulation of STIM1 and Orai1 proteins by PPC

To assess whether the increase in protein abundance of STIM1 and Orai1 proteins in PPC cardiomyocytes shown in Fig. 1 depends on ROS and on the opening of mitoKATP channels, we used the specific mito KATP channel blocker 5-HD and the ROS scavenger NAC in western blot experiments under the experimental conditions described in the legend. We found that STIM1 and Orai1 protein abundance remained unchanged in PPC cardiomyocytes that were pretreated with 5-HD or NAC, as shown in the representative immunoblots of Fig 5 *A* and *C*. Actin bands were used as standard for normalization of STIM1 and Orai1 bands. Results from several experimental replicates are summarized in Fig. 5 *B* and *D*.

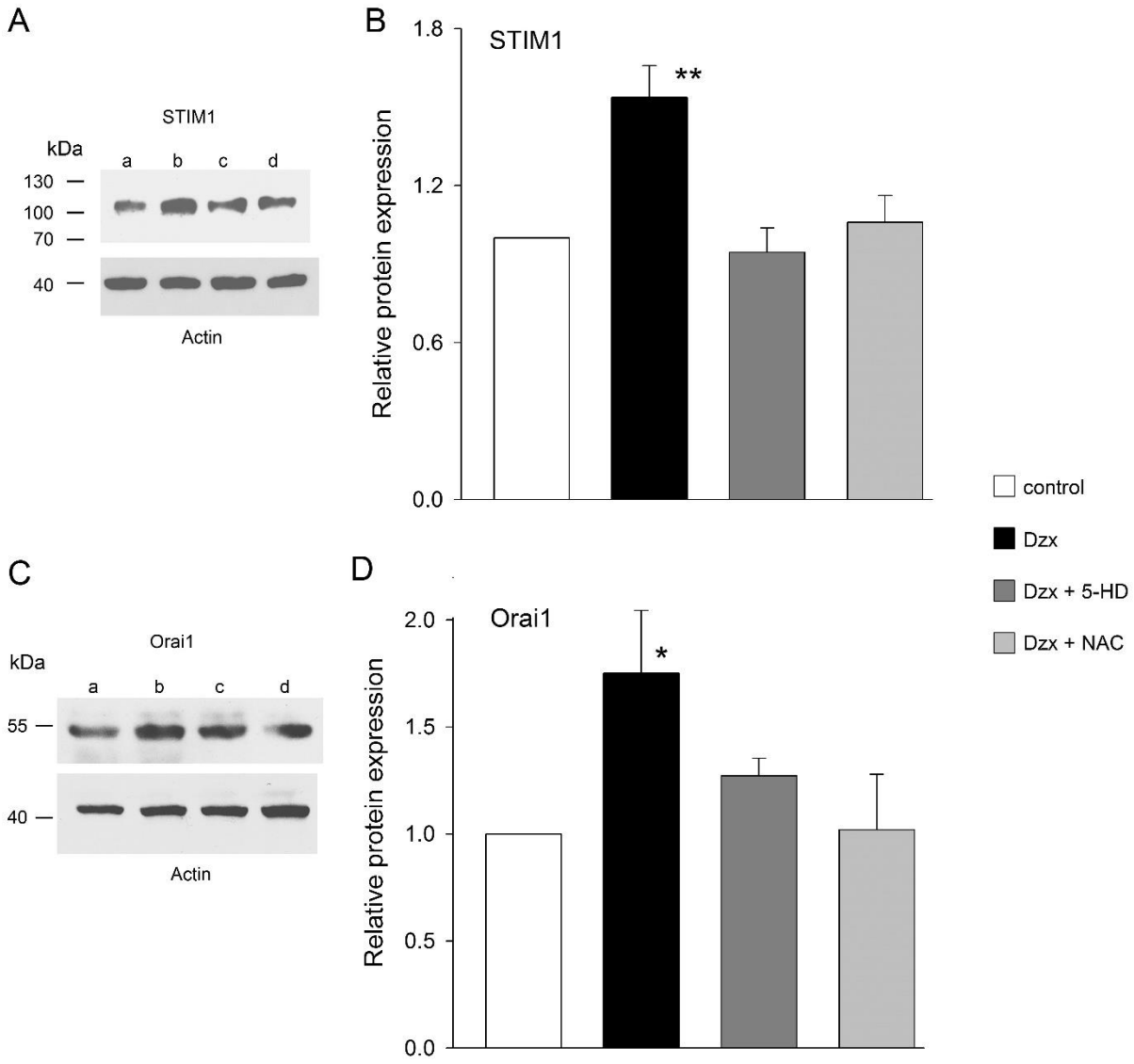

Figure 3.5. Upregulation of STIM1 and Orai1 proteins by PPC depends on ROS and opening of mitoKATP channels. A: Representative western blots of STIM1 and actin of whole membrane fractions of ventricles. Lane a, control; lane b, Dzx; lane c, Dzx + 5-HD; lane d, Dzx + NAC. B: Mean values (± SEM, n=3-7) of normalized densities of STIM1 bands under the indicated experimental conditions. Actin was used as a loading control. C: Representative western blots of Orai1 and actin of whole membrane fractions of ventricles under experimental conditions as in A. D: Mean values (± SEM, n=4) of normalized densities of Orai1 bands under the indicated experimental conditions. Actin was used as a loading control. *p<0.05, **p<0.01.

3.6. The role of mitoKATP channels and ROS on STIM 1 distribution changes by PPC

The possibility that mitoKATP channels and ROS also play a role in change in distribution of STIM1 by PPC was investigated next. Figure 6*A* shows representative immunofluorescence images of cardiomyocytes obtained under the experimental conditions indicated above images. Consistent with results shown in Fig. 2, PPC disrupted the distribution pattern of STIM1. However, the distribution pattern observed in control experiments was preserved when 5-HD or NAC were added to the Dzx-containing solution. This is shown in more detail after magnification of the areas indicated by yellow boxes shown below images. Mean fluorescence intensity values of the images shown in panel *A* are plotted in Fig. 6*B* and confirm the role of ROS and mitoKATP channels in the distribution changes of STIM1 by PPC.

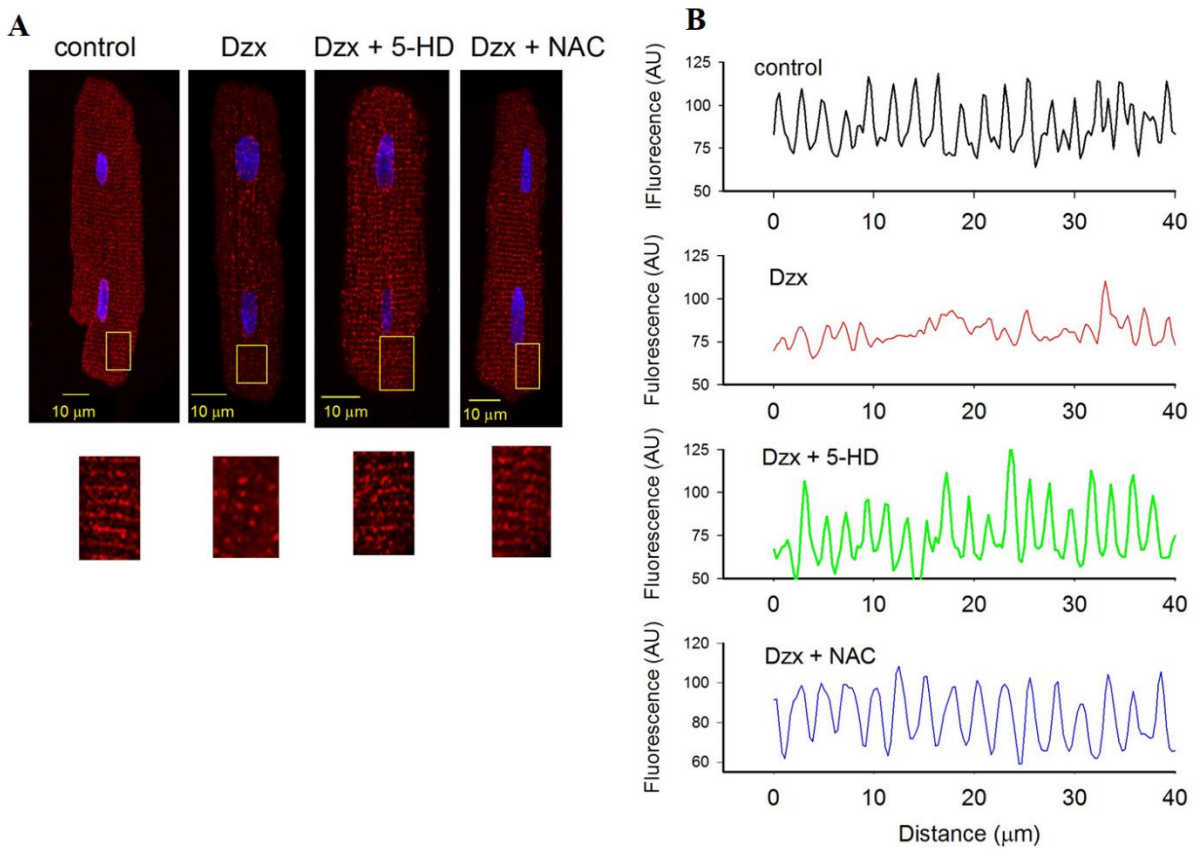

Figure 3.6. Role of ROS and mitoKATP channels on STIM1 distribution changes by PPC. A: Upper panels, representative confocal images of myocytes under the indicated experimental conditions. Lower panels are enlargements of yellow boxed areas. Images show localization of STIM1 (red) with DAPI-labeled nuclei (blue). Calibration bars: 10 μm. B: Plot fluorescence intensity profiles along the longitudinal axis of myocytes shown in A.

3.7. The role of mitoKATP channels and ROS on localization of Orai 1 by PPC

The possibility that mitoKATP channels and ROS also play a role in change in Orai1 by PPC was examined. Fig. 7*A* illustrates representative immunofluorescence images of Orai1 in cardiomyocytes incubated under the indicated experimental conditions. The increase in surface expression of Orai1 by PPC was completely abrogated by blocking mitoKATP channels with 5-HD or using NAC. Similarly, the increase in the number of particles by PPC was blocked by the same compounds as shown in the graph of Fig. 7*B* that summarizes results from several experimental replicates.

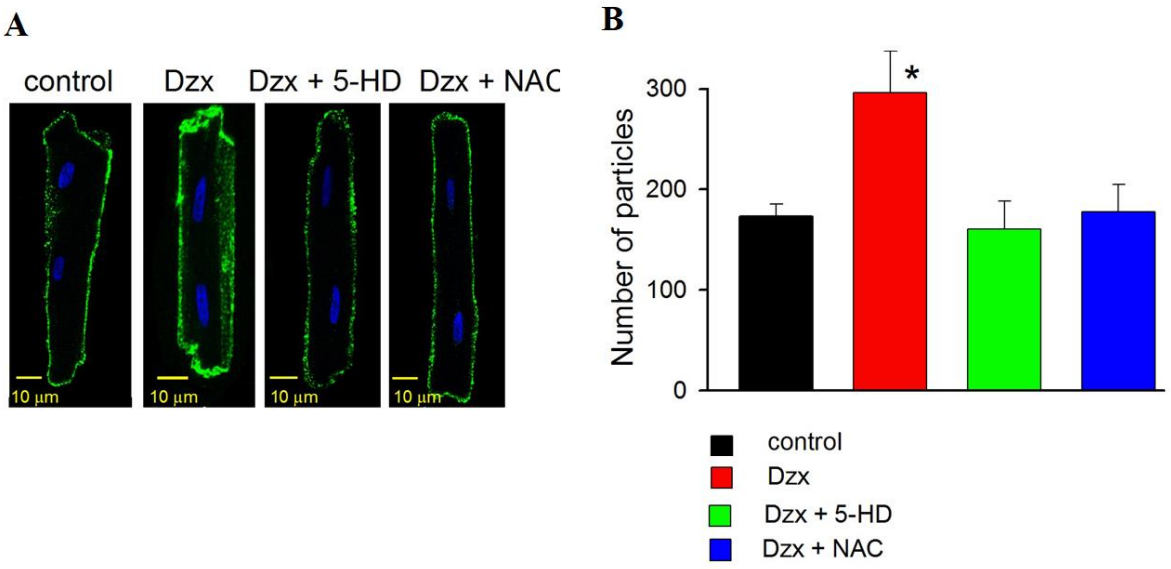

Figure 3.7: Role of ROS and mitoKATP channels on Orai1 distribution changes by PPC. A: Representative confocal images of myocytes under the indicated experimental conditions. Images show localization of Orai1 (green) with DAPI-labeled nuclei (blue). Calibration bars: 10 μm. B: Particle analysis of myocytes under the same conditions as in A. Illustrated are mean values of number of particles (± SEM, n=5-7). *p<0.05.

3.8. PPC and SGK 1

The increase in protein abundance by PPC could be due to reduced degradation or increased synthesis or both. The possibility that decreased degradation could play a role was investigated by measuring the protein expression of SGK1, an enzyme that has been associated with an increase in the abundance of Orai1, disrupting its degradation (Lang et al., 2012), but no changes were observed (Fig.9 *A and B*). On the other hand, as expected from the western blot results, qRT-PCR experiments revealed no changes in the relative values of mRNA expression of SGK1 (Fig.9 *C*).

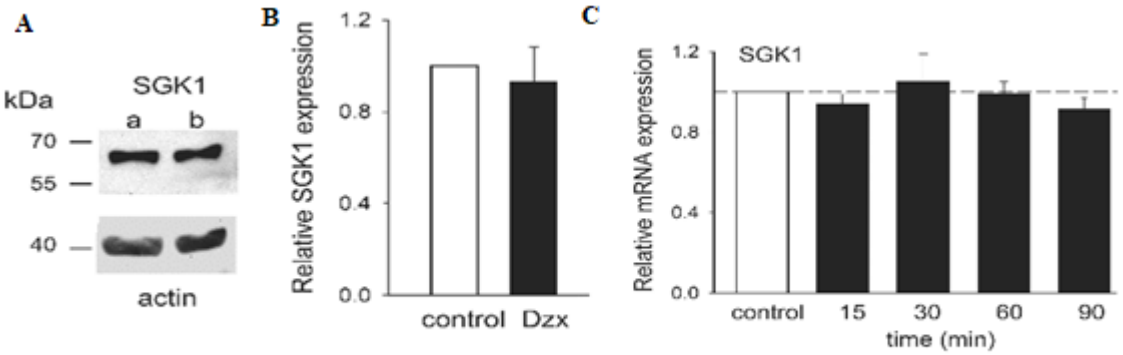

Figure 3.8. PPC has no effect on SGK 1. A: Representative western blots of SGK1 and actin of cytosolic fractions from control and Dzx-treated hearts. B: Mean values of normalized densities of SGK1 bands. Actin was used as a loading control in panel A. C: Mean relative values (± SEM, n=4) of SGK1 mRNA from cardiomyocytes at the indicated incubation times in Dzx.

3.9. Increased STIM1 protein levels produced by de novo protein synthesis

The possibility that PPC increases the abundance of STIM1 proteins by *de novo* synthesis was further supported by experiments done with the protein synthesis inhibitor, CHX. Fig. 9*A* shows representative western blots of STIM1 and actin from cardiomyocytes under the experimental conditions described in the legend. The increase in STIM1 protein expression by PPC was blocked in part by CHX, which by itself had negligible effects on STIM1 abundance. Fig. 9*B* shows summarized results from several experiments as in A. CHX also blocked the changes in the distribution pattern of STIM1 produced by PPC. Fig. 9*C* shows representative confocal images of cardiomyocytes incubated under the experimental conditions indicated above panels. Enlarged images of selected areas of the same cardiomyocytes (yellow boxes) are illustrated in the lower panels. The change in the distribution pattern of STIM1 produced by PPC was prevented by CHX, which by itself had no effect on the distribution pattern.

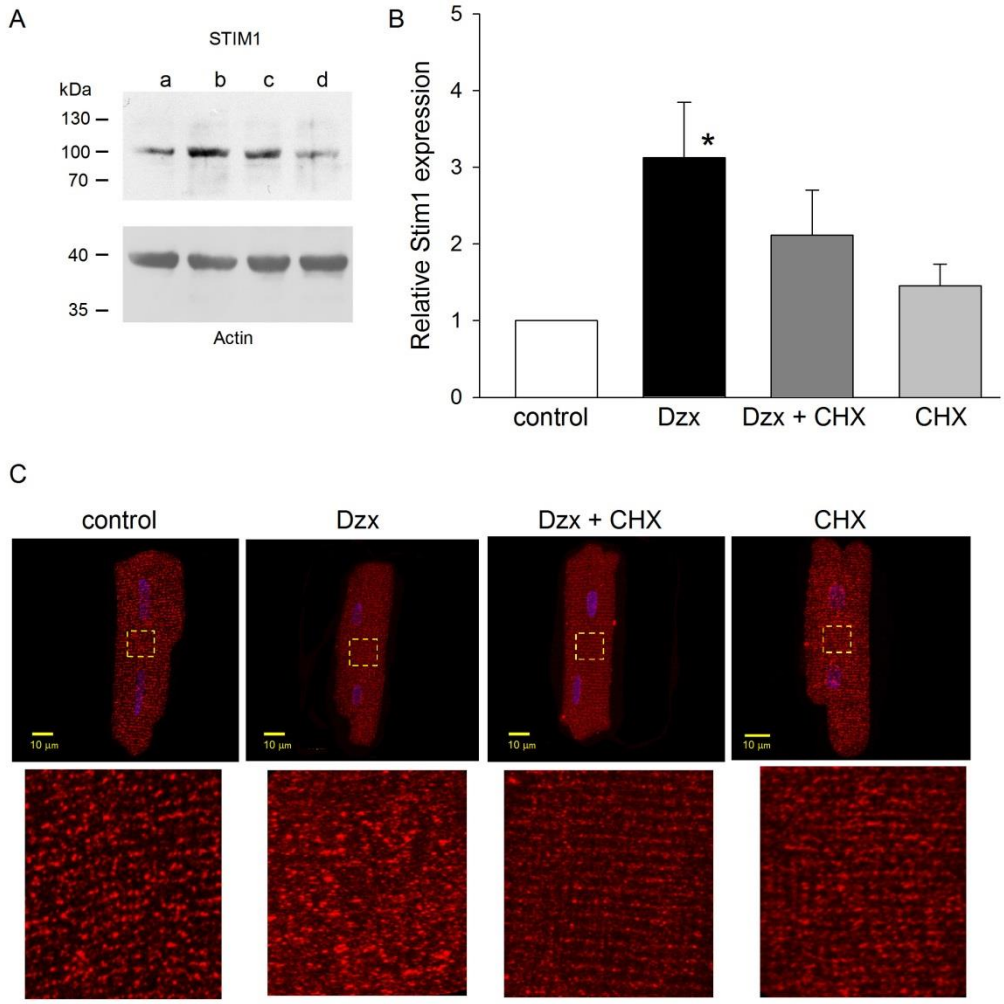

Figure 3.9. The effect of PPC on STIM1expression and localization is prevented by CHX. A: Representative western blots of STIM1 and actin from myocytes incubated under the following experimental conditions: lane a, control; lane b:Dzx, lane c: Dzx + CHX; lane d: CHX. B: Mean values of normalized densities of STIM11 bands (± SEM, n=6-10). Actin was used as a loading control. *$p<0.05$. C: Upper panels, confocal microscopy images of myocytes under the experimental conditions indicated above panels. Images show localization of STIM1 (red) with DAPI-labeled nuclei (blue). Calibration bars: 10 μm. Lower panels are enlargements of the corresponding yellow boxed areas.

3.10. Increased STIM1 protein levels produced by de novo protein synthesis

The effect of CHX on upregulation of Orai1 protein by PPC was investigated next. Figure 10 *A* shows representative immunoblots of Orai1 and actin under the experimental conditions described in the legend. PPC increased the density of the band corresponding to Orai1, an effect that was completely prevented by CHX. CHX by itself had negligible effects on Orai1 abundance. Actin was used as a loading control to normalize the values of Orai1 band densities. Results from several experiments as in Fig. 10*A* are summarized in the graph of Fig. 10*B.* Illustrated are mean values (±SEM) of the relative expression of Orai1. PPC had no effect on Orai1 abundance in the presence of CHX, confirming the hypothesis that the increase in the expression of Orai1 by PPC is related to *de novo* protein synthesis As expected from the western blot results, confocal microscopy revealed that CHX prevented the effects of PPC.

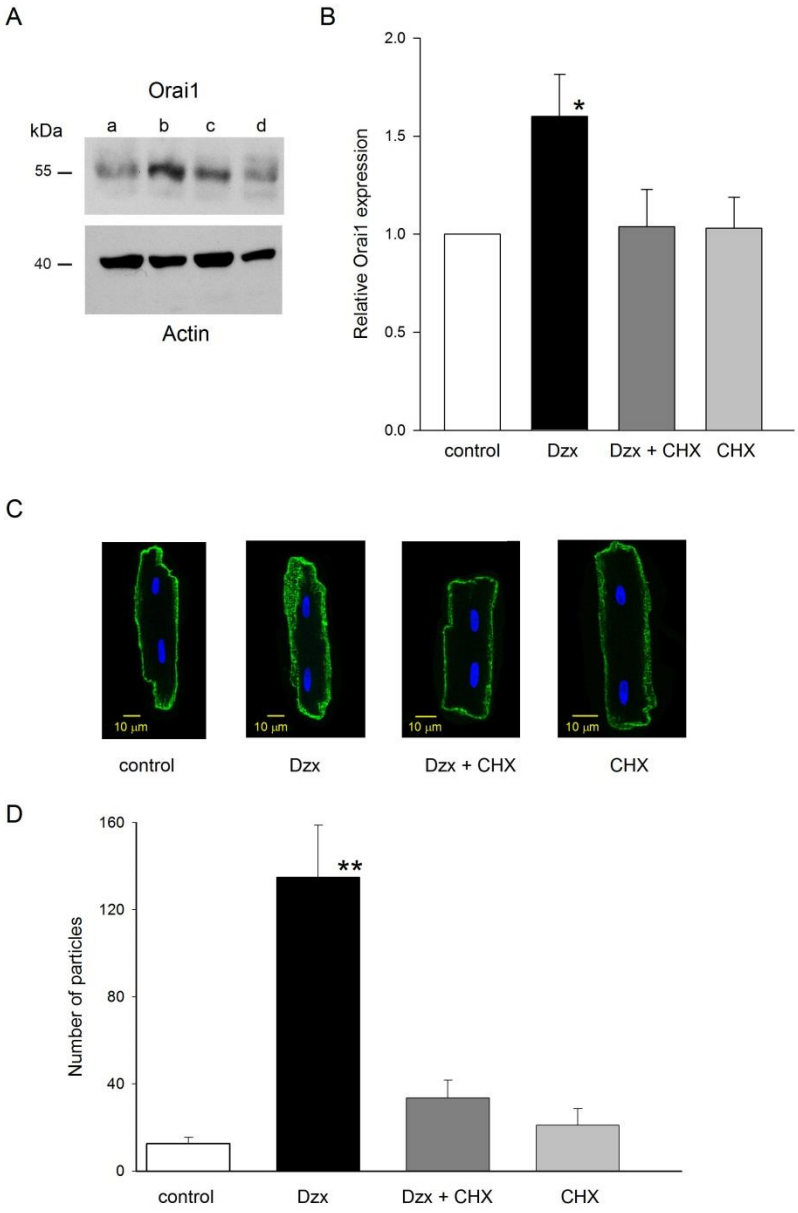

Figure 3.10. The effect of PPC on Orai1expression is prevented by CHX. A: Representative western blots of Orai1 and actin from myocytes incubated under the following experimental conditions: lane a, control; lane b:Dzx, lane c: Dzx + CHX; lane d: CHX. B: Mean values of normalized densities of Orai1 bands (± SEM, n=4). Actin was used as a loading control. C: Confocal microscopy images of myocytes under the experimental conditions indicated below panels. Images show localization of Orai1 (green) with DAPI-labeled nuclei (blue). Calibration bars: 10 µm. D: Mean values (± SEM, n=10) of number of particles under the indicated experimental conditions from experiments as in C.** $p<0.01$. *$p<0.05$.

3.11. PPC increases the mRNA expression of STIM1 and Orai1

Based on the results of cycloheximide, we speculated that PPC increases the mRNA expression of STIM1 and Orai1. To test this possibility, the time course of the expression levels of mRNA of STIM1 and Orai1 from cardiomyocytes incubated in Dzx was measured with the qRT-PCR technique. We found a significant increase in the levels of STIM1 and Orai1 mRNA after preincubation with Dzx for 15 min. As shown in Figure 11*A-B*, overexpression of both messengers was transient and mRNA levels decreased below control values after 60 min of Dzx preincubation.

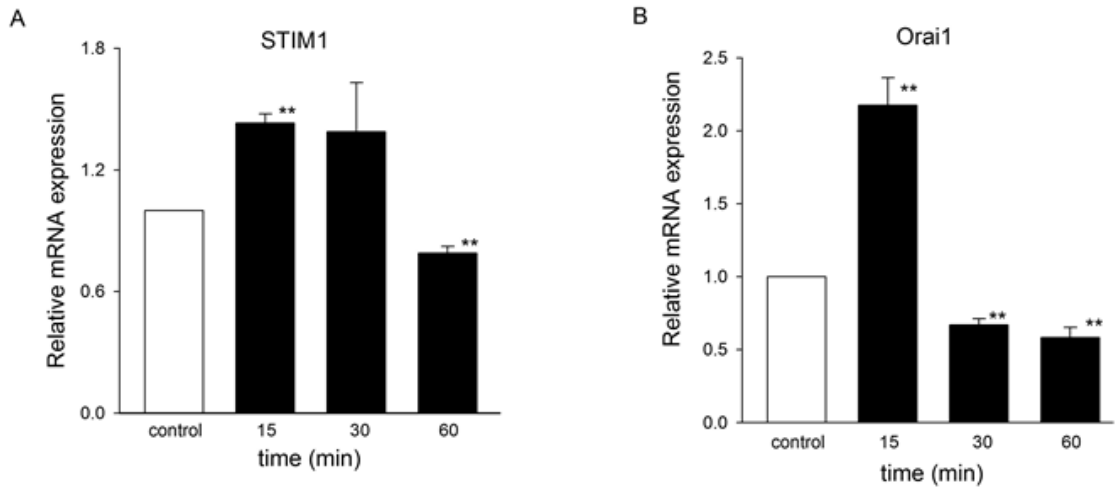

Figure 3.11. PPC increases the expression of STIM1 and Orai1 mRNA. A-B: Mean relative values (± SEM, n=9-11) of STIM1 and Orai1 mRNA expression from cardiomyocytes incubated in Dzx at the indicated times (filled bars). **p<0.01.

3.12. Regulation of Orai1 and STIM1 expression by PPC are mediated by the MAPK/ERK pathway

We made the hypothesis that the MAPK (mitogen-activated protein kinases) /ERK pathway is involved in upregulation of Orai1 and STIM1 proteins by PPC. To test this hypothesis, we performed western blot experiments to detect possible changes in the abundance of pERK. Figure 12*A* shows representative western blots of pERK and actin under the experimental

conditions indicated in the legend. The density of the pERK band increased by PPC and this effect was prevented by the MAPK/ERK inhibitor UO126 which by itself decreased pERK abundance below the control level. The expression of actin remained unchanged in all treatments and was used to normalize the density values of pERK bands. Results from several experimental replicates are summarized in Fig. 12*B*, confirming that pERK expression significantly increased by PPC.

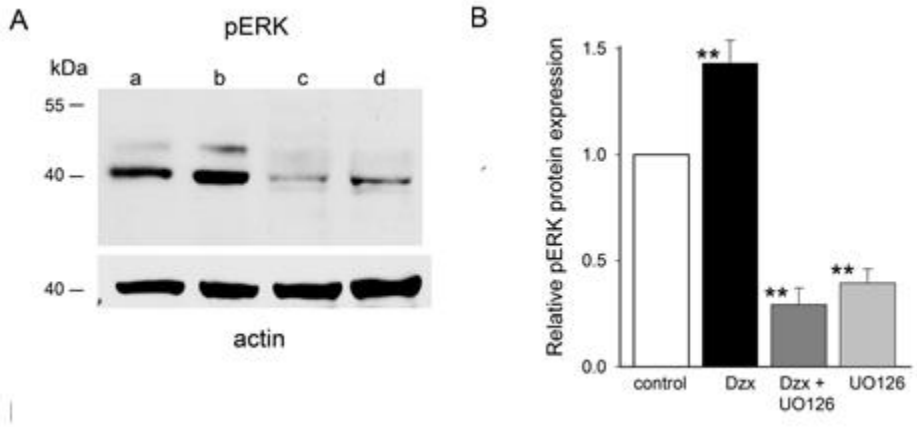

Figure 3.12. PPC upregulates pERK. A: Upper panels, representative western blots of pERK of membrane fractions from whole ventricle extracts. Lane a, control; lane b, Dzx; lane c, Dzx + UO126; lane d, UO126. Lower panels, the corresponding blots of actin used as loading controls. B: Mean values (± SEM, n=4-8) of normalized densities of pERK bands under the same conditions as in A.

3.13. Regulation of Orai1 and STIM1 expression by PPC are mediated by the MAPK/ERK pathway is through ROS

In other systems phosphorylation of ERK is mediated by an increase in mitochondrial ROS production that follows the opening of mitoKATP channels (Samavati et al., 2002). To assess whether this also holds true for cardiomyocytes, the abundance of pERK was measured in western blot experiments in lysates from total fractions of cardiomyocytes preincubated with 5-HD or NAC. Fig. 13*A* shows representative western blots under the experimental conditions

indicated in the legend. Preincubation with Dzx increased the density of the pERK band, as described in (Fig. 12*A*-*B*) while in the presence of Dzx and 5-HD or Dzx and NAC, no such changes were observed (Fig. 13*A*). 5-HD and NAC by themselves had negligible effects on the expression of pERK. The graph in Fig. 13 B summarizes results from several experimental replicates as in *A*. The density values of pERK were normalized by the densities of the GAPDH bands that did not change by the treatments and were used as standard.

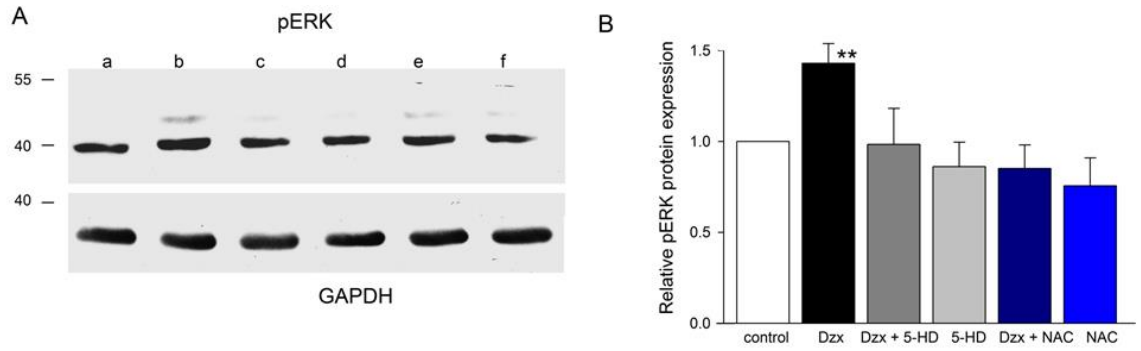

Figure 3.13. PPC upregulates pERK through ROS.A: representative western blots of pERK and GAPDH. Lane a, control; lane b, Dzx; lane c, DZX + 5-HD; lane d, 5-HD; lane e, DZX + NAC; lane f, NAC. B: The graph shows mean values (±SEM, n=4-8) of the relative expression of pERK under the indicated experimental conditions. ** $p<0.01$.

3.14. Regulation of STIM1 by PPC is mediated by the MAPK/ERK pathway

The possibility that MAPK/ERK pathway is involved in up-regulation of STIM1 was checked by using MAPK/ERK inhibitor UO126. Preincubation in Dzx increased STIM1 expression (lane b) compared to the control (lane a) and this increase was blocked by UO126 (lane c) while the inhibitor had little effect on STIM1 expression by itself (lane d). Fig. 14*B* summarizes

results from several experimental replicates confirming the role of the pERK/MAPK pathway on STIM1 expression.

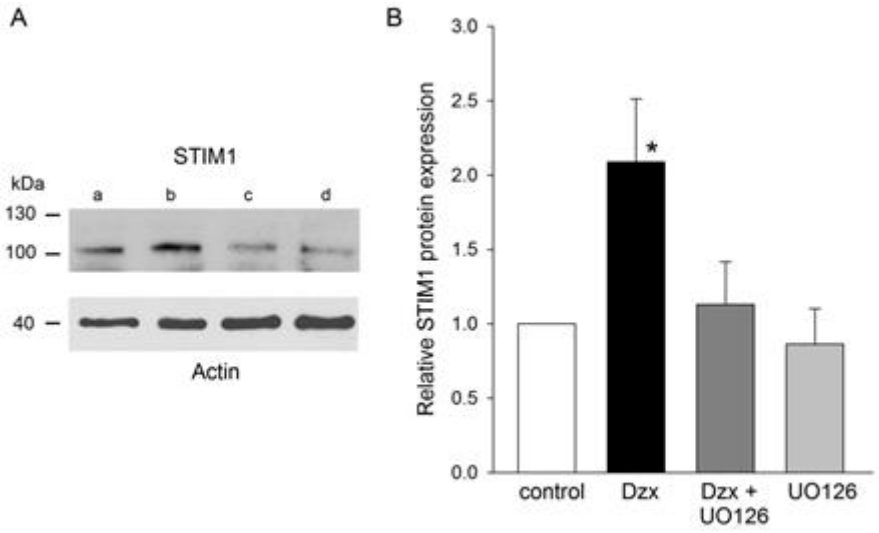

Figure 3.14. The MAPK/pERK pathway is involved in upregulation of STIM1 by PPC. A: Representative western blots of STIM1 and actin. Lane a, control; lane b, Dzx; lane c, Dzx + UO126: lane d, UO126. B: Mean values (±SEM, n=4-8) of the relative expression of STIM1 under experimental conditions as in A.

3.15. Regulation of Orai 1 by PPC is mediated by the MAPK/ERK pathway

The possibility that MAPK/ERK pathway is involved in up-regulation of Orai 1 was checked by using MAPK/ERK inhibitor UO126. Preincubation in Dzx increased Orai 1 expression (lane b) compared to the control (lane a) and up-regulation of Orai1 expression by PPC was completely abrogated by UO126 (lane c).

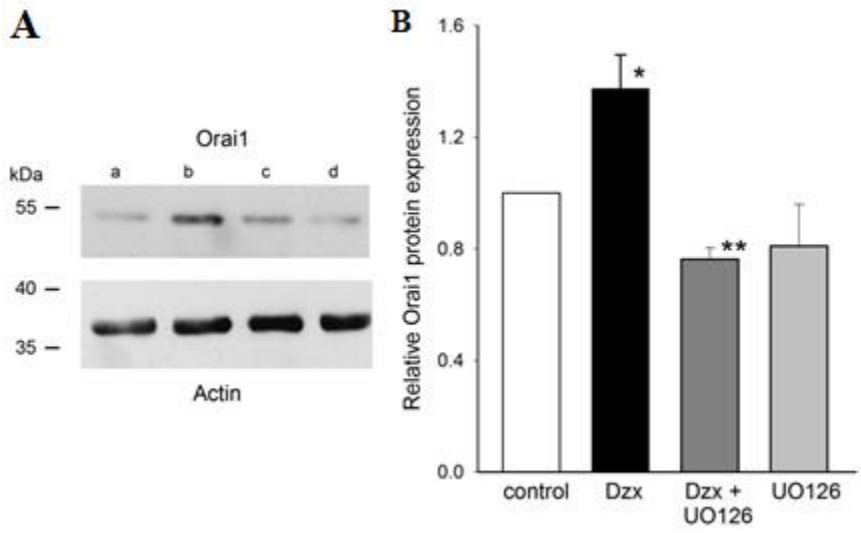

Figure 3.15. The MAPK/pERK pathway is involved in upregulation of Orai 1 by PPC. A: Representative western blots of Orai1 and actin. Lane a, control; lane b, Dzx; lane c, Dzx + UO126: lane d, UO126. D: Mean values (±SEM, n=4-8) of the relative expression of Orai1under the indicated experimental conditions* $p<0.05$, **$p<0.01$.

3.16. Regulation of STIM1 and Orai 1 distribution pattern by PPC are mediated by the MAPK/ERK pathway through ROS

Confocal microscopy experiments also suggested the involvement of the pERK/MAPK pathway in the changes of the distribution pattern of STIM1 by PPC. Figure 16*A* shows representative confocal images of STIM1 under the experimental conditions described above images. UO126 completely suppressed the changes in the distribution pattern produced by Dzx as illustrated in the enlarged segments (yellow boxes) of the images. Likewise, UO126 also blocked overexpression of Orai1 by Dzx along the surface membrane of cardiomyocytes as shown in Fig. 16*B*. This was confirmed by evaluating the number of particles under each experimental condition as summarized in the graph shown in Fig. 16*C*.

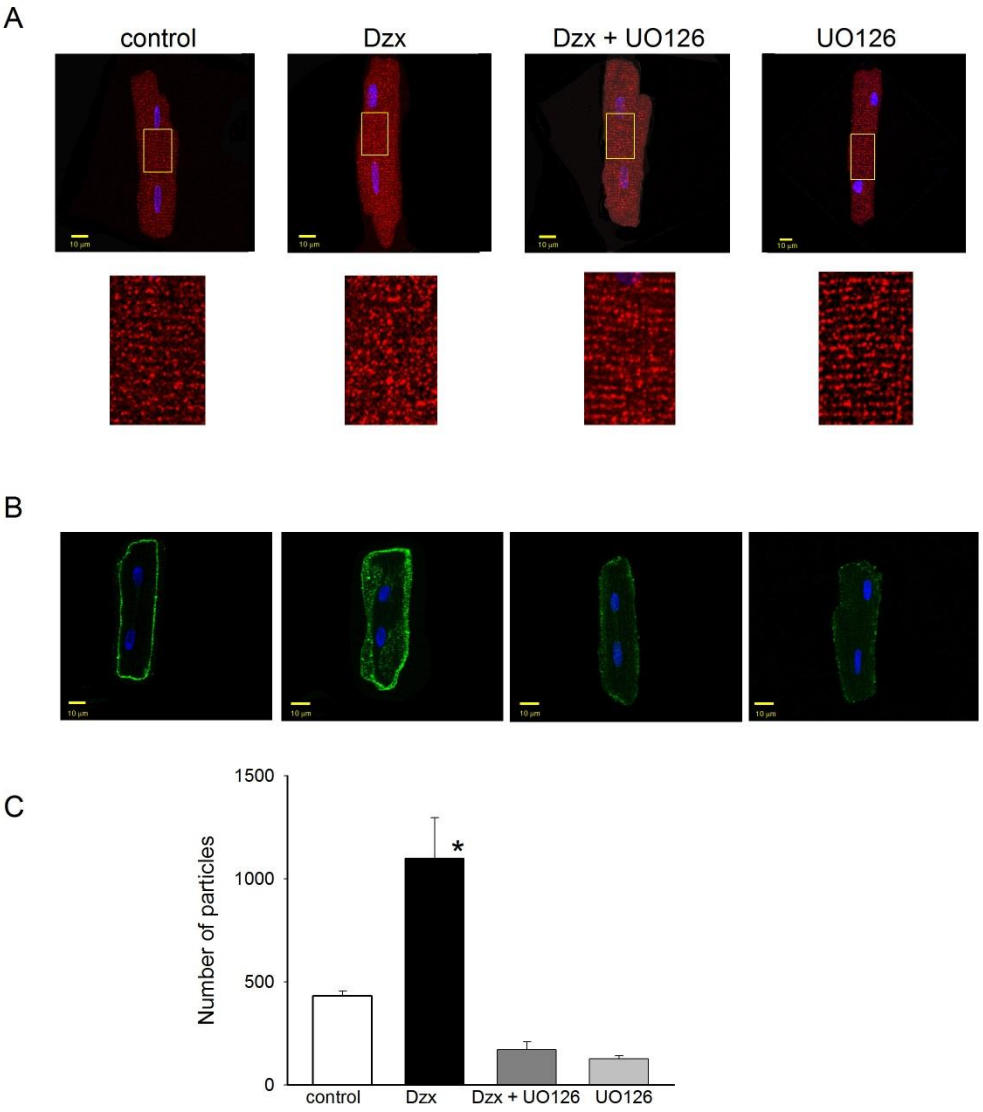

Figure 3.16. Role of the MAPK/pERK pathway on changes in STIM1 localization pattern and upregulation of Orai1 by PPC. A: Upper panels: Confocal microscopy images of myocytes under the indicated experimental conditions. Images show localization of STIM1 (red) with DAPI-labeled nuclei (blue). Calibration bars: 10 μm. Lower panels, amplification of the corresponding yellow boxed areas. B: Representative confocal images of cardiomyocytes under conditions as in A. Images show localization of Orai1 (green) with DAPI-labeled nuclei (blue). C: The graph shows the mean (±SEM, n=5-6) number of particles of Orai1 from confocal images as in B. * $p<0.05$.

3.17. PPC induces translocation of transcription factors NFkB and c-Fos into the nucleus

The possibility that changes in the expression of SOCE components by PPC depend NFkB and c-Fos transcription factors was investigated next. We found that after 15-60 min preincubation in Dzx both factors were translocated to the nucleus by PPC, as illustrated in the representative confocal images shown in **Figure 17*A*-*B***. Similar results were obtained in two separate experimental replicates.

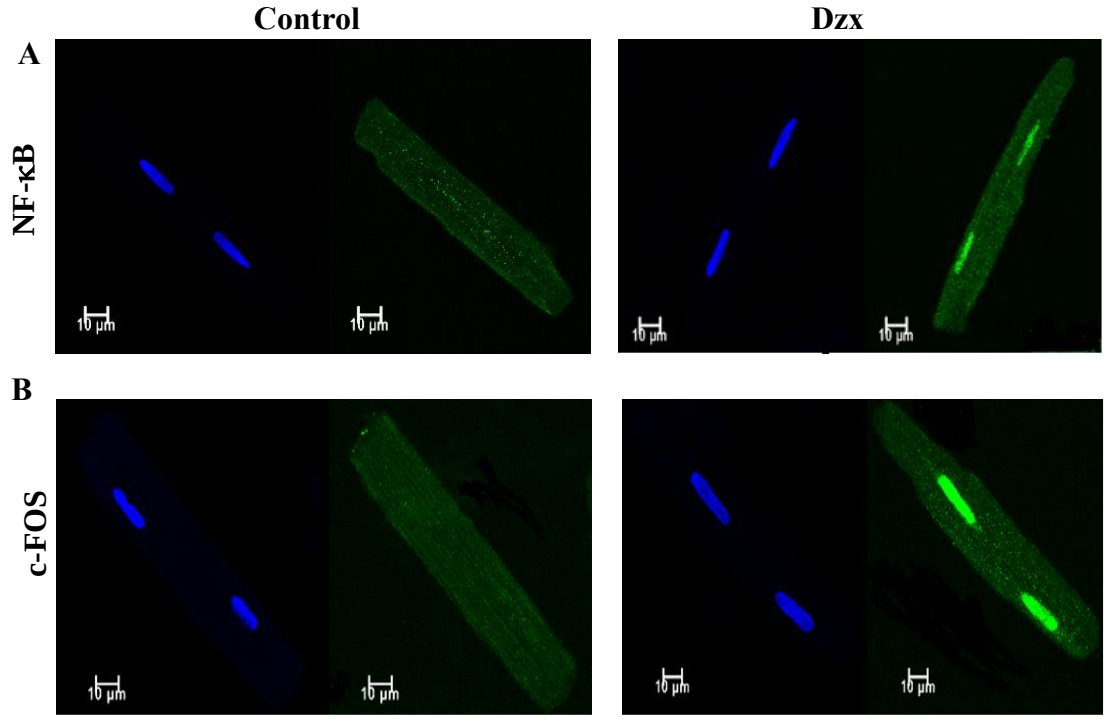

Figure 3.17. PPC induces translocation of transcription factors NFkB and c-Fos into the nucleus. A: Confocal microscopy images of myocytes under the experimental conditions indicated above panels. Images show localization of NFkB (green) with DAPI-labeled nuclei (blue). B: Representative confocal images of cardiomyocytes under conditions as in A. Images show localization of c-Fos (green) with DAPI-labeled nuclei (blue). Calibration bars: 10 μm.

3.18. Translocation of NFκB and c-Fos into the nucleus by PPC is mediated by ROS

To check the possibility that ROS is involved in translocation of both transcription factors into the nucleus by PPC was checked by using ROS scavenger NAC and found that translocation of NFκB and c-Fos was completely blocked by NAC, suggesting the involvement of ROS. Similar results were obtained in two separate experimental replicates.

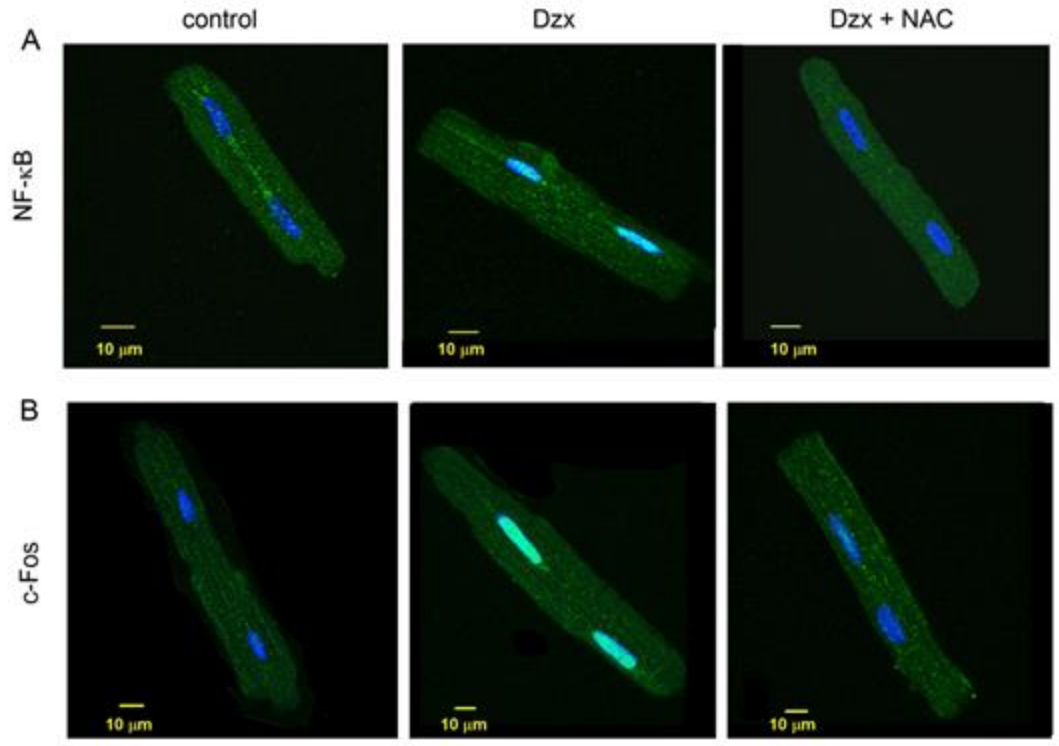

Figure 18. PPC induced translocation of transcription factors NFκB and c-Fos into the nucleus is mediated by ROS. A: Confocal microscopy images of myocytes under the experimental conditions indicated above panels. Images show localization of NFκB (green) with DAPI-labeled nuclei (blue). B: Representative confocal images of cardiomyocytes under conditions as in A. Images show localization of c-Fos (green) with DAPI-labeled nuclei (blue). Calibration bars: 10 μm

3.19. Translocation of NFκB and c-Fos into the nucleus by PPC is via MAPK/ERK pathway

The possibility that MAPK/ERK pathway is involved in the translocation of transcription factors NFκB and c-Fos into the nucleus was checked by using MAPK/ERK inhibitor UO126. We found that after 15-60 min preincubation in Dzx both factors were translocated to the nucleus by PPC and the translocation was completely blocked by UO126 , suggesting the involvement of MAPK/ERK pathway. Similar results were obtained in two separate experimental replicates.

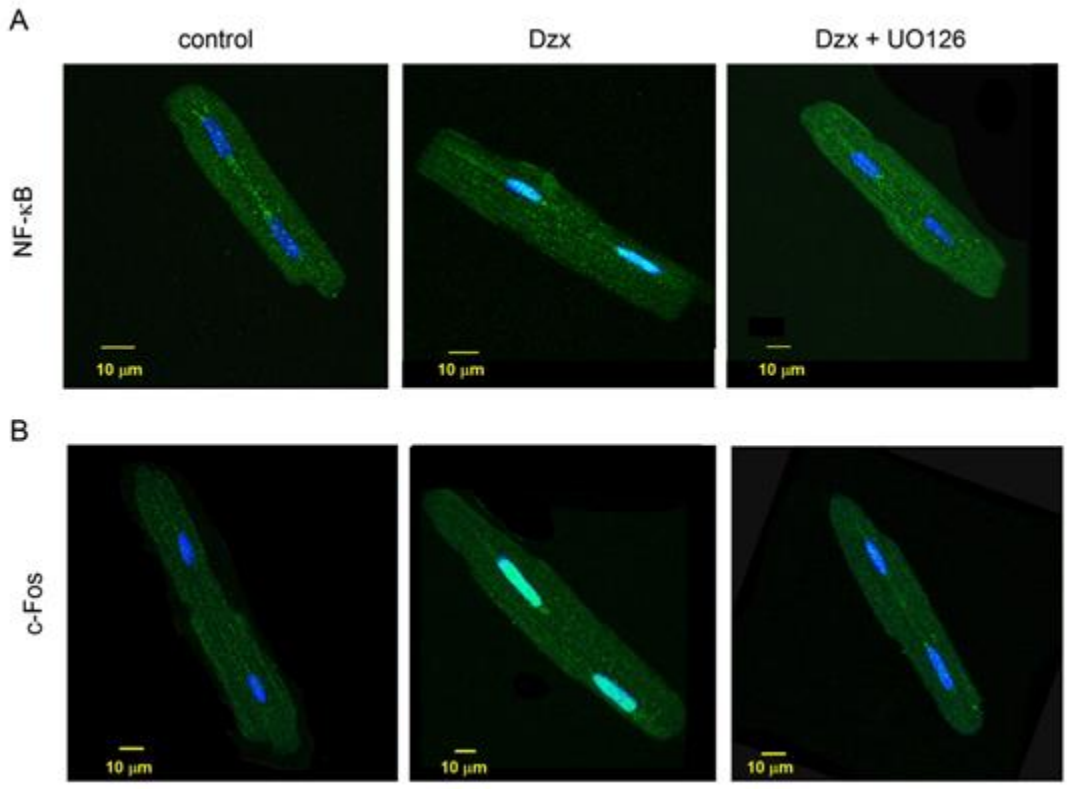

Figure 19. that MAPK/ERK pathway is involved in the translocation of transcription factors NFκB and c-Fos into the nucleus. A: Confocal microscopy images of myocytes under the experimental conditions indicated above panels. Images show localization of NFκB (green) with DAPI-labeled nuclei (blue). B: Representative confocal images of cardiomyocytes under

conditions as in A. Images show localization of c-Fos (green) with DAPI-labeled nuclei (blue). Calibration bars: 10 μm.

4. DISCUSSION

4.1. Up-regulation of Stim 1 and Orai1 by PPC

In the present work we present the novel observation that both protein components of SOCE, stim 1 and Orai1, are upregulated by PPC. We also demonstrated for the first time in adult cardiomyocytes that Stim 1 and Orai1 expression are upregulated by ROS through the MAPK pathway. Upregulation of these two proteins was shown to be dependent upon *de novo* synthesis, as evidenced by the associated changes in the expression of their mRNA and protein abundance, with the protein synthesis inhibitor CHX (Rivera-Pagán et al.,2015) preventing upregulation of Stim 1 and Orai1. Moreover, we found no evidence that protein degradation pathway play an active role in upregulation of Stim 1 and Orai regulation. Orai1 is a target of Nedd4-2, a ubiquitin ligase which prepares several plasma membrane proteins for degradation. STIM is similarly regulated by ubiquitination (Keil *et al.,*2010). Phosphorylation of Nedd4-2 by the SGK1(serum and glucocorticoid regulated kinase 1) leads to binding of Nedd4-2 to the protein 14-3-3 thus preventing its interaction with Orai1 (Lang *et al.,* 2012). In the present work we found no changes in the expression of SGK1 in PPC. Rivera-Pagán et al in 2015 demonstrated that the increase of TREK-2 protein expression requires De novo protein synthesis, while protein degradation pathways do not contribute to TREK-2 up-regulation after ischemic conditions.

4.2. The effect ROS on up-regulation of Stim 1 and Orai1

PPC-cardioprotection is mediated by mitochondrial ROS whose production increases by opening mitoKATP channels with drugs like Dzx (Garlid et al., 1997; Pain et al., 2000; Gonzalez, 2010). Dzx is known to increase the rate of mitochondrial production of ROS

(Forbes et al., 2001; Oldenburg et al., 2003; Pasdois et al., 2008; Gonzalez et al., 2010). Gonzalez et al. (2010) described that down-regulation of Cav1.2 channels is mediated by ROS and in the present study we found that opening of mitoKATP channels and ROS production are also required for overexpression of SOCE components since we observed that the specific blocker 5-HD (Hu et al., 1999;Garid et al.,1997; McCullough et al.,1991) and the ROS scavenger NAC completely abrogated the increase in Stim 1 and Orai1 protein expression by PPC. Previous study done in adult rat cardiomyocytes has shown that 5-HD inhibits cardiac ATP sensitive potassium channels. The open probability of the channel was reduced in the presence of 5-HD by suggesting that 5-HD is specific blocker of ATP sensitive potassium channel (McCullough et al.,1991). Several studies have shown that the 5-HD completely antagonized the effect of diazoxide (Hu et al., 1999; Garid et al.,1997; Gonzalez et al.,2010). We also found changes in the localization pattern of Stim 1 by PPC and previous observations in human osteosarcoma cells under hypoxia revealed translocation of Stim 1 to plasma membrane junctions in a ROS dependent manner (Mungai et al., 2011).

4.3. Upregulation of STIM1 and Orai1 by PPC involves ROS activation of the MAPK signaling pathway

ROS are important signaling molecules for activation of MAPKs. Several studies have demonstrated that ROS can induce activation of MAPK pathways. (Bae et al., 1997; Guyton et al., 1996; Sundaresan et al., 1995). The prevention of ROS by antioxidants also blocks MAPK activation indicating the involvement of ROS in activation of MAPK pathways (Guyton et al., 1996). Samavati et al in 2002 demonstrate that diazoxide can activate the ERK MAPK in THP-1 cells and this activation was inhibited in cells pretreated with the oxygen radical scavenger NAC indicating the role of ROS in activation of MAPK pathway.

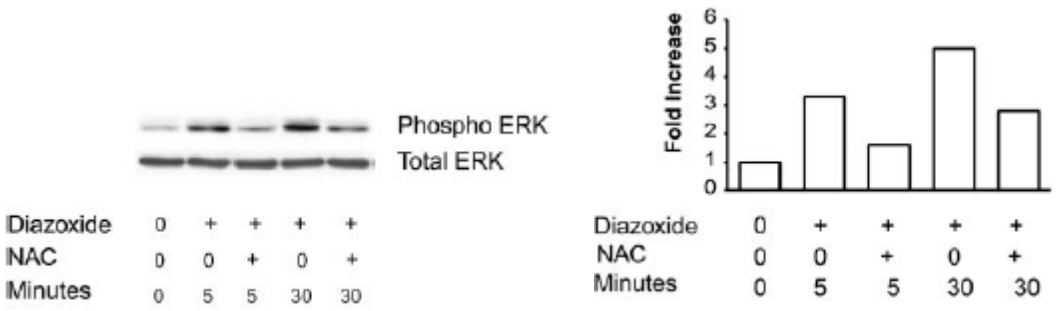

Figure 4.3.1. *N*-acetylcysteine (NAC) attenuates ERK activation mediated by diazoxide. Cells were preincubated for 90 min with 30 mM NAC. After 90 min, 100 µM diazoxide was added for indicated times.

The activation of ERK is associated with cell survival and cell proliferation in response to growth factors (Seger and Krebs, 1995). In non-excitable cells depletion of intracellular Ca^{2+} stores by the SERCA inhibitor thapsigargin results in a time and concentration dependent activation of ERK (Rosado and Sage, 2001) and opening of mitoKATP channels with Dzx increases phosphorylation of ERK (Samavati et al., 2002). Involvement of ROS in MAPK activation during PPC of cardiomyocytes is supported by several observations. Firstly, phosphorylation of ERK increased following PPC, an effect that was blocked by 5-HD and NAC in the present study (Fig 13). Secondly, we found that PPC-induced overexpression of Stim 1 and Orai1 was blocked by UO126, a MAPK pathway inhibitor. Several studies have demonstrated that UO126 is a specific blocker of MAPK (Hotokezaka et al.,2002; Planz et al.,2001; Namura et al.,2001). Consistent with our observations, it has been reported that the opening of mKATP channels with Dzx increases phosphorylation of ERK in human monocytic cells (Samavati et al., 2002). ROS are activated by various stresses and prevented by intracellular antioxidants. When ROS production exceeds the capacity of the antioxidants, induces oxidative modification of MAPK signaling proteins, thereby leading to MAPK

activation. Potentially, ROS could activate MAPK pathways by oxidative modifications of MAPK signaling proteins and/or by inactivation of MAPK phosphatases. (Son et al., 2011).

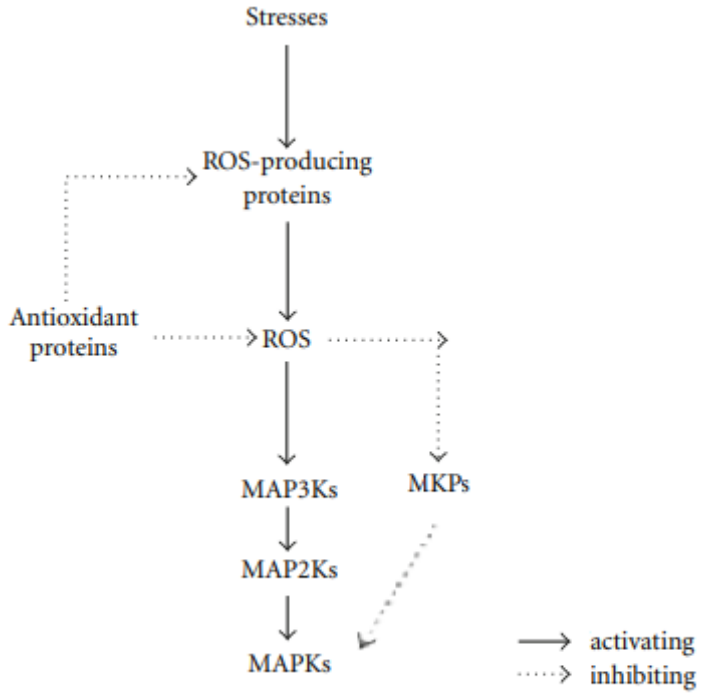

Figure 4.3.2. Mechanisms for ROS-mediated activation of MAPK pathways.

4.4. Upregulation of Stim 1 and Orai1 expression by PPC and SOCE

Upregulation of Stim 1 and Orai1 by PPC would be expected to be accompanied by an increase in SOCE. Previous study have demonstrated that mast cell activation is related to increased Ca2+ entry through SOCs. Ovalbumin stimulation increased intracellular ROS production in mast cells through activation of phosphoinositide 3-kinase (PI3K) pathway, which results in upregulation of the expression levels of Stim 1 and Orai 1, leading to increase in SOCE and subsequent mast cell activation (Yang et al.,2012)However, previous observations in cardiomyocytes showed a drastic decrease and not an increase in Ca^{2+} influx through SOCs in PPC cardiomyocytes. The reduction in Ca^{2+} influx by PPC was explained by ROS and Ca^{2+} dependent inactivation of Orai1 channels (Sampieri et al., 2019).

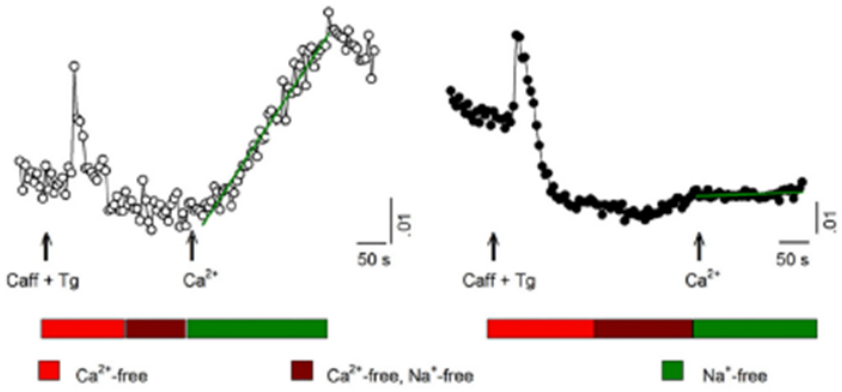

Figure 4.4.1. Decrease in Ca^{2+} influx through SOCs in PPC (Sampieri et al.,2019).

Our present results suggest that additional factors also contribute to a reduction in SOCE. For example, although PPC increased the expression of Stim 1, it completely disrupted its distribution pattern in the cardiomyocyte. Previous work has shown that the localization of Stim 1 resembles the distribution of the junctional SR along the Z-disk (Bonilla et al., 2019). We confirmed this distribution in control cardiomyocytes and found peaks of fluorescence evenly distributed along the longitudinal axis. Peaks were separated by a distance that is consistent with the sarcomere length. In PPC cardiomyocytes the number and size of particles associated to Stim 1 fluorescence increased but peaks of fluorescence were no longer regularly spaced. Furthermore, the stoichiometry between Orai1 and Stim 1 is critical for channel function. A ratio of 2 Stim 1s per 1 Orai1 is generally accepted (Hoover and Lewis, 2011; Yen and Lewis, 2019) and as evidenced by experiments in HEK cells, expressing Stim 1 and Orai1 at varying ratios results in a highly non-linear, bell-shaped relation between Orai1 expression and the amplitude of SOC currents in which currents peak at a ratio ~ 2 Stim 1 per 1 Orai1 (Fig.4.4.3) (Hoover and Lewis, 2011), leading to the paradoxical observation that increased Orai1 expression reduces SOCE (Yen and Lewis, 2019).

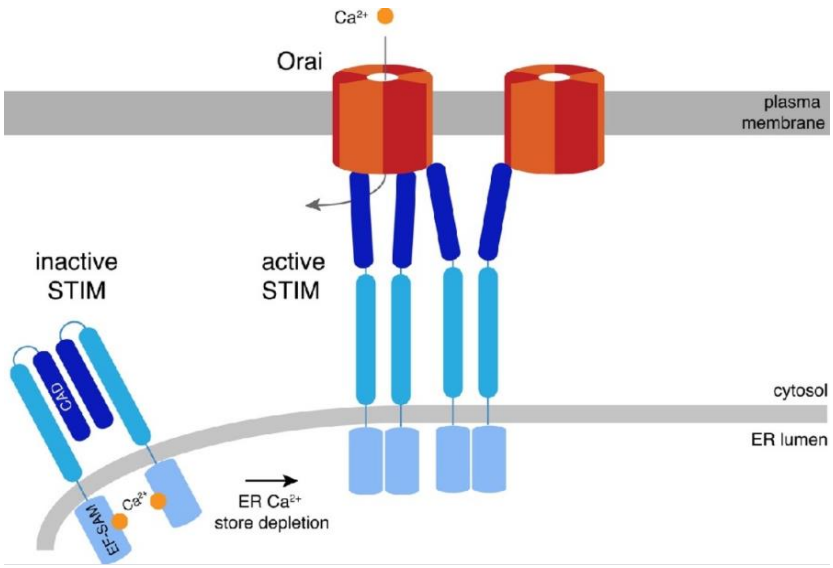

Figure 4.4.2. **STIM-Orai complex stoichiometry for the regulation of store-operated calcium entry:** Depletion of ER Ca^{2+} triggers STIM1 to accumulate at ER-plasma membrane junctions where it binds and activates SOCE. STIM1 is a dimer, and dissociation of Ca^{2+} from its two luminal domains associates STIM1 oligomerization. The CRAC channel is a hexamer of Orai1 subunits based on crystallographic and electrophysiological studies. STIM1 binding activates CRAC channels in a highly nonlinear way, such that all six Orai1 binding sites must be occupied to account for the activation. STIM1 dimers bind to individual or pairs of Orai1 subunits (Yen and Lewis, 2019).

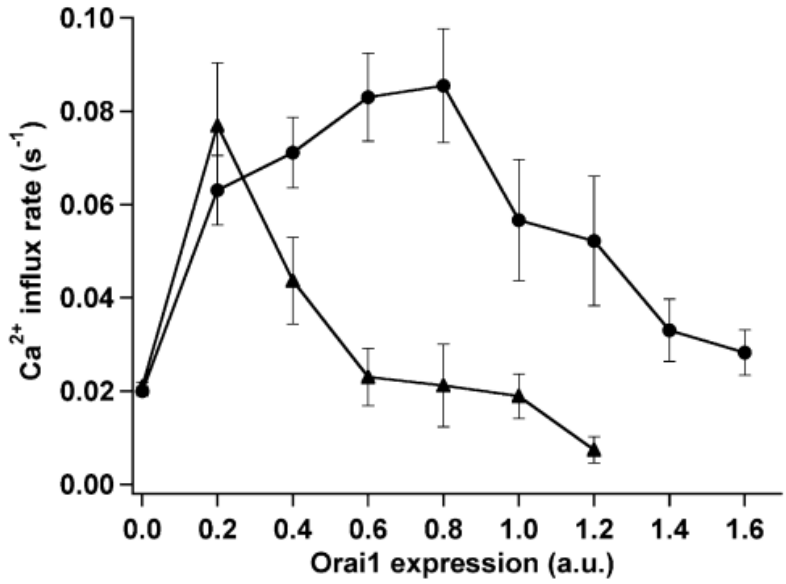

Figure 4.4.3. CRAC channel activity is a highly nonlinear function of Orai expression. Reduced level of STIM lowers the threshold for Orai-induced suppression of SOCE. After store depletion, Ca^{2+} influx rates were measured on Ca^{2+} readdition in cells with moderate (circles) or low (triangles) levels of mChSTIM.

This paradox has been explained by an excess of Orai1 competing for a limited number of Stim 1 proteins. Our western blot experiments showed that in PPC cardiomyocytes Stim 1 and Orai1 protein expression increased by a similar amount and therefore a deficit in the number of Stim 1 proteins would be expected. This would result in a deficient activation of Orai1 channels and therefore in a decrease of SOCE. A reduction in SOCE is likely beneficial under conditions of ischemic stress. The SR Ca^{2+} content is markedly depleted in intact hearts subjected to I/R (Valverde et al., 2010) which would be expected to be followed by activation of SOCE.

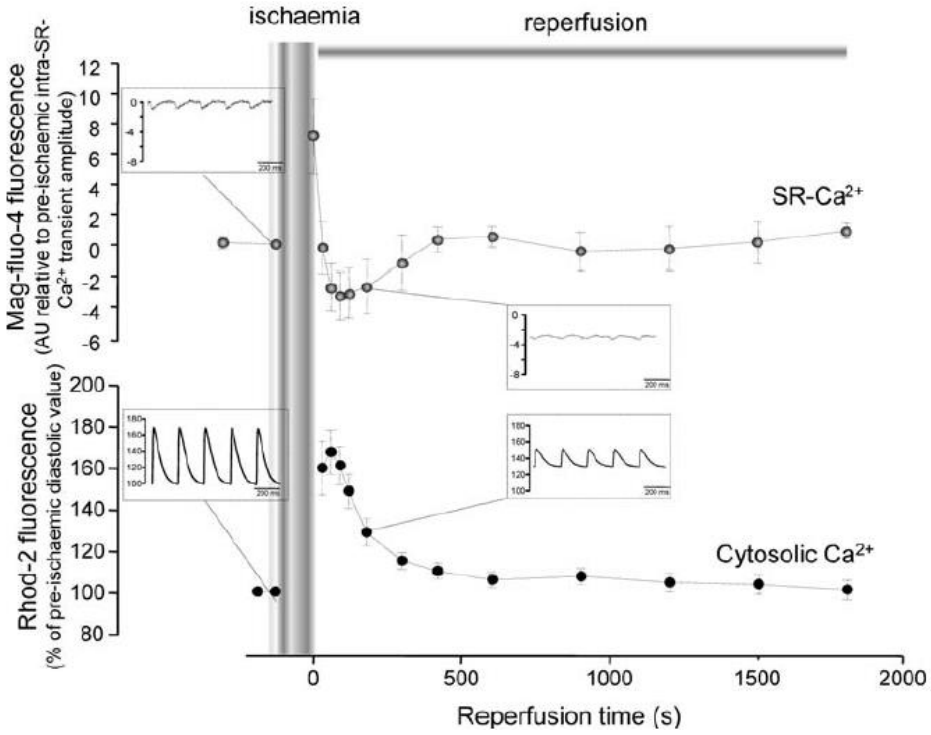

Figure 4.4.4. The increase in diastolic Ca^{2+} is the mirror-like image of the decrease in SR-Ca^{2+} content. Overall results of Mag-fluo-4 fluorescence (upper panel) in pre-ischaemia and

reperfusion. Results of Rhod-2 obtained in experiments from the same group (lower panel) are shown for comparison. Changes in diastolic level of Rhod-2 fluorescence are expressed as percentage of the pre-ischaemic diastolic value. As shown, the recovery profile of SR- Ca^{2+} (Mag-fluo-4) was a mirror-like image of cytosolic Ca^{2+} (Rhod-2) (Valverde et al., 2010).

A decrease in SOCE by PPC would mitigate the drastic increase in cytosolic Ca^{2+} caused by ischemia that is associated to cell death allowing protection of the heart from ischemic insults.

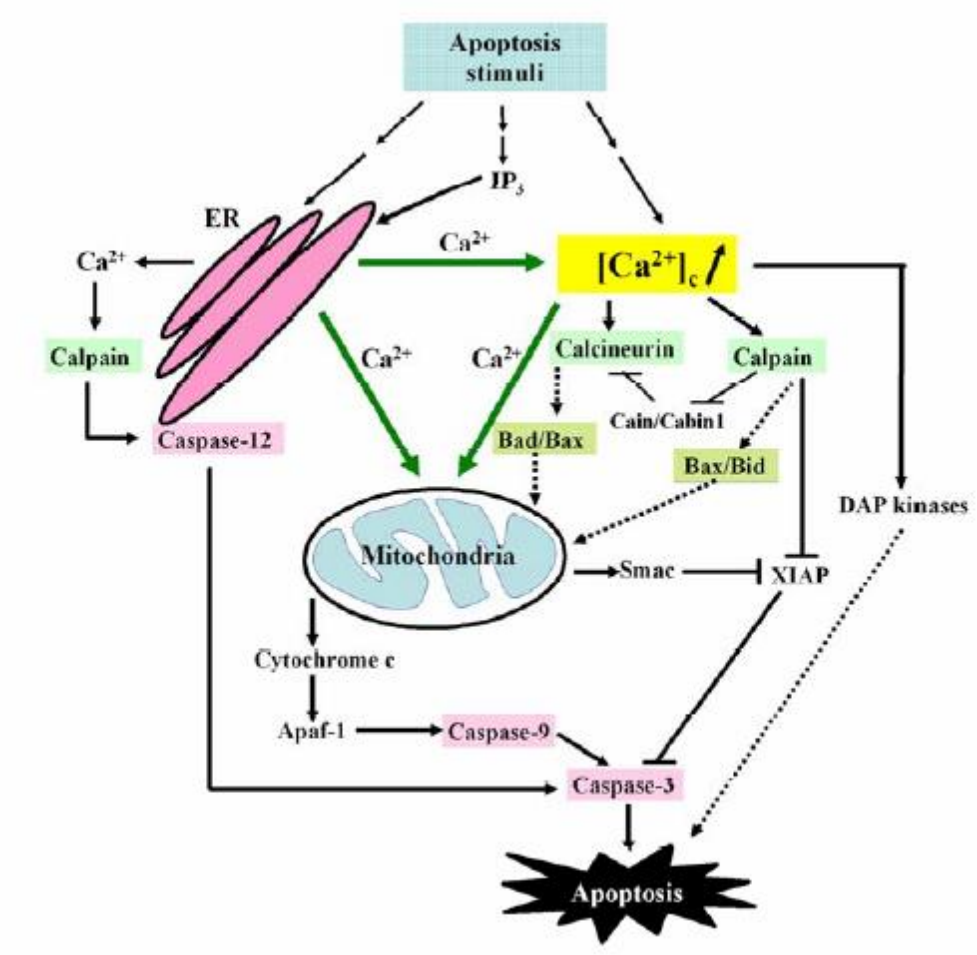

Figure 4.4.5. The mechanisms of Ca^{2+} signaling in regulating cell death. Upon apoptotic stimulation, an increase of Ca^{2+} in the cytosol is generated via Ca^{2+} release from the ER or Ca^{2+} influxes from the extracellular medium. These excessive Ca^{2+} ions then bind to Ca^{2+} dependent enzymes, such as calpain and calcineurin, by activating their downstream targets including the Bcl-2 family proteins. Alternatively, the released Ca^{2+} is directly taken up by mitochondria

through mitochondrial Ca^{2+} uniporter (MCU). Mitochondrial overload with Ca^{2+} releases cytochrome c into cytosol. All these events lead to apoptosis. (Guo et al., 2005)

4.5. Role of NFκB in upregulation and ROS of Stim 1 and Orai1 expression

Several lines of evidence suggest that the increase in expression of Stim 1 and Orai1 by PPC involves the protein complex NFκB. Firstly, our experiments demonstrated translocation of this nuclear factor into the nuclei of PPC cardiomyocytes and both translocation and upregulation of Stim 1 and Orai1 were related to ROS elevations since they were blocked by NAC. Second, Promoter region of Orai 1 has binding sites for several transcription factors such as Pax-4a, c-Rel, CUTL1, FOXO1, RelA, NFκB, and RSRFC4 whereas Stim1 has AP-1, NFκB, SRF, c-Fos, c-Jun, hepatic nuclear factor 1 (HNF1), and POU2F1.Among the several regulators of Stim 1 and Orai1 expression, NFκB is common to both. (Niemeyer, 2016).Work done in mast cells and heterologous expression systems has demonstrated binding of NFκB to specific sites of the promoter regions of STIM1 and Orai1 genes increasing transcription. Inhibition of the NFκB by Wogonin or silencing of NFκB subunits p65, p50, or p52 decreased Stim 1 and Orai1 at mRNA level while overexpression of NFκB increased Stim 1 and Orai1 mRNA (Eylenstein et al., 2012).

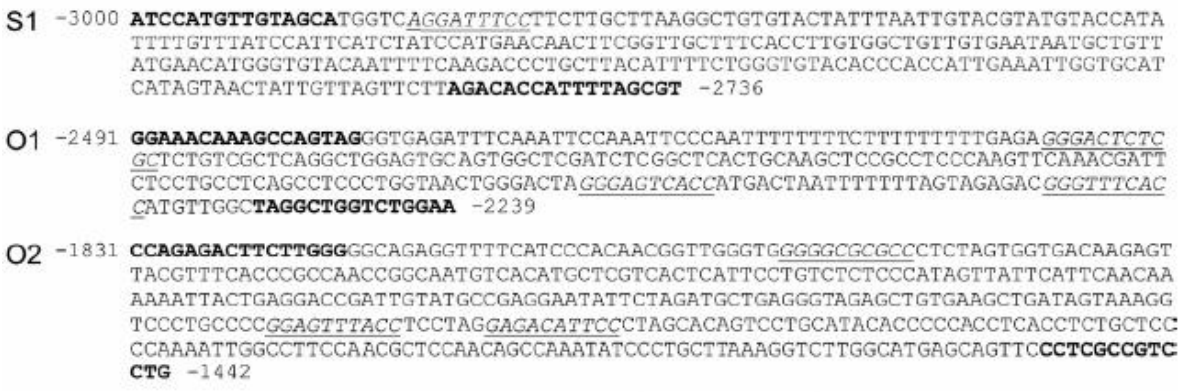

Figure 4.5.1. NFκB binding sites to the promoter region of Stim 1 and Orai 1. analysis of

the DNA sequence of STIM1 transcriptional start site (S1) and Orai1 transcriptional start site (O1 and O2) revealed putative NFκB binding sites (*italic*, *underlined*) is shown.

Although the targets of ROS remained to be identified, several possibilities may be suggested. It has been previously demonstrated in non-excitable cells that ROS activate SGK1 (Eylenstein et al., 2012). This enzyme is located upstream of NFκB (Kobayashi and Cohen, 1999; Prasad et al., 2000) and is expressed in adult cardiomyocytes (Kobayashi et al., 1999). However, it has been recently demonstrated that glucocorticoid stimulation increases SGK1-dependent SOCE activation but decreases mRNA expression of Orai1 in rat cardiomyocytes (Wester et al., 2019), while in our present experiments we observed a ROS-dependent upregulation of Orai1 mRNA in PPC cardiomyocytes. Other alternatives to explain the action of ROS on translocation of NFκB include:1.Activation of NFκB by oxidation (Oeckinghaus and Ghosh, 2009). Micromolar amounts of hydrogen peroxide were found to activate NFκB in lurkat T cells and HeLa cells whereas variety of antioxidative have been reported to potently suppress the activation of NFkB (Schreck et al.,1991). 2. The interaction of ROS with NFκB at several locations within the signaling pathway(Morgan and Liu, 2011). A distinct redox regulation of NFκB between cytoplasm and nucleus have been reported. ROS stimulates the NFκB pathway in the cytoplasm whereas it inhibits NFκB activity in the nucleus. ROS can be involved in both the activation and the inhibition of NFκB signaling (Kabe et al.,2005). 3. In many cases ROS activate NFκB through phosphorylation of proteins like IkBa that binds to NFκB. Exogenously added H_2O_2 regulates NFκB activation through alternative phosphorylation of IκBα (Takada et al.,2003). Further research is needed to elucidate the detailed mechanism through which ROS activate NFκB in PPC cardiomyocytes.

4.6. The involvement of pERK and c-Fos in upregulation of Stim 1 and Orai1 by PPC and role of ROS

Our experiments demonstrated that upregulation of Stim 1 and Orai1 by PPC also involves activation of the MAPK signaling pathway by ROS. These important signaling molecules have been shown to activate MAPKs in smooth muscle and other systems (Sundaresan et al., 1995; Guyton et al., 1996; Bae et al., 1997; Son et al., 2011). Involvement of ROS on MAPK activation during PPC in cardiomyocytes is supported by the following observations: Firstly, phosphorylation of the mitogen-activated protein kinase (MAPK) ERK increased by PPC, an effect that was blocked by 5-HD and NAC. Secondly, overexpression of Stim 1 and Orai1 by PPC was blocked by UO126, an inhibitor of MEK in the upstream activation of MAPK. Consistent with our observations, it has been previously reported that opening of mitoKATP channels with Dzx increases phosphorylation of ERK in a human monocytic cell line (Samavati et al., 2002). The mechanisms by which ROS can activate MAPK pathways include oxidative modifications of MAPK signaling proteins and inactivation of MAPK phosphatases (Son et al., 2011). Among the several molecules downstream ERK, the immediate early gene c-Fos plays a prominent role (Plotnikov et al., 2011). In this study, we also observed translocation of c-Fos to the nucleus of PPC cardiomyocytes which depended on ROS and ERK, as suggested by the action of NAC and UO126. The role of ROS on c-Fos translocation is consistent with previous observations in cultured neonatal cardiomyocytes showing that H_2O_2 treatment rapidly increases the expression of c-Fos (Cheng et al., 1999). Furthermore, the promoter region of the STIM gene has a putative c-Fos binding site (Fig. 4.6.1) (DebRoy et al., 2014).

Figure 4.6.1. AP1 (c-Fos, and c-Jun) binding site to the STIM1 promoter. The putative nucleotide sequence identified in the 5-regulatory region of human (A) and mouse (B) STIM1 genes. Nucleotides are numbered relative to the transcription start site as 1. Potential consensus sequences for the transcription factors NF-B and AP1 are indicated in boldface and are underlined.

Previous work in endothelial cells has revealed that STIM1 is upregulated during sepsis, its expression depends on the cooperative action between NFκB and p38, another MAPK. Bacterial endotoxin induces time-dependent binding of NF-κB and c-Fos to Stim 1 promoter (DebRoy et al., 2014). Silencing of c-Fos markedly reduces Stim 1 overexpression indicating a key role of this transcription factor in the regulation of Stim 1 expression (Fig.4.6.2) (DebRoy et al., 2014). Taken this background into consideration, it is plausible that c-Fos also upregulates Stim 1 in adult cardiomyocytes during PPC.

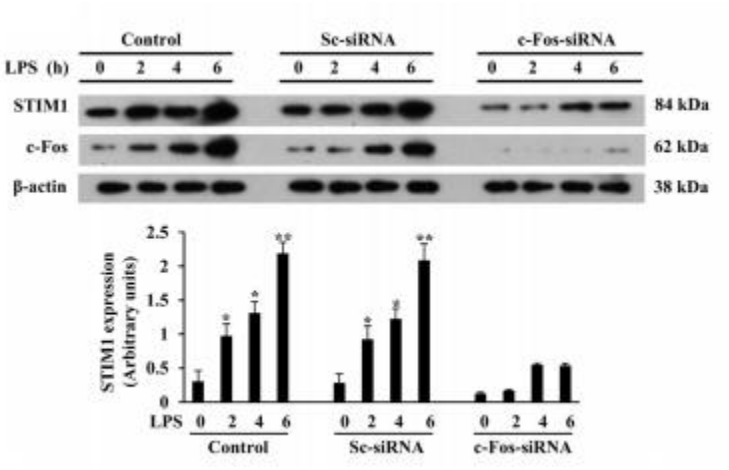

Figure 4.6.2. c-Fos is required for LPS induced STIM1 expression. HLMVE cells were transfected with control, siRNA (Sc-siRNA) or c-Fos-siRNA. After transfection, cells were exposed to LPS for indicated time periods.

4.7. Cav1.2 channels and SOCs

Voltage and store-operated Ca^{2+} channels are the major routes of Ca^{2+} influx in mammalian cells. In cardiomyocytes, the influx of Ca^{2+} through voltage-activated Cav1.2 channels is crucial for excitation-contraction coupling (Bers, 2002). Cardiomyocytes also express the Ca^{2+} sensor Stim 1 and Orai1, its associated Ca^{2+} channel, both components of SOCE (Saliba et al.,2015; Hulot et al.,2011). Previous work has shown a coordinated regulation between Cav1.2 channels and SOCs. When Stim 1 is activated it binds to the C-terminus of Cav1.2 channels, inhibits gating and causes internalization of the Cav1.2 channel (Park et al., 2010, Wang et al., 2010). Gonzalez et al in 2010 have demonstrated that PPC brings about a decrease in the expression of Cav1.2 channels while the opposite is true for SOCs as our present observations indicate. However, increased expression of Stim 1 and Orai11 by PPC appears not to be directly related to down-regulation of Cav1.2 channels by preconditioning. This is because down-regulation of the voltage activated Ca^{2+} channel is due to increased degradation of the principal

subunit of the channel (Gonzalez et al., 2010), while in the present experiments, changes in the expression of Stim 1 and Orai1 were related to *de novo* protein synthesis.

CONCLUSION

- Pharmacological preconditioning increases the expression of Stim 1 and Orai 1.
- An increase in the expression of STIM 1 and Orai 1 in preconditioning is mediated by ROS.
- Up-regulation of STIM 1 and Orai 1 involves increased mRNA levels and *de novo* synthesis of proteins.
- PPC produces *de novo* synthesis of STIM1 and Orai1 by a mechanism that involves NFkB, c-Fos, and ROS via MAPK/ERK signaling.

6. APPENDIX

A. Preliminary data shows that PPC increases NFκB

The protein level of transcription factor NFκB was determined in nuclear fraction by using Western blot and found that the expression of NFκB increases by PPC.

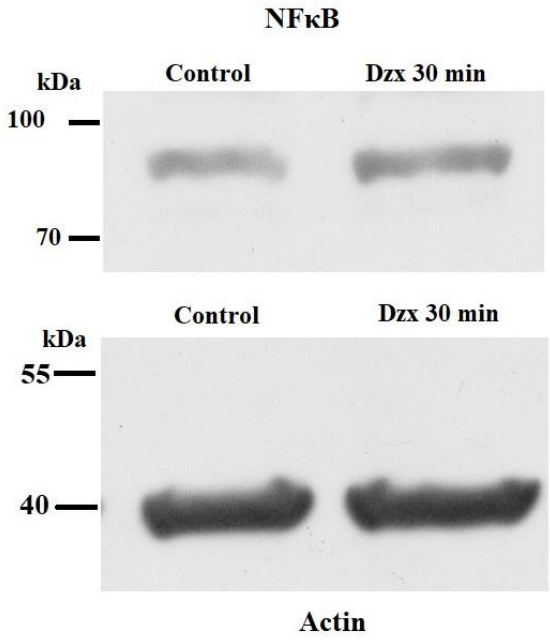

Figure A1. An increase in NFκB by PPC . A: Upper panels, representative western blots of NFκB of nuclear fractions from cardiomyocytes. Lower panels, the corresponding blots of actin used as loading controls.

B. Glycosylation pattern in Orai 1

The molecular weight of Orai 1 is 33 kDa but in our study we found Orai 1 at 55 kDa and we always have been observing multiple banding in Orai 1. To confirm the non-specific binding of Orai 1 we have used two different antibodies from Abcam and Thermofisher where in both

we have got consistent multiple banding and the most abundant band was at 55 kDa (Figure B1 A-B). This was again confirmed by using liver sample as a positive control (Figure B1 C).

Dorr *et al* in 2016 reported that multiple banding in Orai 1 is because of Glycosylation. We also have analysed total glycosylation sites in adult rat by using NetOGlyc 4.0 Server and found that there are total 16 glycosylation sites of Orai 1 present in rat (Figure B2). To test whether glycosylation was primarily responsible for the variations in the band pattern, we compared protein lysates before and after treatment with peptide N-glycosidase F (PNGase F), an amidase that cleaves off the innermost N-acetylglucosamine, thereby removing all N-glycans. Indeed, treatment with PNGase reduced the patterns to bands with molecular mass of ~33kDa and the intensity of band at 55 kDa is also reduced, suggesting that in these cells, Orai1 may be subjected to additional posttranslational modifications (Figure B3).

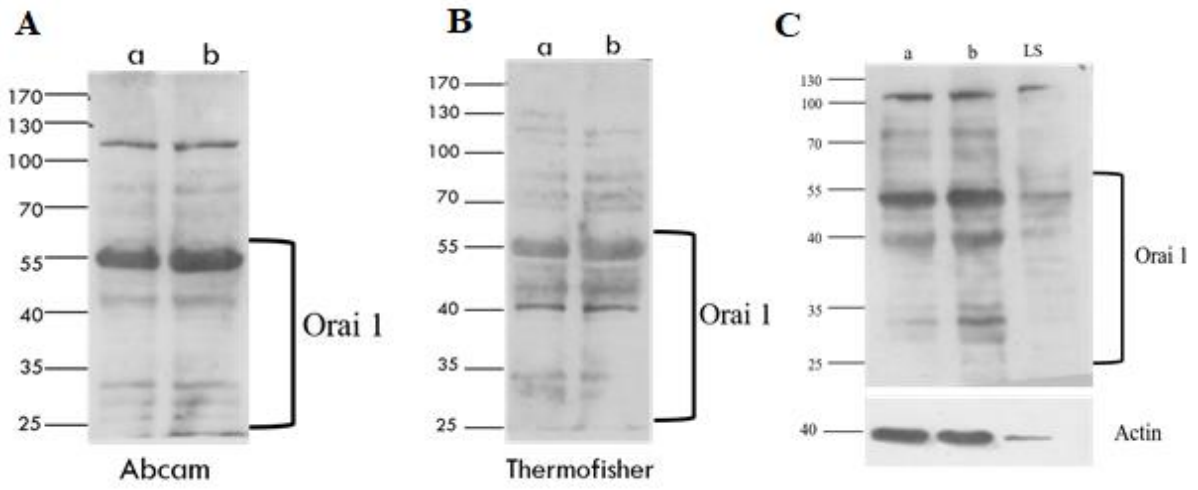

Figure B1. Multile banding in Orai 1. A-C: Representative western blots of Orai 1 of whole membrane fractions from control (lane a) and Dzx-treated hearts (lane b) and liver sample (lane c).

#seqname	source	feature	start	end	score	strand	frame	comment			
SEQUENCE	netOGlyc-4.0.0.13	CARBOHYD	10	10	0.907765	.	.	#POSITIVE
SEQUENCE	netOGlyc-4.0.0.13	CARBOHYD	12	12	0.782627	.	.	#POSITIVE
SEQUENCE	netOGlyc-4.0.0.13	CARBOHYD	19	19	0.945226	.	.	#POSITIVE
SEQUENCE	netOGlyc-4.0.0.13	CARBOHYD	22	22	0.881983	.	.	#POSITIVE
SEQUENCE	netOGlyc-4.0.0.13	CARBOHYD	23	23	0.96425 .	.	#POSITIVE	
SEQUENCE	netOGlyc-4.0.0.13	CARBOHYD	24	24	0.905395	.	.	#POSITIVE
SEQUENCE	netOGlyc-4.0.0.13	CARBOHYD	25	25	0.877656	.	.	#POSITIVE
SEQUENCE	netOGlyc-4.0.0.13	CARBOHYD	27	27	0.942929	.	.	#POSITIVE
SEQUENCE	netOGlyc-4.0.0.13	CARBOHYD	30	30	0.939838	.	.	#POSITIVE
SEQUENCE	netOGlyc-4.0.0.13	CARBOHYD	34	34	0.964768	.	.	#POSITIVE
SEQUENCE	netOGlyc-4.0.0.13	CARBOHYD	40	40	0.97131 .	.	#POSITIVE	
SEQUENCE	netOGlyc-4.0.0.13	CARBOHYD	53	53	0.852785	.	.	#POSITIVE
SEQUENCE	netOGlyc-4.0.0.13	CARBOHYD	61	61	0.28391 .	.		
SEQUENCE	netOGlyc-4.0.0.13	CARBOHYD	63	63	0.221335	.	.	
SEQUENCE	netOGlyc-4.0.0.13	CARBOHYD	67	67	0.141316	.	.	
SEQUENCE	netOGlyc-4.0.0.13	CARBOHYD	72	72	0.120963	.	.	
SEQUENCE	netOGlyc-4.0.0.13	CARBOHYD	77	77	0.268947	.	.	
SEQUENCE	netOGlyc-4.0.0.13	CARBOHYD	84	84	0.454813	.	.	
SEQUENCE	netOGlyc-4.0.0.13	CARBOHYD	91	91	0.257001	.	.	
SEQUENCE	netOGlyc-4.0.0.13	CARBOHYD	92	92	0.100948	.	.	
SEQUENCE	netOGlyc-4.0.0.13	CARBOHYD	94	94	0.0309608	.	.	
SEQUENCE	netOGlyc-4.0.0.13	CARBOHYD	95	95	0.112855	.	.	
SEQUENCE	netOGlyc-4.0.0.13	CARBOHYD	99	99	0.0693385	.	.	
SEQUENCE	netOGlyc-4.0.0.13	CARBOHYD	113	113	0.0123505	.	.	
SEQUENCE	netOGlyc-4.0.0.13	CARBOHYD	126	126	0.0109404	.	.	
SEQUENCE	netOGlyc-4.0.0.13	CARBOHYD	129	129	0.0138106	.	.	
SEQUENCE	netOGlyc-4.0.0.13	CARBOHYD	130	130	0.00537799	.	.	
SEQUENCE	netOGlyc-4.0.0.13	CARBOHYD	143	143	7.8107e-06	.	.	
SEQUENCE	netOGlyc-4.0.0.13	CARBOHYD	144	144	4.71e-06	.	.	
SEQUENCE	netOGlyc-4.0.0.13	CARBOHYD	154	154	0.0315502	.	.	
SEQUENCE	netOGlyc-4.0.0.13	CARBOHYD	161	161	0.012926	.	.	
SEQUENCE	netOGlyc-4.0.0.13	CARBOHYD	165	165	0.0266456	.	.	
SEQUENCE	netOGlyc-4.0.0.13	CARBOHYD	181	181	0.0231905	.	.	
SEQUENCE	netOGlyc-4.0.0.13	CARBOHYD	182	182	0.0150059	.	.	
SEQUENCE	netOGlyc-4.0.0.13	CARBOHYD	186	186	5.45521e-06	.	.	
SEQUENCE	netOGlyc-4.0.0.13	CARBOHYD	212	212	0.788679	.	.	#POSITIVE
SEQUENCE	netOGlyc-4.0.0.13	CARBOHYD	214	214	0.821632	.	.	#POSITIVE
SEQUENCE	netOGlyc-4.0.0.13	CARBOHYD	220	220	0.660641	.	.	#POSITIVE
SEQUENCE	netOGlyc-4.0.0.13	CARBOHYD	227	227	0.557129	.	.	#POSITIVE
SEQUENCE	netOGlyc-4.0.0.13	CARBOHYD	229	229	0.199077	.	.	
SEQUENCE	netOGlyc-4.0.0.13	CARBOHYD	230	230	0.232384	.	.	
SEQUENCE	netOGlyc-4.0.0.13	CARBOHYD	233	233	0.111421	.	.	
SEQUENCE	netOGlyc-4.0.0.13	CARBOHYD	242	242	0.0430987	.	.	
SEQUENCE	netOGlyc-4.0.0.13	CARBOHYD	243	243	0.0364493	.	.	
SEQUENCE	netOGlyc-4.0.0.13	CARBOHYD	263	263	0.0136413	.	.	
SEQUENCE	netOGlyc-4.0.0.13	CARBOHYD	266	266	0.0505666	.	.	
SEQUENCE	netOGlyc-4.0.0.13	CARBOHYD	269	269	0.0148183	.	.	
SEQUENCE	netOGlyc-4.0.0.13	CARBOHYD	296	296	0.0728303	.	.	
SEQUENCE	netOGlyc-4.0.0.13	CARBOHYD	298	298	0.0793541	.	.	
SEQUENCE	netOGlyc-4.0.0.13	CARBOHYD	301	301	0.0278817	.	.	

Figure B2. Glycosylation sites of Orai 1 in Rat

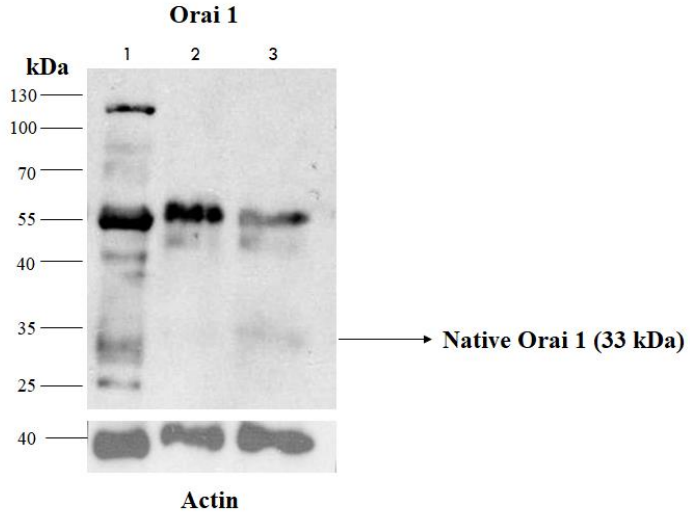

Figure B3. De-glycosylation of Orai 1 by PNGase (Peptide -*N*-Glycosidase). Upper panels, Representative western blot of Orai 1 of whole membrane fractions from control heart. Lane 1-Without denaturation, Lane 2-Denatured without enzyme, Lane 3-Denatured with enzyme. Lower panels, the corresponding blots of actin used as loading controls.

C. Stim1 and Orai1 colocalization

Stim1 interacts with Orai1 to activate SOCE. To check whether Stim 1 interacts with Orai1 in PPC, dual staining experiments were done by using confocal microscopy. We also checked the possible interaction of Stim 1 and Orai1 by depleting intracellular Ca^{2+} store. To deplete the intracellular Ca^{2+} store we had used thapsigargin (Tg), an inhibitor of SERCA.

The colocalization of two proteins is demonstrated by the yellow staining as showed in enlarged panels (Fig C2). Images were analyzed for colocalization utilizing the Pearson's Correlation. Pearson's Correlation of both increased after store depletion with Tg. This increased colocalization is expected to increase the opportunity for physical interaction between Stim 1 and Orai1, resulting in activation of calcium influx through Orai1. Whereas, the Pearson's Correlation of Stim1 and Orai 1 seems to be decreasing after PPC. However, recent studies from our lab reported that PPC decreases SOCE (Sampieri *et al*.,2019). Based on colocalization results, decrease in physical interaction of Stim 1 and Orai1 in PPC could reduce SOCE.

Control

ColocalizationOverall

	Colocalization
Pearson's Correlation	0.2288
Overlap Coefficient	0.3113
Colocalization Rate	3.58 %
Colocalization Area	42.32 µm²
Area Image	4506.52 µm²
Area Foreground	1182.67 µm²
Area Background	3323.85 µm²

Tg

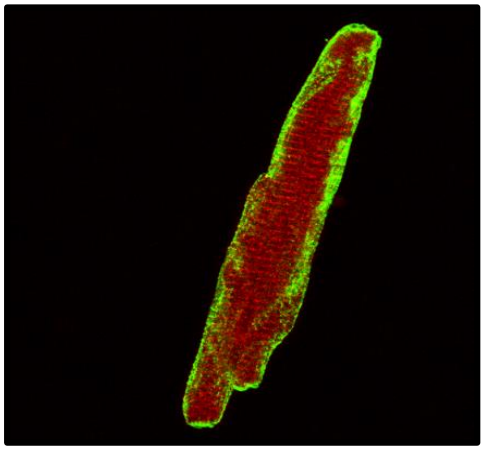

ColocalizationOverall

	Colocalization
Pearson's Correlation	0.7115
Overlap Coefficient	0.7535
Colocalization Rate	29.92 %
Colocalization Area	566.57 µm²
Area Image	12493.83 µm²
Area Foreground	1893.62 µm²
Area Background	10600.21 µm²

Dzx

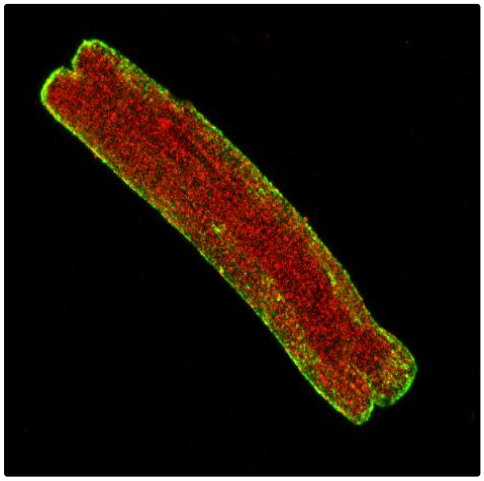

	Colocalization
Pearson's Correlation	0.5816
Overlap Coefficient	0.6399
Colocalization Rate	18.06 %
Colocalization Area	366.33 µm²
Area Image	13045.20 µm²
Area Foreground	2028.55 µm²
Area Background	11016.66 µm²

Figure C1. Stim 1-Orai1colocalization. Confocal microscopy images of cardiomyocytes under control condition, after Tg and PPC. Left panels: Images show colocalization of STIM1 (red)

with Orai1 (green).Right panels: Analysis of the colocalization of Stim 1 and Orai1 by Pearson's Coefficient.

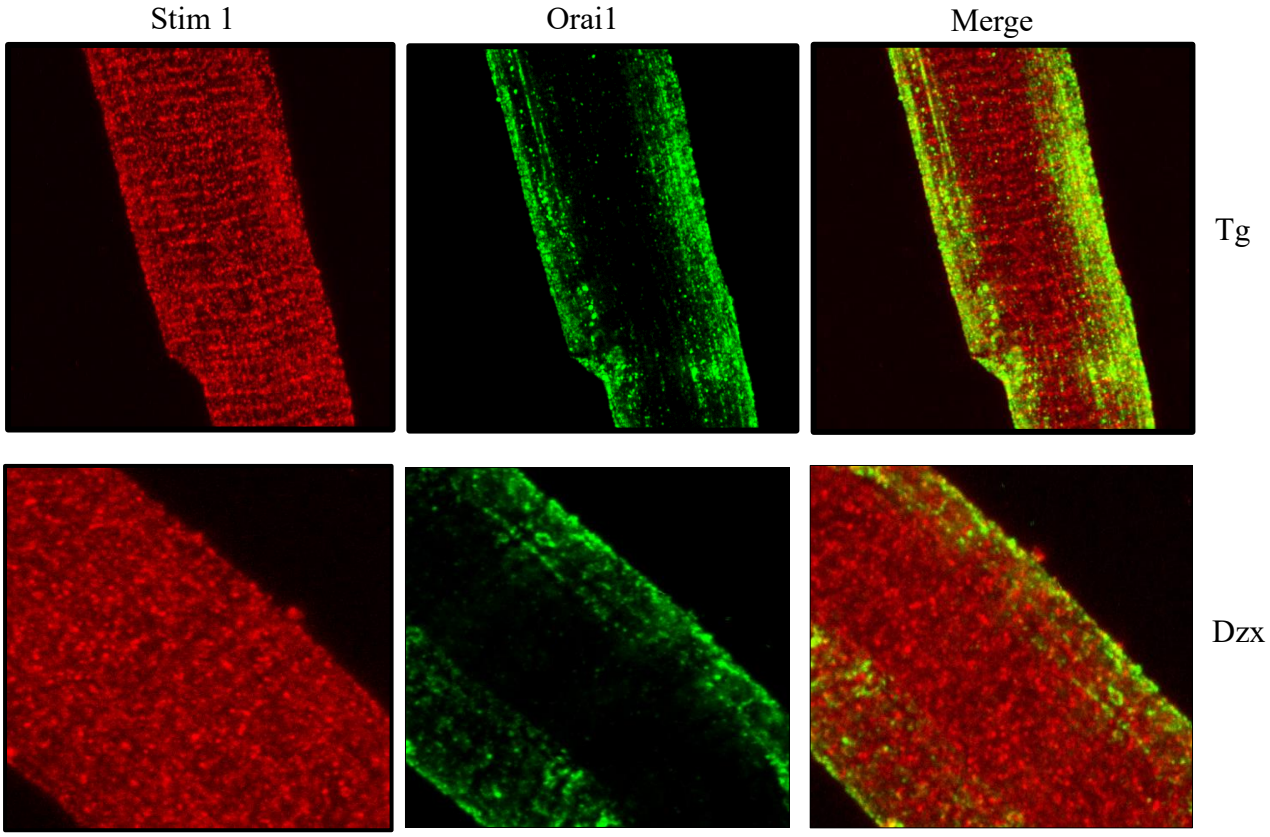

Figure C2. Zoomed confocal images of cardiomyocytes after Tg and PPC. Images show colocalization of STIM1 (red) with Orai1 (green).

D. Calmodulin is involved in disruption of Stim 1 in PPC

Li et al in 2017 have reported that the binding of calmodulin to the Stim 1 disrupts the Stim1-Orai1 complex by disassembling Stim1 oligomer and inhibits SOCE. Based on this we made hypothesis that change in distribution of Stim1 in PPC is because of disassembling of Stim1 oligomer and calmodulin is involved in this. To test this hypothesis, an inhibitor of calmodulin W-7 was used. PPC disrupted the distribution pattern of STIM1. However, the distribution

pattern observed in control experiments was preserved when W7 was added to the Dzx-containing solution. This is shown in more detail after magnification of the selected areas of the same cardiomyocytes shown below images (Fig D).

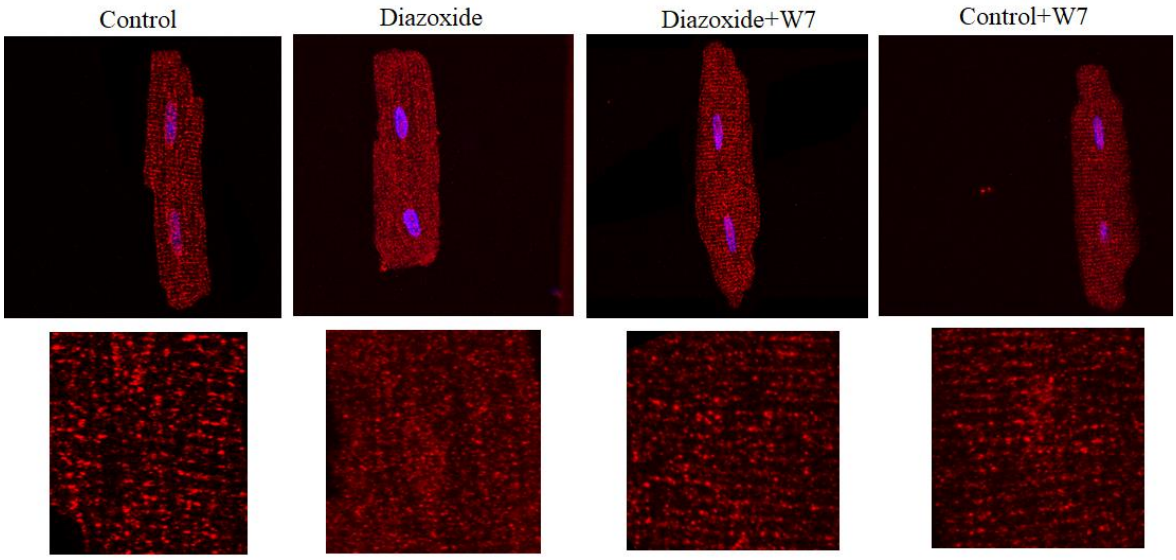

Figure D. Immunofluorescence images show the cellular distribution of STIM 1 in cardiomyocytes with control or with Dzx or with Dzx+W7 (30 min with W7 (30µM) followed by 90 min with Dzx in same solution) or with Control+W7 (30 min with W7 (30µM) followed by 90 min with tyrode solution). Enlarged images of selected areas of the same cardiomyocytes are illustrated in the lower panels.

E. Intracellular Ca^{2+} plays a role in change in localization of Stim 1 and Orai 1.

Sampieri et el in 2019 reported that inactivation of SOCE in PPC depends on intracellular Ca^{2+}. The possibility that intracellular Ca^{2+} could play a role in change in localization of Stim 1 and Orai 1 was investigated by using a cell-permeant Ca^{2+} chelator BAPTA-AM. PPC disrupted the distribution pattern of STIM1. However, the distribution pattern observed in control experiments was preserved when BAPTA-AM was added to the Dzx-containing solution. This

is shown in more detail after magnification of the selected areas of the same cardiomyocytes shown below images (Fig E1). Fig.E2 illustrates representative immunofluorescence images of Orai1 in cardiomyocytes incubated under the indicated experimental conditions. The increase in surface expression of Orai1 by PPC was completely abrogated by BAPTA-AM. Based on these results we confirmed that changes in Stim 1 and Orai 1 by PPC are related to intracellular Ca^{2+}.

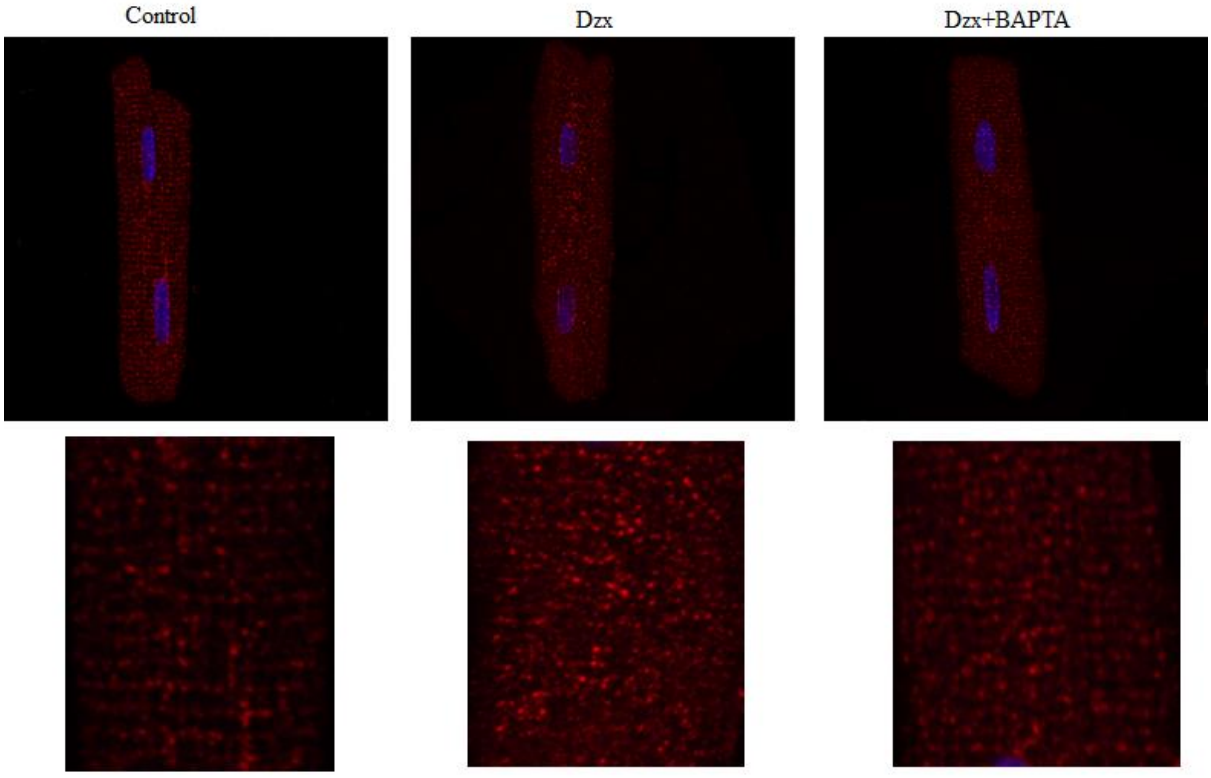

Figure E1. Immunofluorescence images show the cellular distribution of STIM 1 in cardiomyocytes with control or with Dzx or with Dzx+BAPTA-AM (30 min with BAPTA-AM (30μM) followed by 90 min with Dzx in same solution. Enlarged images of selected areas of the same cardiomyocytes are illustrated in the lower panels.

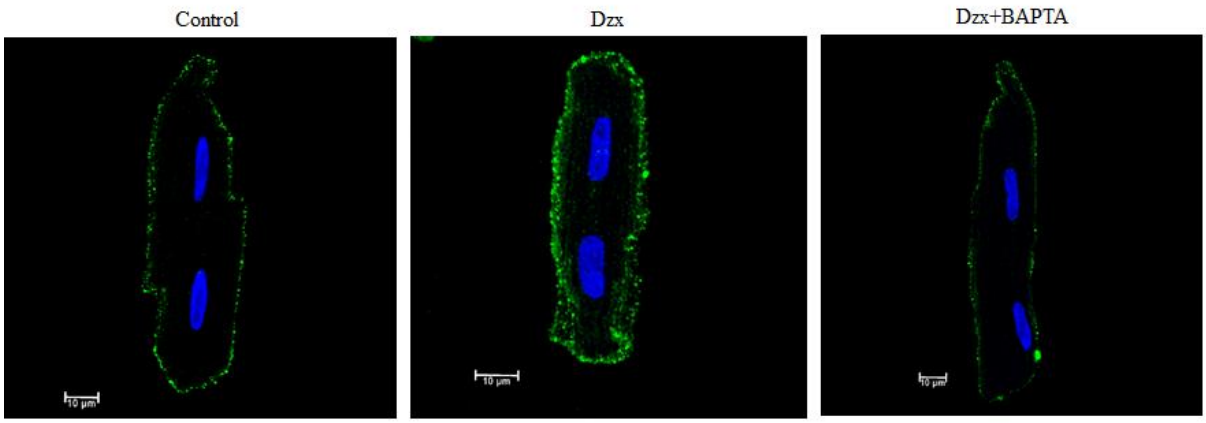

Figure E2. Immunofluorescence images show the cellular distribution of Orai 1 in cardiomyocytes with control or with Dzx or with Dzx+BAPTA-AM (30 min with BAPTA-AM (30µM) followed by 90 min with Dzx in same solution.

7. REFERENCE

Amcheslavsky, A., Wood, M. L., Yeromin, A. V., Parker, I., Freites, J. A., Tobias, D. J., & Cahalan, M. D. (2015). Molecular biophysics of Orai store-operated Ca2+ channels. Biophysical Journal, 108(2), 237–246. https://doi.org/10.1016/j.bpj.2014.11.3473

Bae, Y. S., Kang, S. W., Seo, M. S., Baines, I. C., Tekle, E., Chock, P. B., & Rhee, S. G. (1997). Epidermal growth factor (EGF)-induced generation of hydrogen peroxide. Role in EGF receptor-mediated tyrosine phosphorylation. The Journal of Biological Chemistry, 272(1), 217–221.

Baines, C. P. (2009). The mitochondrial permeability transition pore and ischemia-reperfusion injury. Basic Research in Cardiology, 104(2), 181–188. https://doi.org/10.1007/s00395-009-0004-8

Baines, C. P. (2009). The Molecular Composition of the Mitochondrial Permeability Transition Pore. Journal of Molecular and Cellular Cardiology, 46(6), 850–857. YOhttps://doi.org/10.1016/j.yjmcc.2009.02.007

Baines, C. P. (2010). The cardiac mitochondrion: Nexus of stress. Annual Review of Physiology, 72, 61–80. https://doi.org/10.1146/annurev-physiol-021909-135929

Baines, C. P. (2011). How and when do myocytes die during ischemia and reperfusion: The late phase. Journal of Cardiovascular Pharmacology and Therapeutics, 16(3–4), 239–243. https://doi.org/10.1177/1074248411407769

Bers, D. M. (2002). Cardiac excitation-contraction coupling. Nature, 415(6868), 198–205. https://doi.org/10.1038/415198a

Bonilla, I. M., Belevych, A. E., Baine, S., Stepanov, A., Mezache, L., Bodnar, T., … Gyorke, S. (2019). Enhancement of Cardiac Store Operated Calcium Entry (SOCE) within Novel Intercalated Disk Microdomains in Arrhythmic Disease. Scientific Reports, 9(1), 10179. https://doi.org/10.1038/s41598-019-46427-x

Cheng, T. H., Shih, N. L., Chen, S. Y., Wang, D. L., & Chen, J. J. (1999). Reactive oxygen species modulate endothelin-I-induced c-fos gene expression in cardiomyocytes. Cardiovascular Research, 41(3), 654–662. https://doi.org/10.1016/s0008-6363(98)00275-2

Collins, H. E., Zhu-Mauldin, X., Marchase, R. B., & Chatham, J. C. (2013). STIM1/Orai1-mediated SOCE: Current perspectives and potential roles in cardiac function and pathology. American Journal of Physiology. Heart and Circulatory Physiology, 305(4), H446-458. https://doi.org/10.1152/ajpheart.00104.2013

Contreras, L., Drago, I., Zampese, E., & Pozzan, T. (2010). Mitochondria: The calcium connection. Biochimica et Biophysica Acta (BBA) - Bioenergetics, 1797(6), 607–618. https://doi.org/10.1016/j.bbabio.2010.05.005

Correll, R. N., Goonasekera, S. A., van Berlo, J. H., Burr, A. R., Accornero, F., Zhang, H., … Molkentin, J. D. (2015). STIM1 elevation in the heart results in aberrant Ca2+ handling and cardiomyopathy. Journal of Molecular and Cellular Cardiology, 87, 38–47. https://doi.org/10.1016/j.yjmcc.2015.07.032

DebRoy, A., Vogel, S. M., Soni, D., Sundivakkam, P. C., Malik, A. B., & Tiruppathi, C. (2014). Cooperative signaling via Transcription Factors NF-κB and AP1/c-Fos mediates endothelial cell STIM1 expression and hyperpermeability in response to endotoxin. The Journal of Biological Chemistry, 289(35), 24188–24201. https://doi.org/10.1074/jbc.M114.570051

Dhalla, N. S., Takeda, N., Singh, M., & Lukas, A. (2002). Myocardial Ischemia and Preconditioning. Springer Science & Business Media.

Dörr, K., Kilch, T., Kappel, S., Alansary, D., Schwär, G., Niemeyer, B. A., & Peinelt, C. (2016). Cell type-specific glycosylation of Orai1 modulates store-operated Ca2+ entry. Science Signaling, 9(418), ra25. https://doi.org/10.1126/scisignal.aaa9913

Eylenstein, A., Gehring, E.-M., Heise, N., Shumilina, E., Schmidt, S., Szteyn, K., … Lang, F. (2011). Stimulation of Ca2+-channel Orai1/STIM1 by serum- and glucocorticoid-inducible kinase 1 (SGK1). FASEB Journal: Official Publication of the Federation of American Societies for Experimental Biology, 25(6), 2012–2021. https://doi.org/10.1096/fj.10-178210

Forbes, R. A., Steenbergen, C., & Murphy, E. (2001). Diazoxide-induced cardioprotection requires signaling through a redox-sensitive mechanism. Circulation Research, 88(8), 802–809. https://doi.org/10.1161/hh0801.089342

Garlid, K. D., Dos Santos, P., Xie, Z.-J., Costa, A. D. T., & Paucek, P. (2003). Mitochondrial potassium transport: The role of the mitochondrial ATP-sensitive K(+) channel in cardiac function and cardioprotection. Biochimica Et Biophysica Acta, 1606(1–3), 1–21. https://doi.org/10.1016/s0005-2728(03)00109-9

Garlid, K. D., Paucek, P., Yarov-Yarovoy, V., Murray, H. N., Darbenzio, R. B., D'Alonzo, A. J., … Grover, G. J. (1997). Cardioprotective effect of diazoxide and its interaction with mitochondrial ATP-sensitive K+ channels. Possible mechanism of cardioprotection. Circulation Research, 81(6), 1072–1082. https://doi.org/10.1161/01.res.81.6.1072

González, G., Zaldívar, D., Carrillo, E., Hernández, A., García, M., & Sánchez, J. (2010). Pharmacological preconditioning by diazoxide downregulates cardiac L-type Ca2+ channels. British Journal of Pharmacology, 161(5), 1172–1185. https://doi.org/10.1111/j.1476-5381.2010.00960.x

Guo, J., Lao, Y., & Chang, D. C. (2009). Calcium and Apoptosis. In A. Lajtha & K. Mikoshiba (Eds.), Handbook of Neurochemistry and Molecular Neurobiology: Neural Signaling Mechanisms (pp. 597–622). https://doi.org/10.1007/978-0-387-30370-3_33

Gusarova, G. A., Trejo, H. E., Dada, L. A., Briva, A., Welch, L. C., Hamanaka, R. B., … Sznajder, J. I. (2011). Hypoxia leads to Na,K-ATPase downregulation via Ca(2+) release-activated Ca(2+) channels and AMPK activation. Molecular and Cellular Biology, 31(17), 3546–3556. https://doi.org/10.1128/MCB.05114-11

Guyton, K. Z., Liu, Y., Gorospe, M., Xu, Q., & Holbrook, N. J. (1996). Activation of mitogen-activated protein kinase by H2O2. Role in cell survival following oxidant injury. The Journal of Biological Chemistry, 271(8), 4138–4142. https://doi.org/10.1074/jbc.271.8.4138

Harraz, O. F., & Altier, C. (2014). STIM1-mediated bidirectional regulation of Ca2+ entry through voltage-gated calcium channels (VGCC) and calcium-release activated channels (CRAC). Frontiers in Cellular Neuroscience, 8. https://doi.org/10.3389/fncel.2014.00043

Hawkins, B. J., Irrinki, K. M., Mallilankaraman, K., Lien, Y.-C., Wang, Y., Bhanumathy, C. D., … Madesh, M. (2010). S-glutathionylation activates STIM1 and alters mitochondrial homeostasis. The Journal of Cell Biology, 190(3), 391–405. https://doi.org/10.1083/jcb.201004152

Hoover, P. J., & Lewis, R. S. (2011). Stoichiometric requirements for trapping and gating of Ca2+ release-activated Ca2+ (CRAC) channels by stromal interaction molecule 1 (STIM1). Proceedings of the National Academy of Sciences of the United States of America, 108(32), 13299–13304. https://doi.org/10.1073/pnas.1101664108

Hoth, M., & Penner, R. (1992). Depletion of intracellular calcium stores activates a calcium current in mast cells. Nature, 355(6358), 353–356. https://doi.org/10.1038/355353a0

Hotokezaka, H., Sakai, E., Kanaoka, K., Saito, K., Matsuo, K., Kitaura, H., … Nakayama, K. (2002). U0126 and PD98059, specific inhibitors of MEK, accelerate differentiation of RAW264.7 cells into osteoclast-like cells. The Journal of Biological Chemistry, 277(49), 47366–47372. https://doi.org/10.1074/jbc.M208284200

Hou, X., Burstein, S. R., & Long, S. B. (2018). Structures reveal opening of the store-operated calcium channel Orai. ELife, 7. https://doi.org/10.7554/eLife.36758

Hu, H., Sato, T., Seharaseyon, J., Liu, Y., Johns, D. C., O'Rourke, B., & Marbán, E. (1999). Pharmacological and histochemical distinctions between molecularly defined sarcolemmal KATP channels and native cardiac mitochondrial KATP channels. Molecular Pharmacology, 55(6), 1000–1005.

Hulot, J.-S., Fauconnier, J., Ramanujam, D., Chaanine, A., Aubart, F., Sassi, Y., … Engelhardt, S. (2011). Critical role for stromal interaction molecule 1 in cardiac hypertrophy. Circulation, 124(7), 796–805. https://doi.org/10.1161/CIRCULATIONAHA.111.031229

Hunton, D. L., Lucchesi, P. A., Pang, Y., Cheng, X., Dell'Italia, L. J., & Marchase, R. B. (2002). Capacitative calcium entry contributes to nuclear factor of activated T-cells nuclear translocation and hypertrophy in cardiomyocytes. The Journal of Biological Chemistry, 277(16), 14266–14273. https://doi.org/10.1074/jbc.M107167200

Kabe, Y., Ando, K., Hirao, S., Yoshida, M., & Handa, H. (2005). Redox regulation of NF-kappaB activation: Distinct redox regulation between the cytoplasm and the nucleus. Antioxidants & Redox Signaling, 7(3–4), 395–403. https://doi.org/10.1089/ars.2005.7.395

Kalogeris, T., Baines, C. P., Krenz, M., & Korthuis, R. J. (2012). Chapter Six—Cell Biology of Ischemia/Reperfusion Injury. In K. W. Jeon (Ed.), International Review of Cell and

Molecular Biology (Vol. 298, pp. 229–317). https://doi.org/10.1016/B978-0-12-394309-5.00006-7

Keil, J. M., Shen, Z., Briggs, S. P., & Patrick, G. N. (2010). Regulation of STIM1 and SOCE by the ubiquitin-proteasome system (UPS). PloS One, 5(10), e13465. https://doi.org/10.1371/journal.pone.0013465

Kobayashi, T., & Cohen, P. (1999). Activation of serum- and glucocorticoid-regulated protein kinase by agonists that activate phosphatidylinositide 3-kinase is mediated by 3-phosphoinositide-dependent protein kinase-1 (PDK1) and PDK2. The Biochemical Journal, 339 (Pt 2), 319–328.

Kobayashi, T., Deak, M., Morrice, N., & Cohen, P. (1999). Characterization of the structure and regulation of two novel isoforms of serum- and glucocorticoid-induced protein kinase. The Biochemical Journal, 344 Pt 1, 189–197.

Lang, F., Eylenstein, A., & Shumilina, E. (2012). Regulation of Orai1/STIM1 by the kinases SGK1 and AMPK. Cell Calcium, 52(5), 347–354. https://doi.org/10.1016/j.ceca.2012.05.005

Lesnefsky, E. J., Chen, Q., Tandler, B., & Hoppel, C. L. (2017). Mitochondrial Dysfunction and Myocardial Ischemia-Reperfusion: Implications for Novel Therapies. Annual Review of Pharmacology and Toxicology, 57, 535–565. https://doi.org/10.1146/annurev-pharmtox-010715-103335

Li, X., Wu, G., Yang, Y., Fu, S., Liu, X., Kang, H., … Shen, Y. (2017). Calmodulin dissociates the STIM1-Orai1 complex and STIM1 oligomers. Nature Communications, 8(1), 1042. https://doi.org/10.1038/s41467-017-01135-w

Liu, J., Pang, Y., Chang, T., Bounelis, P., Chatham, J. C., & Marchase, R. B. (2006). Increased hexosamine biosynthesis and protein O-GlcNAc levels associated with myocardial protection against calcium paradox and ischemia. Journal of Molecular and Cellular Cardiology, 40(2), 303–312. https://doi.org/10.1016/j.yjmcc.2005.11.003

Luo, X., Hojayev, B., Jiang, N., Wang, Z. V., Tandan, S., Rakalin, A., … Hill, J. A. (2012). STIM1-dependent store-operated Ca2+ entry is required for pathological cardiac hypertrophy. Journal of Molecular and Cellular Cardiology, 52(1), 136–147. https://doi.org/10.1016/j.yjmcc.2011.11.003

Mancarella, S., Wang, Y., & Gill, D. L. (2011). Signal transduction STIM1 senses both Ca2+ and heat. Nature Chemical Biology, 7(6), 344–345. https://doi.org/10.1038/nchembio.587

McCullough, J. R., Normandin, D. E., Conder, M. L., Sleph, P. G., Dzwonczyk, S., & Grover, G. J. (1991). Specific block of the anti-ischemic actions of cromakalim by sodium 5-hydroxydecanoate. Circulation Research, 69(4), 949–958. https://doi.org/10.1161/01.res.69.4.949

Morgan, M. J., & Liu, Z. (2011). Crosstalk of reactive oxygen species and NF-κB signaling. Cell Research, 21(1), 103–115. https://doi.org/10.1038/cr.2010.178

Muallem, S., Zhao, H., Mayer, E., & Sachs, G. (1990). Regulation of intracellular calcium in epithelial cells. Seminars in Cell Biology, 1(4), 305–310.

Mungai, P. T., Waypa, G. B., Jairaman, A., Prakriya, M., Dokic, D., Ball, M. K., & Schumacker, P. T. (2011). Hypoxia triggers AMPK activation through reactive oxygen species-mediated activation of calcium release-activated calcium channels. Molecular and Cellular Biology, 31(17), 3531–3545. https://doi.org/10.1128/MCB.05124-11

Murphy, E., & Steenbergen, C. (2008). Mechanisms underlying acute protection from cardiac ischemia-reperfusion injury. Physiological Reviews, 88(2), 581–609. https://doi.org/10.1152/physrev.00024.2007

Murry, C. E., Jennings, R. B., & Reimer, K. A. (1986). Preconditioning with ischemia: A delay of lethal cell injury in ischemic myocardium. Circulation, 74(5), 1124–1136. https://doi.org/10.1161/01.cir.74.5.1124

Namura, S., Iihara, K., Takami, S., Nagata, I., Kikuchi, H., Matsushita, K., … Alessandrini, A. (2001). Intravenous administration of MEK inhibitor U0126 affords brain protection against forebrain ischemia and focal cerebral ischemia. Proceedings of the National Academy of Sciences of the United States of America, 98(20), 11569–11574. https://doi.org/10.1073/pnas.181213498

Niemeyer, B. A. (2016). Changing calcium: CRAC channel (STIM and Orai) expression, splicing, and posttranslational modifiers. American Journal of Physiology. Cell Physiology, 310(9), C701-709. https://doi.org/10.1152/ajpcell.00034.2016

Oeckinghaus, A., & Ghosh, S. (2009). The NF-kappaB family of transcription factors and its regulation. Cold Spring Harbor Perspectives in Biology, 1(4), a000034. https://doi.org/10.1101/cshperspect.a000034

Oldenburg, O., Cohen, M. V., & Downey, J. M. (2003). Mitochondrial KATP channels in preconditioning. Journal of Molecular and Cellular Cardiology, 35(6), 569–575. https://doi.org/10.1016/S0022-2828(03)00115-9

Pain, T., Yang, X. M., Critz, S. D., Yue, Y., Nakano, A., Liu, G. S., … Downey, J. M. (2000). Opening of mitochondrial K(ATP) channels triggers the preconditioned state by generating free radicals. Circulation Research. https://doi.org/10.1161/01.RES.87.6.460

Park, C. Y., Hoover, P. J., Mullins, F. M., Bachhawat, P., Covington, E. D., Raunser, S., … Lewis, R. S. (2009). STIM1 clusters and activates CRAC channels via direct binding of a cytosolic domain to Orai1. Cell, 136(5), 876–890. https://doi.org/10.1016/j.cell.2009.02.014

Park, C. Y., Shcheglovitov, A., & Dolmetsch, R. (2010). The CRAC channel activator STIM1 binds and inhibits L-type voltage-gated calcium channels. Science (New York, N.Y.), 330(6000), 101–105. https://doi.org/10.1126/science.1191027

Pasdois, P., Beauvoit, B., Tariosse, L., Vinassa, B., Bonoron-Adèle, S., & Dos Santos, P. (2008). Effect of diazoxide on flavoprotein oxidation and reactive oxygen species generation during ischemia-reperfusion: A study on Langendorff-perfused rat hearts using optic fibers. American Journal of Physiology. Heart and Circulatory Physiology, 294(5), H2088-2097. https://doi.org/10.1152/ajpheart.01345.2007

Patterson, R. L., van Rossum, D. B., & Gill, D. L. (1999). Store-operated Ca2+ entry: Evidence for a secretion-like coupling model. Cell, 98(4), 487–499. https://doi.org/10.1016/s0092-8674(00)81977-7

Penna, A., Demuro, A., Yeromin, A. V., Zhang, S. L., Safrina, O., Parker, I., & Cahalan, M. D. (2008). The CRAC channel consists of a tetramer formed by Stim-induced dimerization of Orai dimers. Nature, 456(7218), 116–120. https://doi.org/10.1038/nature07338

Planz, O., Pleschka, S., & Ludwig, S. (2001). MEK-specific inhibitor U0126 blocks spread of Borna disease virus in cultured cells. Journal of Virology, 75(10), 4871–4877. https://doi.org/10.1128/JVI.75.10.4871-4877.2001

Prakriya, M., & Lewis, R. S. (2015). Store-Operated Calcium Channels. Physiological Reviews, 95(4), 1383–1436. https://doi.org/10.1152/physrev.00020.2014

Putney, J. W. (1986). A model for receptor-regulated calcium entry. Cell Calcium, 7(1), 1–12. https://doi.org/10.1016/0143-4160(86)90026-6

Rivera-Pagán, A. F., Rivera-Aponte, D. E., Melnik-Martínez, K. V., Zayas-Santiago, A., Kucheryavykh, L. Y., Martins, A. H., … Eaton, M. J. (2015). Up-Regulation of TREK-2 Potassium Channels in Cultured Astrocytes Requires De Novo Protein Synthesis: Relevance to Localization of TREK-2 Channels in Astrocytes after Transient Cerebral Ischemia. PLoS ONE, 10(4). https://doi.org/10.1371/journal.pone.0125195

Roos, J., DiGregorio, P. J., Yeromin, A. V., Ohlsen, K., Lioudyno, M., Zhang, S., … Stauderman, K. A. (2005). STIM1, an essential and conserved component of store-operated Ca2+ channel function. The Journal of Cell Biology, 169(3), 435–445. https://doi.org/10.1083/jcb.200502019

Rosado, J. A., & Sage, S. O. (2001). Role of the ERK pathway in the activation of store-mediated calcium entry in human platelets. The Journal of Biological Chemistry, 276(19), 15659–15665. https://doi.org/10.1074/jbc.M009218200

Saliba, Y., Keck, M., Marchand, A., Atassi, F., Ouillé, A., Cazorla, O., … Lompré, A.-M. (2015). Emergence of Orai3 activity during cardiac hypertrophy. Cardiovascular Research, 105(3), 248–259. https://doi.org/10.1093/cvr/cvu207

Samavati, L., Monick, M. M., Sanlioglu, S., Buettner, G. R., Oberley, L. W., & Hunninghake, G. W. (2002). Mitochondrial K(ATP) channel openers activate the ERK kinase by an oxidant-dependent mechanism. American Journal of Physiology. Cell Physiology, 283(1), C273-281. https://doi.org/10.1152/ajpcell.00514.2001

Schreck, R., Rieber, P., & Baeuerle, P. A. (1991). Reactive oxygen intermediates as apparently widely used messengers in the activation of the NF-kappa B transcription factor and HIV-1. The EMBO Journal, 10(8), 2247–2258.

Seger, R., & Krebs, E. G. (1995). The MAPK signaling cascade. FASEB Journal: Official Publication of the Federation of American Societies for Experimental Biology, 9(9), 726–735.

Soboloff, J., Rothberg, B. S., Madesh, M., & Gill, D. L. (2012). STIM proteins: Dynamic calcium signal transducers. Nature Reviews. Molecular Cell Biology, 13(9), 549–565. httpYou s://doi.org/10.1038/nrm3414

Son, Y., Cheong, Y.-K., Kim, N.-H., Chung, H.-T., Kang, D. G., & Pae, H.-O. (2011). Mitogen-Activated Protein Kinases and Reactive Oxygen Species: How Can ROS Activate MAPK Pathways? Journal of Signal Transduction, 2011, 792639. https://doi.org/10.1155/2011/792639

Stathopulos, P. B., Zheng, L., Li, G.-Y., Plevin, M. J., & Ikura, M. (2008). Structural and mechanistic insights into STIM1-mediated initiation of store-operated calcium entry. Cell, 135(1), 110–122. https://doi.org/10.1016/j.cell.2008.08.006

Sundaresan, M., Yu, Z. X., Ferrans, V. J., Irani, K., & Finkel, T. (1995). Requirement for generation of H2O2 for platelet-derived growth factor signal transduction. Science (New York, N.Y.), 270(5234), 296–299. https://doi.org/10.1126/science.270.5234.296

Szydlowska, K., & Tymianski, M. (2010). Calcium, ischemia and excitotoxicity. Cell Calcium, 47(2), 122–129. https://doi.org/10.1016/j.ceca.2010.01.003

Takada, Y., Mukhopadhyay, A., Kundu, G. C., Mahabeleshwar, G. H., Singh, S., & Aggarwal, B. B. (2003). Hydrogen peroxide activates NF-kappa B through tyrosine phosphorylation of I kappa B alpha and serine phosphorylation of p65: Evidence for the involvement of I kappa B alpha kinase and Syk protein-tyrosine kinase. The Journal of Biological Chemistry, 278(26), 24233–24241. https://doi.org/10.1074/jbc.M212389200

Takemura, H., & Putney, J. W. (1989). Capacitative calcium entry in parotid acinar cells. The Biochemical Journal, 258(2), 409–412. https://doi.org/10.1042/bj2580409

Talukder, M. A. H., Zweier, J. L., & Periasamy, M. (2009). Targeting calcium transport in ischaemic heart disease. Cardiovascular Research, 84(3), 345–352. https://doi.org/10.1093/cvr/cvp264

Testai, L., Rapposelli, S., Martelli, A., Breschi, M. C., & Calderone, V. (2015). Mitochondrial potassium channels as pharmacological target for cardioprotective drugs. Medicinal Research Reviews, 35(3), 520–553. https://doi.org/10.1002/med.21332

Valverde, C. A., Kornyeyev, D., Ferreiro, M., Petrosky, A. D., Mattiazzi, A., & Escobar, A. L. (2010). Transient Ca2+ depletion of the sarcoplasmic reticulum at the onset of reperfusion. Cardiovascular Research, 85(4), 671–680. https://doi.org/10.1093/cvr/cvp371

Wang, Y., Deng, X., Mancarella, S., Hendron, E., Eguchi, S., Soboloff, J., … Gill, D. L. (2010). The Calcium Store Sensor, STIM1, Reciprocally Controls Orai and CaV1.2 Channels. Science (New York, N.Y.), 330(6000), 105–109. https://doi.org/10.1126/science.119108

Williams, R. T., Manji, S. S., Parker, N. J., Hancock, M. S., Van Stekelenburg, L., Eid, J. P., … Dziadek, M. A. (2001). Identification and characterization of the STIM (stromal interaction molecule) gene family: Coding for a novel class of transmembrane proteins. Biochemical Journal, 357(Pt 3), 673–685.

Yang, X., Jin, H., Cai, X., Li, S., & Shen, Y. (2012). Structural and mechanistic insights into the activation of Stromal interaction molecule 1 (STIM1). Proceedings of the National Academy of Sciences of the United States of America, 109(15), 5657–5662. https://doi.org/10.1073/pnas.1118947109

Yen, M., & Lewis, R. S. (2019). Numbers count: How STIM and Orai stoichiometry affect store-operated calcium entry. Cell Calcium, 79, 35–43. https://doi.org/10.1016/j.ceca.2019.02.002

Yuan, J. P., Zeng, W., Dorwart, M. R., Choi, Y.-J., Worley, P. F., & Muallem, S. (2009). SOAR and the polybasic STIM1 domains gate and regulate Orai channels. Nature Cell Biology, 11(3), 337–343. https://doi.org/10.1038/ncb1842

Zhang, S. L., Yeromin, A. V., Zhang, X. H.-F., Yu, Y., Safrina, O., Penna, A., … Cahalan, M. D. (2006). Genome-wide RNAi screen of Ca(2+) influx identifies genes that regulate Ca(2+) release-activated Ca(2+) channel activity. Proceedings of the National Academy of Sciences of the United States of America, 103(24), 9357–9362. https://doi.org/10.1073/pnas.0603161103

Zhang, S. L., Yu, Y., Roos, J., Kozak, J. A., Deerinck, T. J., Ellisman, M. H., … Cahalan, M. D. (2005). STIM1 is a Ca2+ sensor that activates CRAC channels and migrates from the Ca2+ store to the plasma membrane. Nature, 437(7060), 902–905. https://doi.org/10.1038/nature04147